DE TTK

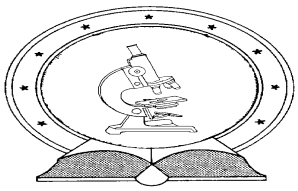

Thermodynamic, kinetic and relaxation studies on lanthanide complexes of open-chain and macrocyclic ligands

PhD Thesis

Zoltán Pálinkás

Supervisiors:

Dr. Éva Jakab Tóth (University of Orléans)

Dr. Imre Tóth, Dr. Ernő Brücher (University of Debrecen)

University of Debrecen

Debrecen, 2012.

UNIVERSITÉ D'ORLÉANS

ÉCOLE DOCTORALE SCIENCES ET TECHNOLOGIES

Centre de Biophysique Moléculaire, CNRS, Orléans

Department of Inorganic and Analytical Chemistry, University of Debrecen

THÈSE EN COTUTELLE INTERNATIONALE présentée par:

Zoltan PALINKAS

soutenue le : **13 juillet 2012**

pour obtenir le grade de: **Docteur de l'université d'Orléans et de l'université de Debrecen**

Discipline : Chimie Inorganique

Thermodynamic, kinetic and relaxation studies on lanthanide complexes of open-chain and macrocyclic ligands

THÈSE dirigée par :

Mme. Eva JAKAB TÓTH	Dr., CBM, CNRS, Orléans
M. Imre TÓTH	Prof., Université de Debrecen
M. Ernő Brücher	Prof., Université de Debrecen

RAPPORTEURS :

M. Carlos F. G. C. GERALDES	Prof., Université de Coimbra
M. Ivan LUKES	Prof., Université de Charles, Prague

JURY :

M. Gyula RÁBAI	Prof., Université de Debrecen, président du jury
Mme. Eva JAKAB TÓTH	Dr., CBM, CNRS, Orléans, directrice thése
M. István BÁNYAI	Prof., Université de Debrecen
M. Stéphane PETOUD	Prof., Université d'Orléans
M. Carlos F. G. C. GERALDES	Prof., Université de Coimbra, rapporteur
M. Ivan LUKES	Prof., Université de Charles, Prague, rapporteur
M. Béla NOSZÁL	Prof., Université de SOTE

Ezen értekezést a Debreceni Egyetem Természettudományi Doktori Tanács Kémiai Doktori Iskola Koordinációs Kémiai programja keretében készítettem a Debreceni Egyetem természettudományi doktori (PhD) fokozatának elnyerése céljából.

Debrecen, 2012. április 16.

Tanúsítom, hogy Pálinkás Zoltán doktorjelölt 2007-2011 között a fent megnevezett Doktori Iskola Koordinációs Kémiai programjának keretében irányításommal végezte munkáját. Az értekezésben foglalt eredményekhez a jelölt önálló alkotó tevékenységével meghatározóan hozzájárult. Az értekezés elfogadását javasolom.

Debrecen, 2012. április 16.

Thermodynamic, kinetic and relaxation studies on lanthanide complexes of open-chain and macrocyclic ligands

Értekezés a doktori (Ph.D.) fokozat megszerzése érdekében
a Kémia tudományágban

Írta: Pálinkás Zoltán okleveles vegyész

Készült a Debreceni Egyetem Kémia doktori iskolája
(Koordinációs Kémia programja) keretében

Témavezető: Dr.Tóth Imre, Dr. Brücher Ernő, Dr. Tóth Éva

A doktori szigorlati bizottság:

elnök:	Dr. Sóvágó Imre
tagok:	Dr. Farkas Etelka
	Dr. Gajda Tamás

A doktori szigorlat időpontja: 2011. 04. 11.

Az értekezés bírálói:

Dr. Ivan Lukes
Dr. Carlos F. Geraldes

A bírálóbizottság:

elnök:	Dr. Rábai Gyula
tagok:	Dr. Bányai István
	Dr. Noszál Béla
	Dr. Tóth Éva
	Dr. Stéphane Petoud

Az értekezés védésének időpontja: 2012. 07. 13.

Table of contents

I. Introduction

Over the last few decades, Magnetic Resonance Imaging (MRI) has become one of the most powerful and highly efficient methods in medical diagnostics. This technique is based on the measurement of water proton relaxation rates in human tissues, and provides three dimensional, high resolution images. Since the water proton relaxation rates differ in healthy and diseased tissues, important diagnostic informations can be obtained with the use of MRI. In order to reduce the time of examinations and significantly increase the contrast of the images, contrast agenst (CA) are widely used in the clinical practice. Contrast agents are paramagnetic compounds – Gd(III) chelates in majority – which can improve the sensitivity and specificity of MRI.[1,2] Nowadays, more than 30 % of the clinical MR examinations are assisted by the use of contrast agents. The efficiency of MRI contrast agents is described with their relaxivity; the longitudinal paramagnetic relaxation rate enhancement of water protons in the presence of 1 mM of the contrast agent.

There are several advantages of MRI: it is a non-invasive technique and in contrast to X-ray or computer tomography, utilizes non-ionizing radiation. In addition, the measurement of the in vivo concentration of certain metabolites (enzymes, endogenous anions and cations, pH, pO_2) might be possible with the use of the so-called smart or intelligent contrast agents, which have been introduced recently and which are in spectacular development.

The most important requirement for a contrast agent to be applied in vivo is non-toxicity. In order to avoid toxicity, Gd^{3+} is complexed with suitable multidentate ligands, poly-amino-carboxylates in general. Indeed, the free gadolinium ion can not be injected into the body since it may interact

with endogenous metabolites in many different ways (it can bind to the donor groups of different proteins or small anions, replace other metal ions in enzymes, or, due to its ionic radius similar to Ca^{2+}, it may interfere in Ca^{2+}-regulated signal transmission processes. Moreover, Gd^{3+} tends to form hydroxo complexes and precipitate under physiological conditions (pH= 7.4). These processes are strongly related to the *in vivo* dissociation of CA, when the highly toxic free Gd^{3+} ion and the toxic free ligand capable of forming chelates appear in the body. By consequence, the dissociation of Gd-based contrast agents leads to toxicity (LD_{50} values for free Gd^{3+} and for uncomplexed ligands are in the range of 0.1-0.2 mmol/kg).[3,4] In addition to the general requirements of being efficient and non-toxic, contrast agents have to meet other demands, such as good water solubility and low osmolality.

The objectives of the thesis are (i) to develop novel Gd^{3+} complexes with improved relaxivity and to understand the relations between the structure of the complex and all parameters that will influence relaxivity and (ii) to investigate the thermodynamic stability and kinetic inertness of the complexes formed with Gd^{3+} and other lanthanide ions, two factors directly related to the *in vivo* safety of contrast agents.

II. Bibliographic review

II. 1. Chemistry of lanthanides

From lanthanum (z= 57) to lutetium (z= 71) (first part of the f-block elements) the fourteen elements in the periodic table are called lanthanides. Lanthanides, together with scandium (z= 21) and yttrium (z= 39) have been called the rare earths for a long time. The use of this name was misleading since these metals are not rare at all. For example, cerium, the most abundant lanthanide, is more common than nickel, or lead. The explanation for the use of this name is that there are only few larger deposits of these metals all over the world. Nowadays, scandium and yttrium are placed together in the group of lanthanides, because of their similar chemical properties.[5]

From lanthanum to lutetium the elements change from [Xe]$4f^0$ to [Xe]$4f^{14}$ electron configuration. The complete list of the lanthanide elements and some of their properties are summarized in Table II. 1.

Table II. 1. List and physico-chemical properties of lanthanide atoms and ions[6]

ATOMIC NUMBER	NAME	SYMBOL	ELECTRONIC CONFIGURATION		E° (V)	RADIUS
			Atom	M^{3+}		M^{3+} (A)
57	Lanthanum	La	[Xe] $5d^1\ 6s^2$	[Xe]	-2.37	1.17
58	Cerium	Ce	[Xe] $4f^1\ 5d^1\ 6s^2$	[Xe] f^1	-2.34	1.15
59	Praseodynium	Pr	[Xe] $4f^2\ 6s^2$	[Xe] f^2	-2.35	1.13
60	Neodynium	Nd	[Xe] $4f^3\ 6s^2$	[Xe] f^3	-2.32	1.12
61	Promethium	Pm	[Xe] $4f^4\ 6s^2$	[Xe] f^4	-2.29	1.11
62	Samarium	Sm	[Xe] $4f^5\ 6s^2$	[Xe] f^5	-2.30	1.10
63	Europium	Eu	[Xe] $4f^6\ 6s^2$	[Xe] f^6	-1.99	1.09
64	Gadolinium	Gd	[Xe] $4f^7\ 6s^2$	[Xe] f^7	-2.29	1.08
65	Terbium	Tb	[Xe] $4f^8\ 6s^2$	[Xe] f^8	-2.30	1.06
66	Dysposium	Dy	[Xe] $4f^9\ 6s^2$	[Xe] f^9	-2.29	1.05
67	Holmium	Ho	[Xe] $4f^{10}\ 6s^2$	[Xe] f^{10}	-2.33	1.04
68	Erbium	Er	[Xe] $4f^{11}\ 6s^2$	[Xe] f^{11}	-2.31	1.03
69	Thulium	Tm	[Xe] $4f^{12}\ 6s^2$	[Xe] f^{12}	-2.31	1.02
70	Ytterbium	Yb	[Xe] $4f^{13}\ 6s^2$	[Xe] f^{13}	-2.22	1.01
71	Lutetium	Lu	[Xe] $4f^{14}\ 5d^1\ 6s^2$	[Xe] f^{14}	-2.30	1.00

As the lanthanide series is ranged from lanthanum to lutetium, the atomic and ionic radius decrease monotonously (lanthanide contraction). The 4*f* electrons are inner electrons in the sense that the maximum of their charge density functions is well inside the outermost electrons ($5s^2 5p^6$), thus they are shielded from the surroundings of the lanthanide ion. The 5*s* and 5*p* orbitals, however, penetrate the 4*f* subshell and thus are not shielded from the increasing nuclear change, leading to a diminution of the ionic size in the lanthanide series, called lanthanide contraction.[5]

Because of the lanthanide contraction, the physico-chemical properties of the lanthanides change monotonously and their separation is quite difficult and requires special technics (selective reduction, ion-

exchange and solvent extraction methods). In lanthanide compounds, the oxidation state of lanthanide ions is predominantly +3. Some exceptions exist, because of the extra stability of the empty (Ce(IV)), semi-occupied (Eu(II)) and fully occupied (Yb(II)) *f*-orbitals.

The coordination chemistry of trivalent lanthanides exhibits some variability across the series, but this variability is much less pronounced than that found for the transition metal ions. Lanthanides form various complexes with high coordination numbers (from 7 to 12), among these the most common are 8 and 9 (for example aqua complexes). The bonds in their binary and coordination compounds are predominantly ionic. They tend to form complexes with decreasing coordination number across the series as the radius of the lanthanide ion decreases. Since trivalent lanthanide ions are hard metal ions, they have a preference for hard donor atoms (such as O and F), in the order of the electronegativities. The geometries found for the lanthanide complexes are quite varied, being determined principally by ligand conformation, ligand donor group-donor group interaction, competition between ligand donor groups and solvent molecules for the available coordination sites, and in some cases, the size of the Ln^{III} ion is also important. In general, lanthanide complexes are quite labile, especially those formed with monodentate ligands, and undergo rapid ligand-exchange reactions.

Stable lanthanide complexation is expected with multidentate ligands (open chained, or macrocycles) containing O- and/or N-donor atoms (amino-acids, polyamino-polycarboxylates, crown-ethers, cryptands).

Except La(III) (f^0) and Lu(III) (f^{14}), lanthanide ions contain unpaired *f* electrons, so they are paramagnetic. The magnetic properties of a given ion are largely independent of the coordination environment. In contrast to the transition metal analogues, lanthanide complexes have sharp line-like

electronic spectra which show little dependence on the ligand. The transitions of the *f*-electrons are responsible for the well-known photophysical properties of the lanthanide ions, such as long-lived luminescence and sharp absorption and emission lines. The *f-f* electronic transitions are forbidden, leading to long excited state lifetimes and low extinction coefficients. These magnetic and electronic properties are characteristic of each lanthanide ion. The lanthanides are chemically similar, but have specific magnetic and photophysical properties.[7]

II. 2. Gd-based contrast agents

The longitudinal and transverse relaxation times of water protons (T_1 and T_2) can be reduced with paramagnetic metal ions containing several unpaired electrons (Mn^{2+}, Fe^{3+}, Eu^{2+}, Gd^{3+}). The effect of Gd^{3+} ion is the most expressed, given its seven unpaired electrons, large magnetic moment and suitable, slow electronic relaxation time (10^{-9} s). Unfortunately, Gd^{3+} has no biological role and thus it is highly toxic for living organisms. To prevent the presence of free Gd^{3+} *in vivo*, a number of multidentate ligands have been developed and investigated for stable complexation of Gd^{3+}. Since lanthanides form predominantly ionic bonds in their complexes, linear or macrocyclic ligands with O- and N-donor atoms are used for the encapsulation of Gd^{3+}. The ligands used in practice are octadentate and all eight donor atoms are coordinated to the metal ion, the remaining 1 (or 2) coordination site of Gd^{3+} is occupied by water molecule(s).

In MRI experiments, contrast agents are used in relatively large dose (0.1-0.3 mmol/kg body weight in general) in order to obtain images with high contrast. The Gd(III) chelates, when used as contrast agents, are injected

intravenously and distribute mainly to the extracellular spaces. The excretion of contrast agents from the body is fast ($t_{1/2}$= 1.5-2.0 h) and the way of excretion depends on the structure of the ligand used for complexation.

The first Gd(III) complex approved for MRI applications was $Gd(DTPA)^{2-}$ (1988).[8,9] This was followed soon by the kinetically more inert, macrocyclic $Gd(DOTA)^{-}$[9] and later by Gd(III) complexes of DTPA or DOTA derivatives. These complexes have negative charge and sometimes cause pain in the patients upon injection. To avoid this effect, neutral contrast agents have been developed: Gd(DTPA-BMA), Gd(HP-DO3A), Gd(DO3A-B) and Gd(DTPA-BMEA). The commercially available contrast agents listed above are hydrophilic and excrete from the body through the kidneys.[10] The investigation of the blood pool, the brain and the liver requires contrast agents containing lipophilic groups such as Gd(EOB-DTPA) and Gd(BOPTA).[11] Because of the presence of the lipophilic groups, these complexes remain in the body longer time and excrete mainly through the liver. Exploring new contrast agents showing organ specificity is of great interest of recent research.

As mentioned above, safety is indispensable for *in vivo* application of Gd(III) complexes. The complexes must stay intact in the body fluids and not dissociate to free gadolinium ion and ligand, both toxic alone. The most important criteria for the safe *in vivo* application are the high thermodynamic stability and kinetic inertness of the applied complexes.

II. 3. Thermodymanic stabilities

The thermodynamic stability of an ML complex can be expressed by the equilibrium constant of the formation reaction of the complex, K_{ML}, called stability constant:

$$K_{ML} = \frac{[ML]}{[M][L]} \quad \text{(II.1)}$$

where [M], [L] and [ML] are the equilibrium concentrations of free metal ion, deprotonated ligand, and complex, respectively.

Since the complex formation is a competitve reaction between the metal and hydrogen ions for the free ligand, the protonation constants of the ligand, K_i, are also necessary for the calculation of the complex stability constant:

$$K_i = \frac{[H_iL]}{[H_{i-1}L][H^+]} \quad \text{(II.2)}$$

On the other hand, complexes formed with polyamino-polycarboxylate and other multidentate ligands might be protonated at low pH, which can be characterized by the protonation constant of the complex:

$$K_{MH_iL} = \frac{[M(H_iL)]}{[M(H_{i-1}L][H^+]} \quad \text{(II.3)}$$

For linear or macrocyclic polyamino-polycarboxylate ligands, the protonation order of the donor groups have been often investigated by ^{1}H-NMR spectroscopy.[12] It was evidenced that the protonation occurs first at the amino-nitrogen atom(s) and then at the less basic carboxylate oxygens.

Lanthanide ions tend to form stable complexes mainly with multidentate ligands containing ionic O- and N-donors. Thus, in general, substitution of one or more carboxylate groups of the ligand by non-charged donors causes a decrease in the complex stabiliy. Comparison of the stability

constants of complexes formed between lanthanides and open chain or macrocyclic ligands clearly shows that macrocyclic ligands form thermodynamically more stable complexes. The complex stabilites are further influenced by many parameters (steric factors, size of the lanthanide ion and the ligand, the number of donor atoms, etc.). Consequently, it is often difficult to draw general tendencies or rules to predict complex stabilities.

Complex stability constants are most often determined by pH-potentiometric titration of the ligand in the absence and presence of the metal ion. This method can be used only when the equilibrium is reached rapidly, which is generally true for linear ligands. In most of the cases, the formation of macrocyclic complexes – DOTA and its derivatives – is a slower process, therefore a batch method is used instead of direct titration.[13,14,15]

It is important to find a correlation between complex stability and *in vivo* toxicity in order to predict whether the complex is a potentially safe contrast agent or not. First, a high thermodynamic stability is required, however, alone, it is not enough for the safe use. One has to take into account that the body fluids are very complex systems from the chemical point of view. The free metal ion, the free ligand or the complex itself can participate in many side reactions under *in vivo* conditions. Among these, the most important are the protonation of the free ligand, its interaction with endogenous metal ions (Mg^{2+}, Ca^{2+}, Zn^{2+}, Cu^{2+}, etc.), the complexation of free Gd^{3+} by different ligands existing in the plasma (citrate, phosphate, hydrogen-carbonate, transferrin, oxalic acid, etc), and the interaction of the Gd(III) complex with small ligands like carbonate, phosphate, dicarboxylic acids, etc. to form ternary complexes. These potential side reactions can be included into another constant, the so-called conditional stability constant, K^*,[16] which describes the stability of the complex under the given conditions

(pH, given concentration of other potential ligands and metal ions in the system).

In order to simulate the coordination equilibria in the blood plasma, May *et al.*[17] proposed a plasma model involving seven metal ions (Mg^{2+}, Ca^{2+}, Mn^{2+}, Fe^{3+}, Cu^{2+}, Zn^{2+} and Pb^{2+}) and fourty low molecular weight ligands (amino acids, dicarboxylic acids, carbonate, phosphate, citrate, lactate, etc.) in a complex equilibrium including ca. 5000 binary and ternary compounds. From this model, Jackson *et al.*[18] estimated the species distribution in the presence of Gd(DTPA). Cacheris *et al.*[19] used a simpler plasma model to calculate the amount of Gd(III) released from $Gd(DTPA)^{2-}$, Gd(DTPA-BMA), and $Gd(EDTA)^{-}$ by using the previously determined conditional stability constanst of the different species. They concluded that the released Gd^{3+} is most likely coordinated to citrate and only negligibly to amino acids or albumin. Based on a simple model, Brücher *et al*. also concluded the citrate coordination of the free Gd^{3+}, liberated from $Gd(DTPA)^{2-}$ by transmetalation reaction with Zn^{2+}.[20]

II. 4. Dissociation kinetics of Gd(III) complexes

The kinetic inertness of the Gd(III) complex depends on the rate of the exchange reactions that may take place in the plasma. The most important one is probably the displacement of Gd^{3+} by the endogenous metals, like Cu^{2+} and Zn^{2+}.[21] This may occur *via* the direct attack of the endogenous metal on GdL, or via the proton-assisted dissociation of the complex, followed by the fast reaction of the ligand with the endogenous metal ion. Ligand exchange reactions between GdL and ligands present in the blood plasma are usually considered to be of low probability. In the last decades, Brücher *et al*. have

published a number of papers relating to the understanding of the dissociation of MRI related Gd(III) complexes.[22] Nowadays it is clear that the dissociation kinetics of macrocyclic and linear lanthanide complexes differ markedly, as the rigidity of macrocyclic complexes leads to significantly slower dissociation kinetics.[20] In the case of $Gd(DTPA)^{2-}$, which is probably the most widely used MRI contrast agent today, a complete kinetic model has been established in order to describe the dissociation of the complex in body.[23] The excretion and the dissociation of $Gd(DTPA)^{2-}$ are regarded as parallel, first-order processes, and by using the kinetic data obtained *in vitro* from the exchange reactions with endogenous Cu^{2+} and Zn^{2+}, the amount of the dissociated complex molecules in the plasma might become calculated at any time after the intravenous injection.

II. 5. Formation kinetics of Ln(III) complexes

There are noteworthy differences between the formation kinetics of lanthanide complexes occurring with linear and macrocyclic ligands. Macrocyclic ligands tend to form complexes much more slowly.[21] The rate of complex formation has been found particularly low for lanthanide complexes of the marcocyclic DOTA. Recently, higher formation rates were determined and reported for the corresponding lanthanide complexes with the 14-membered TETA ligand.[23] The slow complex formation led to discrepancies in complex stability constants obtained by different authors for $Ln(DOTA)^-$ chelates. Moreover, the slow formation kinetics can be a disadvantage, if macrocyclic ligands are used to complex radioactive lanthanides (^{153}Sm, ^{90}Y) in radiopharmaceutical applications. A number of publications have appeared

so far on the complexation kinetics between the macrocyclic ligand DOTA, and the trivalent lanthanide ions, starting with the report of Kasprzyk and Wilkins.[24] This was followed by the reports of Brücher, *et al.*,[25] Wang *et al.*,[26] Kumar and Tweedle,[27] Tóth *et al.*,[22] and Wu and Horrocks.[28] Each of these authors came to similar conclusions about the mechanism of complex formation, differing only in minor specifics. The free ligand has all four acetate pendant arms extended above the plane of the four nitrogens atoms, thus it is rational to conclude that the acetates provide an electrostatic charge potential to charm the lanthanide cation toward the ligand cavity. It is evident that a weak intermediate complex is formed initially between the negatively charged DOTA ligand and the trivalent lanthanide ion, and the rate of this process is similar to those obtained for linear ligands, like DTPA. This weak complex formation is followed by a slow, pH-dependent rearrangement of intermediate to form a final complex, which is orders of magnitude more stable than the initial complex.

The main difference between these kinetic studies was a disagreement about the number of protons attached to the macrocyclic nitrogens, and whether a nitrogen atom is coordinated in the initially formed weak ML complex, or not. Tóth *et al.* proved by spectrophotometry and direct potentiometric titration that the kinetically stable intermediate is diprotonated ($Ln(H_2DOTA)^+$), likely with the H^+'s attached to two macrocyclic nitrogen atoms in trans positions (as found in the crystal structure of the diprotonated ligand) and the Ln^{3+} coordinated only to the extended acetates. The rate of the conversion of the so-called out-of-cage complex, ($Ln(H_2O)_5LH_2^+$), to the in-cage ($Ln(H_2O)L^-$) complex is greatly pH-dependent. In the mechanism proposed by Wu and Horrocks,[28] OH^- catalyzed removal of a single proton from $Ln(H_2O)_5LH_2^+$ is included as a first step to form the neutral compund, $Ln(H_2O)_5LH$. Burai *et al.*[29] tested this hypothesis with the use of ligand

excess and measuring the kinetics of complex formation at higher pH values, when the $Ln(H_2O)_5LH$ species predominates. They have not found any confirmation for the OH^- catalyzed removal of the first proton, but found strong evidence for OH^- catalyzed removal of the second proton. The protonation constants for the formation of $Ce(H_2O)_5LH_2$ and $Yb(H_2O)_5LH_2$ were found to be $4.4 \pm 0.5 \times 10^8$ M^{-1} ($\log K_{CeHL} = 8.64$) and $2.5 \pm 1.4 \times 10^8$ M^{-1} ($\log K_{YbHL} = 8.40$), respectively. These values are considerably lower, than the second protonation constant of DOTA ($\log K_{HL} = 9.67$), consistent with the expectation of the electrostatic repulsion between the Ln^{3+} and nitrogen-bound H^+ in the out-of-cage $Ln(H_2O)_5LH$ compounds. It has been proposed that the rate determining step in the formation of in-cage $Ln(DOTA)^-$ complexes is the deprotonation of the monoprotonated intermediate, $Ln(H_2O)_5LH$. Deprotonation is assisted by Brönsted bases like H_2O, OH^-, or a deprotonated buffers. The mechanistic details of how these protons are catalytically removed from the $Ln(H_2O)_5LH_2^+$ and $Ln(H_2O)_5LH$ species to form the stable, $Ln(H_2O)L^-$ species has not been described yet, but it is now clear that the rate determining step in the formation of this stable chelate is the deprotonation of the monoprotonated species.

II. 6. T_1 and T_2 relaxation, optimization the parameters of CAs

The design of new, more efficient MRI contrast agents requires the detailed understanding of the parameters and mechanisms of water proton relaxation processes.[30,31,32] According to the Solomon-Bloembergen-Morgan theory, which describes the solvent nuclear relaxation in presence of paramagnetic species, a contrast agent will induce an increase of the longitudinal and transversal relaxation rates, $1/T_1$ and $1/T_2$ respectively, of the

surrounding water protons. On Magnetic Resonance images, the increase of $1/T_1$ will lead to an enhancement of the signal (increased brightness), whereas the increase of $1/T_2$ will result in a decreased signal (dark spot). Since in the practice a signal enhancement is easier to detect than a signal decrease, and Gd^{III} is leading to positive contrast, here the discussion will regard T_1-contrast agents only.

The efficiency of a contrast agent is described with its relaxivity (r_1), which is defined as the enhancement of the longitudinal relaxation rate of the water protons per a given concentration (generally millimolar) of the paramagnetic compound (Eq II. 4).

$$\frac{1}{T_{1,obs}} = \frac{1}{T_{1,d}} + r_1[Gd^{3+}] \qquad \text{(II. 4)}$$

where $1/T_{1,obs}$ represents the observed solvent relaxation rate and $1/T_{1,d}$ is the diamagnetic relaxation rate which corresponds to the relaxation rate of the solvent nuclei in the absence of the paramagnetic compound.

The relaxivity can be divided into the sum of two different contributions: the so-called inner sphere, and outer sphere relaxivity, r_1^{IS} and r_1^{OS}, respectively (Eq II. 5).

$$r_1 = r_1^{IS} + r_1^{OS} \qquad \text{(II. 5)}$$

The inner sphere contribution arises from the effect that the magnetic field, caused by the unpaired electrons of the metal ion, has on the protons of the water molecule(s) in the first coordination sphere of the complex, while the outer sphere contribution comes from the interactions between the

electron spin of the metal and the bulk solvent molecules that diffuse in the environment of the paramagnetic compound (Scheme II.1).

Since the outer sphere relaxivity depends mainly on the random translational diffusion, it is hard to control. On the other hand, it is possible to modify the factors influencing the inner sphere relaxivity and this can lead to a considerable growth of this contribution.

The inner sphere relaxivity can be calculated with Eq II. 6,

$$r_1^{IS} = \frac{cq}{55.5}\left(\frac{1}{T_{1m} + \tau_m}\right) \qquad \text{(II. 6)}$$

where c is the molar concentration, q is the number of bound water molecules per Gd^{III}, τ_m is the life-time of the water molecule in the inner sphere of the complex (equal to the reciprocal water exchange rate, $1/k_{ex}$) and T_{1m} is the relaxation time of the bound water protons. T_{1m} is dependent on the rotational correlation time (τ_R), the electron spin relaxation times (T_{1e} and T_{2e}) and the exchange rate of the inner sphere water (k_{ex}).

In the case of some paramagnetic complexes, water molecules not directly bound in the first coordination sphere may also remain in the proximity of the paramagnetic metal for a relatively long time, e. g. due to hydrogen bridges to the ligand, or to the water molecule(s) in the first coordination sphere. The contribution of the relaxivity enhancement from these interactions is called second-sphere relaxivity, and can be described with the same theory that is used for the inner-sphere term. However, this contribution is frequently negligible, or its effect is taken into account just in the outer-sphere term.

It is evident from the Equation (II. 6) which parameters should be modified in order to enhance relaxivity:

- ***q**:* the inner sphere relaxivity is directly proportional to the number of inner sphere water molecules, *q*. However, we need to find a balance between the efficiency and safe use, because increasing *q* might lead to a decrease of the stability of the metal complex. The complex needs to be sufficiently stable and not to dissociate until its complete excretion from the body.
- k_{ex}**:** the exchange rate between the bound water molecules and the solvent water molecules has to be within an optimal value. If the water exchange is too slow, the paramagnetic effect will not be properly transmitted to the solution; if it is too fast, the bound water molecule will not have enough time to feel the paramagnetic effect of the metal ion.

- T_{1e} **and** T_{2e}**:** it is clear that both the longitudinal and transverse electronic relaxation times influence the relaxivity, however, so far very little success has been achieved in trying to relate this effect to the structural features of the ligands.

- τ_R**:** the rotational correlation time, describing the tumbling of the Gd-water proton vector, is the most important parameter which limites the relaxivity of the small molecules currently used as commercial contrast agents.[33]

In the past few years, a variety of approaches has been tried to increase τ_R, mainly involving in the synthesis of higher molecular weight ligands primarily through the attachment of the poly(amino carboxylate) chelate to macromolecules, such as proteins[34], micelles[35], and dendrimers[36].

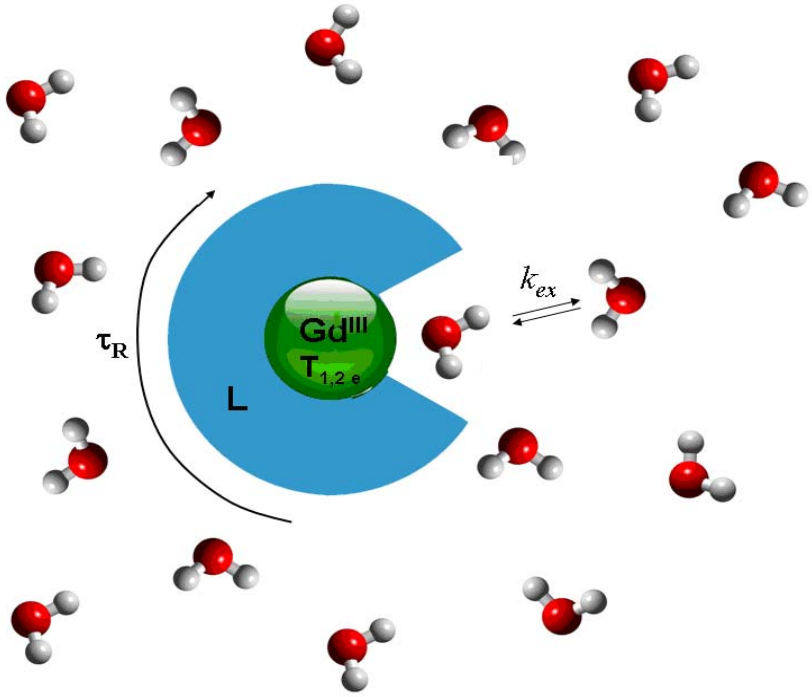

Scheme II. 1. Scheme of the parameters influencing the relaxation of a paramagnetic Gd^{III} complex

All parameters and factors mentioned above should be taken into account in exploring of new ligands and in designing new, highly efficient contrast agents. According to the Solomon-Bloembergen-Morgan theory, a simultaneous optimization of all these parameters could lead to relaxivities of about 100 $mM^{-1}s^{-1}$ (at 20 MHz), while the relaxivities of current contrast agents are in the range of 4-5 $mM^{-1}s^{-1}$.

The determination of the structural and dynamic parameters contributing to the observed relaxivity of Gd^{III} complexes is possible through an array of different experimental techniques.

Nuclear magnetic relaxation dispersion (NMRD) profiles, where the relaxivity is measured as a function of the ^{1}H Larmor frequency, provide a picture of the different interaction mechanisms and dynamic processes that affect the relaxivity of the contrast agent. The water exchange rate, electron relaxation parameters and rotational correlation times all influence the NMRD curves. However, due to the high number of parameters affecting the relaxivity, their determination exclusively from the analysis of these curves can lead to discrepancies. Hence, it is necessary to find other techniques that give independent access to one, or more of these parameters.

One of these techniques is ^{17}O NMR, which uses the oxygen of the bound water as a probe. This oxygen is very close to the central Gd, and therefore feels a greater paramagnetic effect than the corresponding hydrogen atoms. By performing variable temperature ^{17}O T_2 measurements supplemented with variable temperature measurements of the chemical shift difference between bulk and bound water ($\Delta\omega_r$), it is possible to precisely determine the water exchange rate on the contrast agent. ^{17}O NMR also provides direct information about the τ_R and q of the Gd^{III} complex. The rotational correlation time can be assessed by performing variable temperature ^{17}O T_1 measurements. On the other hand, the paramagnetic ^{17}O chemical shifts give an indication also about the q value of the complex.

A reliable determination of the microscopic parameters common to NMRD and ^{17}O NMR can be performed through the simultaneous least-squares fitting of all the data obtained during these experiments.

II. 7. New classes of MRI contrast agents

Beside the optimisation of the efficiency (relaxivity) of MRI contrast agents, another important tendency in MRI research is the development of the so-called smart contrast agents. In this case, the paramagnetic complex acts as a reporter that can provide information on biological processes and/or physiological abnormalities. Changes in any physico-chemical parameter in the body, such as metal concentration, pH or enzymatic activity, will be visualized through the changes in the relaxivity of the gadolinium(III) complex. The relaxivity can be modified by changing the number of water molecules directly coordinated to the lanthanide ion, the water exchange rate and the rotational correlation time.

Paramagnetic complexes which show sharply pH-dependent relaxivity in the physiological pH-range are of particular interest, as they might offer a simple way to distinguish between diseased tissues (pH= 6.9) and healthy (pH= 7.4) tissues (pH-responsive contrast agents). Lanthanide complexes of tetraamide cyclen derivative ligands containing phosphonate side chains show an unusual pH-dependence of their relaxivity, increasing from pH 4.0 to 6.0, then decreasing to a minimum relaxivity around pH= 8.5. This effect is credited to the protonation of uncoordinated phosphonate groups, providing a catalytic pathway for exchange process of the water protons between the complex and the bulk. A Gd(DO3A) derivative mimicking phospholipids has been shown to present a marked pH effect: the relaxivity increases up to 142% from pH 6.0 to 8.0. This behaviour is thought to arise from the formation of colloidal aggregates due to the higher lipophilicity of the neutral complex compared to the protonated one, leading to an increase of the rotation time, and thus the relaxivity.[38] Another example of a pH-

responsive potential contrast agent is water-soluble gadofullerenes $Gd@C_{60}(OH)_x$ (x=27) and $Gd@C_{60}[C(COOH)_2]_{10}$.[39]

Since a number of metal ions are essential for life and many diseases have been associated to abnormal metal ion concentration in the body, another important type of smart contrast agents is the group of ion responsive agents. For this, the lanthanide complex has to contain another coordination site, specific to the metal to be detected. This coordination site must have a high selectivity for the metal ion in question in order to avoid undesired responses coming from the interaction with other metal ions. For example, Zn^{2+} has been reported to play an important role in regulating synaptic transmission and cell death. For these reasons, imaging of Zn^{2+} in the extra- and intracellular environment of tissues is of great interest. A DTPA bis-amide Gd(III)-complex containing pyridyl groups was reported to show a relaxivity decrease on the addition of Zn^{2+} with high selectivity against Ca^{2+} and Mg^{2+}. The decrease of relaxivity is due to the fact that Zn^{2+} coordinates to the pyridyl groups blocking the water access to the gadolinium(III).[40]

Another biologically important cation is calcium. Ca^{2+} plays a significant role in signal transduction pathways, where it acts as a second messenger or in neurotransmitter release from neurons and in contraction of all muscle cell types. Calcium is essential in cell physiology, where movements of Ca^{2+} into and out of the cytoplasm function as a signal for many cellular processes. These important biological functions strongly promoted the creation of MRI probes for calcium detection based on gadolinium(III) complexes that generate a Ca^{2+} dependent relaxivity response. These probes have to have two binding sites that can selectively coordinate Gd^{3+} and Ca^{2+} ions, respectively. Gd(DOPTA) was the first contrast agent designed for sensing Ca^{2+} by MRI. It showed an approximately 80 % increase in water proton relaxivity in the presence of calcium ions in

the micromolar concentration range, corresponding to intracellular Ca^{2+} concentrations.[41]

Later, a series of gadolinium(III)-complexes has been published for extracellular Ca^{2+} sensing.[42,43,44] In these systems, the two Gd^{3+}-containing 1,4,7,10-tetraazacyclododecane-1,4,7-triacetic acid (DO3A) units were connected by a BAPTA-, EGTA-, DTPA- or EDTA-derived linker designed for Ca^{2+} binding.

Chemical exchange saturation transfer (CEST) agents represent a new class of MR imaging probes that operate by altering the total water signal intensity rather than by altering the T_1 or T_2 relaxation times of water protons.[45] A CEST agent by definition contains labile protons (-NH, -OH, -SH or H_2O) that exchange with the protons of bulk water. In order for an effect to be observed, the exchange process between two magnetically distinct environments must be slow on the NMR timescale. "Slow" means that the exchange rate (k_{ex}) must not be higher than the difference in frequency between the two chemical environments ($\Delta\omega >> k_{ex}$).

The main advantage of the CEST technique over Gd(III)- based agents is that one can switch the image contrast "on" or "off" at will by gating the RF presaturation pulse. This exclusive feature eliminates the necessity to acquire pre- and post-injection images to determine signal changes, and therefore, minimizes the possible errors due to time delays and motion-induced artefacts. In addition, multiple CEST agents can be administrated simultaneously and each agent can be activated separately by a RF pulse specific for the chemical shift of its mobile protons offering the possibility of multiple detection.

The first CEST agents proposed by Balaban and co-workers were low molecular weight diamagnetic molecules.[45,46] Many of these molecules showed a significant ability to alter the total water signal intensity, but only

at relatively high concentrations (10-100 mM). The chemical shift difference between the two exchanging proton pools in these systems is about 5 ppm. This small $\Delta\omega$ can lead to partial off-resonance saturation of the bulk water and also limits the maximum k_{ex}.

This limiting factor can be overcome by the use of CEST agents that possess exchangeable protons having a much wider range of chemical shifts. Paramagnetic complexes are the best for this purpose. The paramagnetic complexes used as traditional T_1-shortening agents have at least one water molecule coordinated to the metal centre that exchanges relatively rapidly with bulk water. One class of paramagnetic lanthanide complexes that had been ruled out as T_1-shortening agents, because their water exchange was too slow, are complexes formed with tetraamide derivatives of DOTA. The first example of a PARACEST agent was $Eu(DOTAMGly)^-$, a complex with a bound-water exchange peak at about 50 ppm.[47] The protons of the coordinated water molecule are not the only exchangeable protons. The MR frequency of the amide protons are not shifted so strongly as those of the coordinated water molecule in the case of the $Eu(DOTAMGly)^-$ complex, but they are easily detected in the spectra of other lanthanide complexes with DOTAMGly, for example those formed with ytterbium or dysprosium.

The CEST spectrum of lanthanide (Yb, Tm, Er, Ho, Dy, Eu)-DOTAMGly complexes shows strong CEST effect arising from the amide proton exchange at -16, -51, -22, 39, 77 and -4 ppm, respectively.[48]

In addition, it is possible to design combined PARACEST smart contrast agents that are responsible for pH, metabolite concentration, temperature, enzyme concentration etc.[49,50,51,52]

III. Applied experimental methods

III. 1. pH-potentiometric studies

The most important and wide-spread method for describing the equilibrium processes of lanthanide(III) complexes of polyamino-polycarboxylate ligands in solution is pH-potentiometry. The H^+-ion concentration of an aqueous solution containing the metal complex is influenced by the protonation constants of the ligand and the interaction between the metal ion and differentially protonated ligand forms. Thus, the knowledge of ligand protonation constants is essential for the determination of stability constants.

Generally, protonation constants can be described as follows:

$$K_i = \frac{[H_iL]}{[H_{i-1}L][H^+]} \qquad \text{i= 1, 2…} \qquad \text{(III. 1)}$$

Complex stability constants are most often determined by pH-potentiometric titration of the ligand in the absence and presence of the metal ion. This method can be used only when the equilibrium is reached rapidly, which is generally true for linear ligands. In most of the cases, the formation of macrocyclic complexes – DOTA and its derivatives – is a slower process. In these cases the so-called out of cell (or batch) technique is used instead of direct titration. It requires 15-20 individual samples with the same metal ion and ligand concentration, but with different H^+-ion concentration. When the complex formation reactions are finished – days, or sometimes weeks after the preparation of the samples – the equilibrium pHs of the samples are measured. Using the equilibrium pHs and the protonation constants of the

ligand, the concentration of different species in the M-L-H^+ system, and thus the stability constant of the ML complex can be calculated.

Another limiting factor in the application of pH-potentiometry is the accuracy of the measured pH values. Basically, the measurable pH range is approximately 2 < pH < 12. If an equilibrium process is finished before pH=2 (formation of a highly stable chelate), or after pH=12 (protonation of a ligand donor atom), competitive pH-potentiometric methods, or other techniques (^{1}H-NMR, UV-Vis spectrophotometry) are available for equilibrium constant determinations.

III. 2. UV-Vis spectrophotometry

In most of the cases, the absorption spectra of some lanthanide(III) ions (e. g. Ce^{3+}, Eu^{3+}) change with complex formation. Based on this fact, UV-vis spectrophotometry can be used well for the investigation of complex formation and dissociation kinetics, too.

III. 3. ^{1}H-relaxometry

Since the relaxivity of free Gd^{3+} ion and any GdL chelate complex differ considerably, ^{1}H-relaxometry can be used effectively for the determination of dissociation and formation rates of GdL complexes. In general, if there is a process which modifies the number of coordinated water molecules, the relaxivity of the complex changes, and the process can be studied by measuring the water proton relaxation rates.

During complex formation, the number of inner sphere water molecules in the first coordination sphere of Gd^{3+} ion decreases monotonously, which causes the decrease of the measured water proton

relaxivity. In the case of proton assisted dissociation of a GdL complex, or transmetallation reaction between GdL and a given M^{z+} metal ion, free Gd^{3+} ion appears in the solution resulting in an increase of the relaxivity. If an exchange reaction is taking place between GdL and a ligand L', the relaxivity-change depends on the relative relaxivities of the two complexes.

In addition, in some cases the coordination sphere of GdL is not saturated completely by the multidentate L ligand and ternary – or mixed ligand complexes – might be formed with smaller ligands or anions (X). These reactions can be also followed by relaxometry, and the determination of the stability of GdLX might become possible.

III. 4. ^{17}O NMR

Variable temperature ^{17}O NMR measurements are commonly used to assess the parameters describing water exchange and rotational dynamics on Gd^{3+} complexes. From the measured ^{17}O NMR relaxation rates and angular frequencies of the paramagnetic solutions, $1/T_1$, $1/T_2$ and ω, and of the reference, $1/T_{1A}$, $1/T_{2A}$ and ω_A, one can calculate the reduced relaxation rates and chemical shift, $1/T_{1r}$, $1/T_{2r}$ and ω_r, which may be written as in Equations (III.1)-(III.3), where P_m is the molar fraction of bound water, $1/T_{1m}$, $1/T_{2m}$ are the relaxation rates of the bound water and $\Delta\omega_m$ is the chemical shift difference between bound and bulk water.

$$\frac{1}{T_{1r}} = \frac{1}{P_m}\left[\frac{1}{T_1} - \frac{1}{T_{1A}}\right] = \frac{1}{T_{1m} + \tau_m} \qquad \text{(III.1.)}$$

$$\frac{1}{T_{2r}} = \frac{1}{P_m}\left[\frac{1}{T_2} - \frac{1}{T_{2A}}\right] = \frac{1}{\tau_m}\frac{T_{2m}^{-2} + \tau_m^{-1}T_{2m}^{-1} + \Delta\omega_m^2}{(\tau_m^{-1} + T_{2m}^{-1})^2 + \Delta\omega_m^2} \qquad \text{(III.2.)}$$

$$\Delta\omega_{\mathrm{r}} = \frac{1}{P_{\mathrm{m}}}(\omega - \omega_{\mathrm{A}}) = \frac{\Delta\omega_{\mathrm{m}}}{(1+\tau_{\mathrm{m}}T_{2\mathrm{m}}^{-1})^2 + \tau_{\mathrm{m}}^2\Delta\omega_{\mathrm{m}}^2} + \Delta\omega_{os} \qquad \text{(III.3)}$$

$\Delta\omega_{\mathrm{m}}$ is determined by the hyperfine or scalar coupling constant, $A/\hbar$, according to Equation (III.4), where B represents the magnetic field, S is the electron spin and g_{L} is the isotropic Landé g factor.

$$\Delta\omega_{\mathrm{m}} = \frac{g_L\mu_{\mathrm{B}}S(S+1)B}{3k_{\mathrm{B}}T}\frac{A}{\hbar} \qquad \text{(III.4)}$$

The outer sphere contribution to the chemical shift is assumed to be linearly related to $\Delta\omega_{\mathrm{m}}$ by a constant C_{os} [Eq. (III.5)]

$$\Delta\omega_{\mathrm{os}} = C_{\mathrm{os}}\,\Delta\omega_{\mathrm{m}} \qquad \text{(III.5.)}$$

The ^{17}O longitudinal relaxation rates are given by Equation (III.6), where γ_{S} is the electron and γ_{I} is the nuclear gyromagnetic ratio (γ_{S} = 1.76× 10^{11} rad s^{-1} T^{-1}, γ_{I}=-3.626×10^7 rad s^{-1} T^{-1}), r is the effective distance between the electron charge and the ^{17}O nucleus, I is the nuclear spin (5/2 for ^{17}O), χ is the quadrupolar coupling constant and η is an asymmetry parameter:

$$\frac{1}{T_{1\mathrm{m}}} = \left[\frac{1}{15}\left(\frac{\mu_0}{4\pi}\right)^2\frac{\hbar^2\gamma_{\mathrm{I}}^2\gamma_{\mathrm{S}}^2}{r_{\mathrm{GdO}}^6}S(S+1)\right]\times\left[6\tau_{\mathrm{d1}} + 14\frac{\tau_{\mathrm{d2}}}{1+\omega_{\mathrm{S}}^2\tau_{d2}^2}\right]$$
$$+\frac{3\pi^2}{10}\frac{2I+3}{I^2(2I-1)}\chi^2(1+\eta^2/3)\tau_{\mathrm{RO}} \qquad \text{(III.6)}$$

where:

$$\frac{1}{\tau_{di}} = \frac{1}{\tau_{m}} + \frac{1}{\tau_{RO}} + \frac{1}{T_{ie}} \qquad i = 1\,,\,2 \tag{III.7}$$

The τ_{RO} overall rotational correlation time is assumed to have a simple exponential temperature dependence with an E_R activation energy as follows:

$$\tau_{RO} = \tau_{RO}^{298} \exp\left\{\frac{E_R}{R}\left(\frac{1}{T} - \frac{1}{298.15}\right)\right\} \tag{III.8}$$

In the transverse relaxation the scalar contribution, $1/T_{2sc}$, is the most important [Eq. (III. 9)]. $1/\tau_{s1}$ is the sum of the exchange rate constant and the electron spin relaxation rate.

$$\frac{1}{T_{2m}} \cong \frac{1}{T_{2sc}} = \frac{S(S+1)}{3}\left(\frac{A}{\hbar}\right)^2 \tau_{s1} \tag{III.9}$$

$$\frac{1}{\tau_{s1}} = \frac{1}{\tau_{m}} + \frac{1}{T_{1e}} \tag{III.10}$$

The inverse binding time (or exchange rate, k_{ex}) of water molecules in the inner sphere is assumed to obey the Eyring equation [Eq. (III.11)], where $\Delta S^{\ddagger}$ and $\Delta H^{\ddagger}$ are the entropy and enthalpy of activation for the exchange, and k_{ex}^{298} is the exchange rate at 298.15 K.

$$\frac{1}{\tau_{m}} = k_{ex} = \frac{k_B T}{h} \exp\left\{\frac{\Delta S^{\ddagger}}{R} - \frac{\Delta H^{\ddagger}}{RT}\right\} = \frac{k_{ex}^{298} T}{298.15} \exp\left\{\frac{\Delta H^{\ddagger}}{R}\left(\frac{1}{298.15} - \frac{1}{T}\right)\right\} \tag{III.11}$$

The electron spin relaxation rates, $1/T_{1e}$ and $1/T_{2e}$ for metal ions in solution with S > 1/2 are mainly governed by a transient zero-field-splitting mechanism (ZFS). The ZFS term is expressed by Equations (III.12) and (III.13), where Δ^2 is the trace of the square of the transient zero-field-splitting tensor, τ_v is the correlation time for the modulation of the ZFS with the activation energy E_v, and ω_s is the Larmor frequency of the electron spin:

$$\left(\frac{1}{T_{1e}}\right)^{ZFS} = \frac{1}{25}\Delta^2\tau_v\{4S(S+1)-3\}\left(\frac{1}{1+\omega_S^2\tau_v^2}+\frac{4}{1+4\omega_S^2\tau_v^2}\right) \quad \text{(III.12)}$$

$$\left(\frac{1}{T_{2e}}\right)^{ZFS} = \Delta^2\tau_v\left[\frac{5.26}{1+0.372\omega_S^2\tau_v^2}+\frac{7.18}{1+1.24\omega_S\tau_v}\right] \quad \text{(III.13)}$$

$$\tau_v = \tau_v^{298}\exp\left\{\frac{E_v}{R}\left(\frac{1}{T}-\frac{1}{298.15}\right)\right\} \quad \text{(III.14)}$$

IV. Results

IV. 1. Kinetics of the exchange reactions between $Gd(DTPA)^{2-}$, $Gd(BOPTA)^{2-}$ and Gd(DTPA-BMA) complexes and the TTHA ligand

The complexes of gadolinium(III) formed with the octadentate aminopolycarboxylate ligands DTPA, BOPTA and DTPA-BMA (Scheme IV.1.1.) are clinically used contrast agents in magnetic resonance imaging (MRI) to improve the image contrast (H_5DTPA= diethylenetriamine-N,N,N′,N″,N″-pentaacetic acid, H_5BOPTA= 4-carboxyl-5,6,11-tris(carboxymethyl)-1-phenyl-2-oxa-5,8,11-triazatridecane-13-oic acid, H_3DTPA-BMA= DTPA-bis(methylamide).

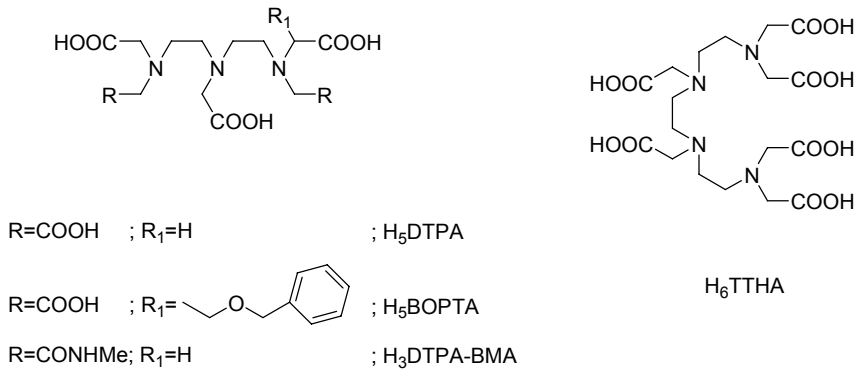

Scheme IV. 1.1. Formulas of the ligands

The contrast agents, injected intravenously, after the distribution in the extracellular space of the body, are eliminated predominantly through the kidneys with a half-time of about 1.5 h.[54,55,56] The elimination of $Gd(BOPTA)^{2-}$ occurs partially through the hepatobiliary system because of

the presence of the lipophilic benzyloxymethyl group. Since both the free Gd^{3+} and the ligands (H_iL) are toxic, the Gd(III) complexes used as contrast agents must have high thermodynamic stability and kinetic inertness.[57] In spite of the strict requirements, numerous experimental data obtained both by animal and human studies, indicate that the excretion of Gd^{3+} from the body is not full.[56,58-62] The amount of the retained Gd^{3+} is generally very low because the elimination of the contrast agents is much faster than their dissociation, which is necessary for the deposition of Gd^{3+}.[59,60] However, the excretion of Gd^{3+} chelates is slower from the body of patients with chronic kidney disease (e. g. dialysed patients), when the half-time of elimination is about 30-40 h.[56] In these cases the amount of retained Gd^{3+} can be higher, which may lead to the development of a newly discovered disease referred to as Nephrogenic Systemic Fibrosis (NSF). The NSF has been observed most frequently in those cases when the contrast agent used was Gd(DTPA-BMA), which has a relatively lower stability constant.[56,63,64] Because of the discovery of NSF, the knowledge of the physico-chemical properties of contrast agents, first of all that of the rate of dissociation, became highly important. The in vivo dissociation of the Gd^{3+} chelates is presumably followed by the reaction of the free Gd^{3+} with some endogenous ligands (e. g. citrate, lactate, etc.), while the free aminopolycarboxylate ligand reacts with the endogenous metal ions, like Zn^{2+}, Cu^{2+} or Ca^{2+}. The dissociation of Gd^{3+} complexes can take place spontaneously and with the assistance of protons, or with the direct attack of the endogenous metals or ligands on the Gd^{3+} complex. Of these reactions the spontaneous and proton assisted dissociation of complexes are generally very slow at physiological pH. The kinetic inertness of Gd^{3+} chelates has been characterized and compared with the proton assisted dissociation rates determined in 0.1 M HCl.[56] More detailed information was obtained for the kinetics of dissociation in the studies on the

rates of metal exchange reactions, occuring between the Gd^{3+} complexes and Eu^{3+}, Cu^{2+} or Zn^{2+} ions in the pH range 3-6. The circumstances of these studies were far from the physiological conditions, moreover the role of the small endogenous ligands in the reactions has not been investigated.[65-69] The possible role of ligand exchange reactions in the *in vivo* dissociation of the Gd^{3+} aminopolycarboxylates has not been studied, probably because the stability constants of the Gd^{3+} complexes formed with the small endogenous ligands are relatively low. However, it was raised that some of the high molecular mass proteins, first of all transferrin may play some role in the dissociation of Gd^{3+} chelates by displacing the aminopolycarboxylate ligand, but the rates of such ligand exchange reactions have not been studied.[63,70]

Ligand exchange reactions can take place during the spectrophotometric determination of Ca^{2+} in serum, if the samples were taken within the first 12-24 h after MRI examinations, performed with Gd(DTPA-BMA) (Omniscan) as contrast agent. For the determination of Ca^{2+} o-cresolphtaleine complexone or methylthymol blue is used, which can displace the DTPA-BMA ligand in the Gd(DTPA-BMA) complex, leading to an apparent decrease in the serum Ca^{2+} level.[71,72] Similar interference was not observed when $Gd(DOTA)^-$ (H_4DOTA= 1,4,7,10-tetraazacyclododecane-1,4,7,10-tetraacetic acid) or $Gd(DTPA)^{2-}$ was used as contrast agent, because the stability constants of these complexes are significantly higher than that of Gd(DTPA-BMA).

The experiments reported by Puttagunta et al. show that the ligand exchange reaction between Gd(DTPA-BMA) and DTPA at 20 mM concentrations, at pH= 7.4 can take place with the release of about 85 % of DTPA-BMA within 2 h. The kinetics of the exchange reactions was not investigated.[73]

Recently a nanostructure silica material, functionalized with 1-hydroxy-2-pyridinone ligand, has been proposed as a sorbent to remove the Gd^{3+} from the blood of dialysed patients, examined by MRI with the use of Gd^{3+} containing contrast agent. The 1-hydroxy-2-pyridinone, bound to the silica, can remove the Gd^{3+} from the Gd(DTPA-BMA) complex. This reaction can also be regarded as a ligand exchange reaction.[74]

In order to obtain information about the kinetics and mechanisms of the ligand exchange reactions of the Gd^{3+} aminopolycarboxylates, we have studied the rates of reactions taking place between the $Gd(DTPA)^{2-}$, $Gd(BOPTA)^{2-}$ and Gd(DTPA-BMA) complexes and the ligand TTHA (Scheme IV.1.) (H_6TTHA=triethylenetetraamine-hexaacetic acid) as model reactions. The stability constant of $Gd(TTHA)^{3-}$ ($\log K_{GdL}$=23.83) is higher than that of $Gd(DTPA)^{2-}$ ($\log K_{GdL}$= 22.46), $Gd(BOPTA)^{2-}$ ($\log K_{GdL}$= 22.59) or Gd(DTPA-BMA) ($\log K_{GdL}$= 16.85)[75,76], and as the species distribution calculations show, the exchange reactions take place practically completely at pH>6.5 in the presence of tenfold TTHA excess. (The charges of ligands and complexes will be used only, when it is necessary.) These ligand exchange reactions could be studied in a broad pH range (6.5< pH< 11) where the hydrolysis of Gd^{3+} did not take place because of the presence of ligand excess. The effect of the presence of small endogenous ligands (citrate, phosphate and carbonate) on the rates of ligand exchange reactions was also investigated in order to obtain information about the role of these ligands in the dissociation of Gd^{3+} complexes.

The ligand exchange reactions taking place between the $Gd(DTPA)^{2-}$, $Gd(BOPTA)^{2-}$ and Gd(DTPA-BMA) complexes and the chelating agent TTHA can be described by Equation (IV.1.1):

$$GdL + H_iTTHA^{(6-i)-} = Gd(TTHA)^{3-} + H_jL + (i-j)H^+ \qquad \text{(IV.1.1)}$$

where the charges of the species GdL and H_jL are not indicated due to the different charges of the ligands.

The rates of the ligand exchange reactions of $Gd(DTPA)^{2-}$ and $Gd(BOPTA)^{2-}$ have been studied in the pH range 6.5-11. The reactions between Gd(DTPA-BMA) and TTHA were found to be relatively fast at pH> 9, so the rates of these reactions had been studied from pH 6.5 to 9. The study of the reaction rates was performed at pH≥ 6.5, because at pH< 6.5 protonated $Gd(HTTHA)^{2-}$ complex could be formed (the protonation constant of $Gd(TTHA)^{3-}$ is $\log K_{GdHX}= 4.73$[75]), which has a higher relaxivity than $Gd(TTHA)^{3-}$.

The rates of the reactions (IV.1.1) have been studied in the presence of TTHA excess, in order to ensure pseudo-first-order conditions. Since the reactions are first-order as regards the complexes GdL, the rates of the ligand exchange can be expressed as follows:

$$-\frac{d[GdL]}{dt} = k_p[GdL] \qquad \text{(IV.1. 2)}$$

where k_p is a pseudo-first-order rate constant and [GdL] is the concentration of the $Gd(DTPA)^{2-}$, $Gd(BOPTA)^{2-}$ or Gd(DTPA-BMA).

In order to obtain the rate law for the ligand exchange reactions, the pseudo-first-order rate constants have been determined at different TTHA and hydrogen ion concentrations. The k_p values determined at physiological pH by the variation of the TTHA concentration, are presented in Figure IV. 1.1.

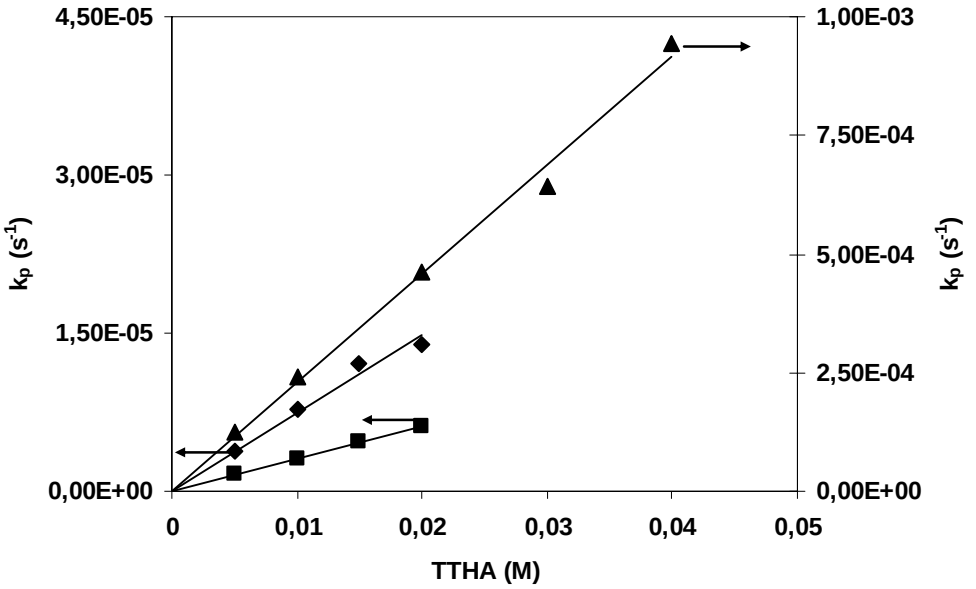

Figure IV.1.1. Dependence of the k_p values, characterizing the rates of the exchange reactions of $Gd(DTPA)^{2-}$ (♦) $Gd(BOPTA)^{2-}$ (■) and Gd(DTPA-BMA) (▲) on the TTHA concentration (pH= 7.4, [GdL]= $1x10^{-3}$ M, 25 ^{o}C, 0.15 M NaCl).

The ligand TTHA is present in different protonated forms in the pH range investigated. The study of the reaction rates as a function of pH gives information about the role of the differently protonated $H_iTTHA^{(6-i)-}$ species in the exchange reactions. The k_p values obtained at different pH-s are shown in Figures IV.1.2 and IV.1.3., where the squares, triangles and diamonds indicate the the experimental k_p data, while the curves show the k_p values calculated with the use of the obtained rate constants (Table IV. 1.1.).

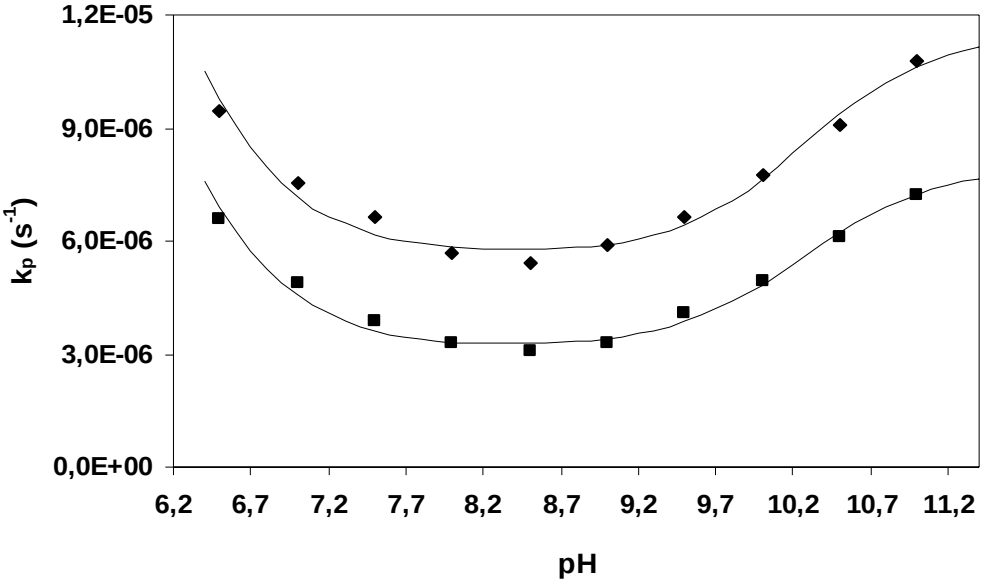

Figure IV.1.2. pH dependence of the k_p values characterizing the rates of exchange reactions between $Gd(DTPA)^{2-}$ (♦), $Gd(BOPTA)^{2-}$ (■) and TTHA ([GdL]= $1x10^{-3}$ M, [TTHA]= $1x10^{-2}$ M, 25 ^{o}C, 0.15 M NaCl).

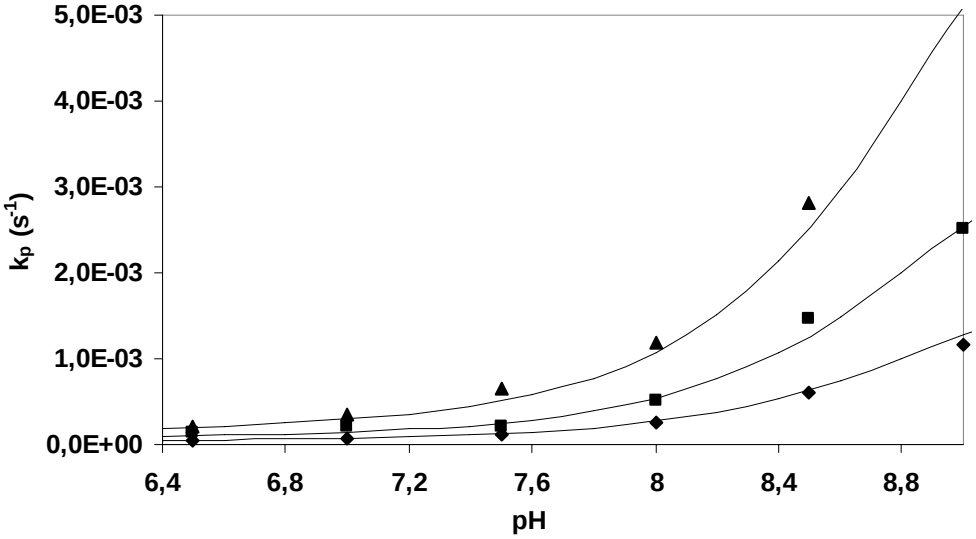

Figure IV.1.3. pH dependence of the k_p values characterizing the rates of exchange reactions between Gd(DTPA-BMA) and TTHA ([GdL]= $1x10^{-3}$ M,

[TTHA]= $5x10^{-3}$ M (♦) , $1x10^{-2}$ M (■) and $2x10^{-2}$ M (▲), 25 ^{o}C, 0.15 M NaCl).

The effect of the endogenous citrate, phosphate and carbonate ions on the rates of ligand exchange reactions has been studied at physiological pH. At pH= 7.4 the citrate is present as fully deprotonated cit^{3-} ligand, while for the phosphate and carbonate the species HPO_4^{2-} and HCO_3^- predominate, respectively. The rate constants, k_p, determined as a function of the total citrate, phosphate and carbonate concentrations are presented in Figures IV.1.4-6.

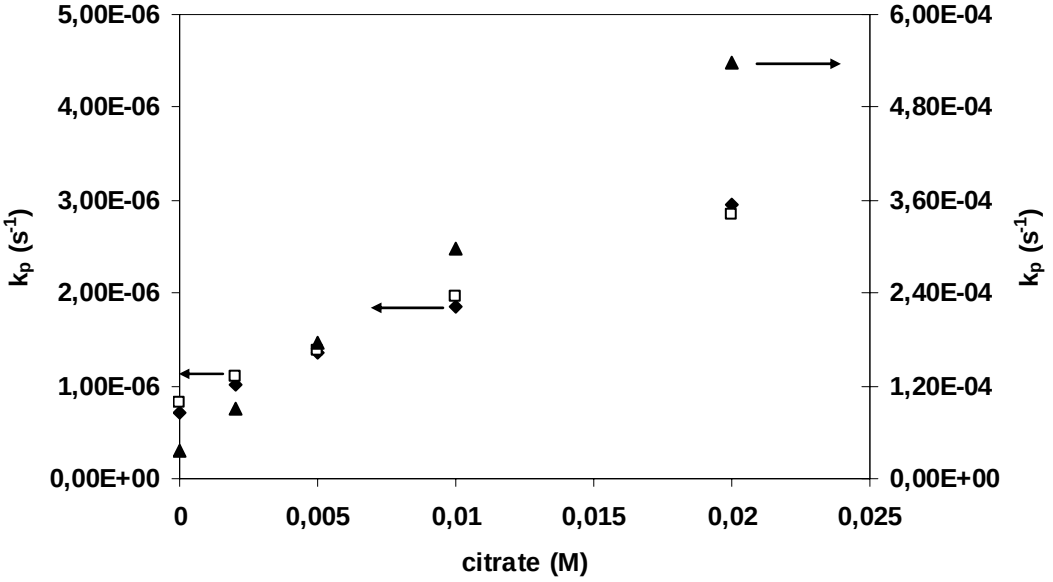

Figure IV.1.4. Dependence of the k_p values on the citrate concentration for the exchange reactions of $Gd(DTPA)^{2-}$ (♦), $Gd(BOPTA)^{2-}$ (□) and Gd(DTPA-BMA) (▲) (pH= 7.4, [GdL]= $1x10^{-3}$ M, [TTHA]= $2x10^{-3}$ M, 25 ^{o}C, 0.15 M NaCl).

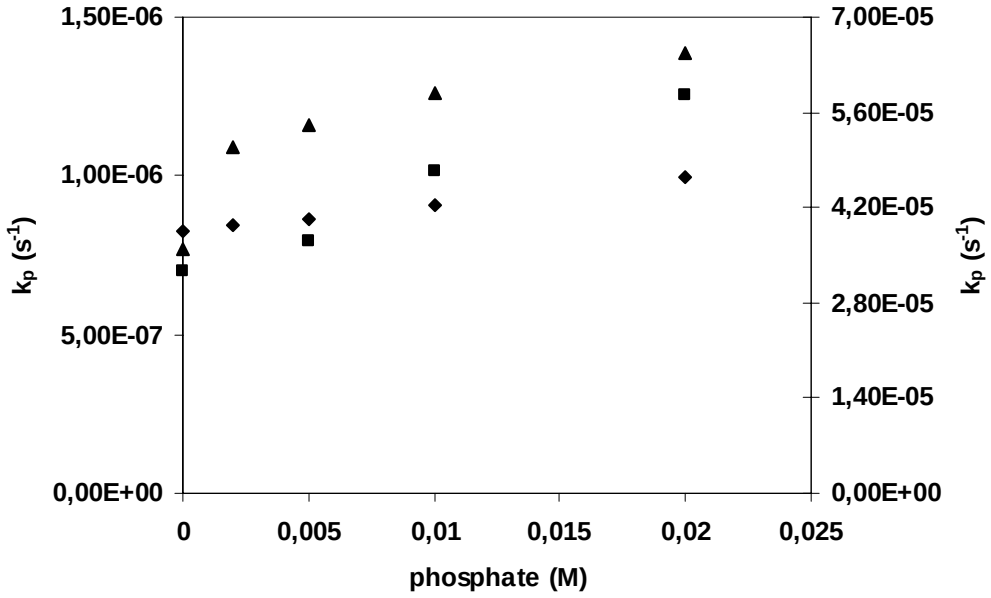

Figure IV.1.5. Dependence of the k_p values on the phosphate concentration for the exchange reactions of $Gd(DTPA)^{2-}$ (♦), $Gd(BOPTA)^{2-}$ (■) and Gd(DTPA-BMA) (▲) (pH= 7.4, [GdL]= $1x10^{-3}$ M, [TTHA]= $2x10^{-3}$ M, 25 ^{o}C, 0.15 M NaCl).

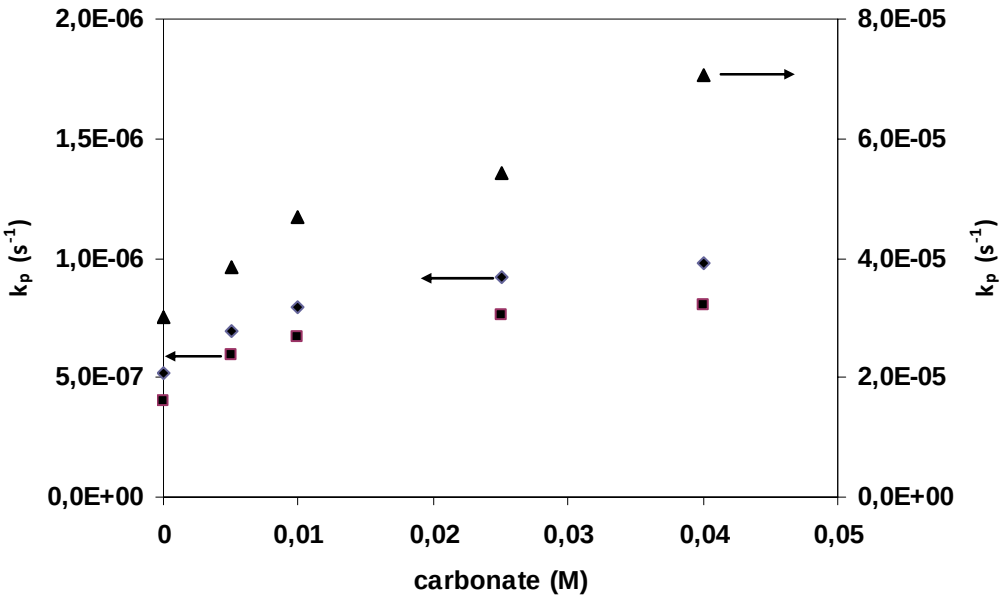

Figure IV.1.6. Dependence of the k_p values on the carbonate concentration for the exchange reactions of $Gd(DTPA)^{2-}$ (♦), $Gd(BOPTA)^{2-}$ (■) and Gd(DTPA-BMA) (▲) (pH= 7.4, [GdL]= $1x10^{-3}$ M, [TTHA]= $2x10^{-3}$ M, 25 ^{o}C, 0.15 M NaCl).

For obtaining well observable rate effects for the endogenous citrate, phosphate and carbonate ions, a lower TTHA excess was used (2 mM), but in these cases the pseudo-first-order rate constants were calculated from the data, obtained for the first 40-50 % conversion of the reactions.

The exchange reactions taking place between the complexes $Gd(DTPA)^{2-}$, $Gd(BOPTA)^{2-}$ and Gd(DTPA-BMA) and the ligand TTHA are very slow at pH values around 7.5-8.5, as it is seen from the rate data presented in Figures IV.1.2. and IV.1.3. The half-life of the exchange reaction for the $Gd(DTPA)^{2-}$ calculated from the k_p value obtained at pH= 8.5 is 36 h, so the reactions had to be followed for a few days.

The ligand exchange reactions in principle can take place with the spontaneous and proton assisted dissociation of complexes, which is followed by the fast reaction between the free Gd^{3+} and TTHA. The other possible pathway is the direct attack of the TTHA on the Gd^{3+} complex, when the TTHA displaces the DTPA, BOPTA or DTPA-BMA ligands from the GdL complexes.

As it is seen in Figure IV.1.1., the k_p values characterizing the rates of ligand exchange reactions, are directly proportional to the total concentration of TTHA. The linear dependence of the first-order rate constants on the TTHA concentration shows that the exchange reactions occur with the participation of the TTHA, presumably with the direct attack of the differently protonated $H_iTTHA^{(6-i)-}$ species on the GdL complexes. On the basis of the direct proportionality between the k_p values and the total

concentration of TTHA ($[TTHA]_t$), the first order rate constants can be expressed as follows:

$$k_p = k_0 + k_L [TTHA]_t \qquad \text{(IV.1. 4)}$$

where k_0 is characteristic for the spontaneous and proton assisted dissociation of the GdL complexes, while k_L characterizes the rates of reactions, occurring with the direct encounter of the $H_iTTHA^{(6-i)-}$ species and the GdL complexes. The k_0 and k_L values have been calculated from the k_p and $[TTHA]_t$ values, presented in Figure IV.1.1. by the least square method. The k_0 values are very low, lower than the calculated errors, so the term, k_0 in Equation (IV.1.4) can be neglected. The rates of the proton assisted dissociation of the GdL complexes can be calculated from the rate data known from the results of the kinetic studies on the metal exchange reactions, taking place between the GdL complexes and the Eu^{3+} ion.[67,68,76] The pseudo-first-order rate constants, calculated for the proton assisted dissociation of $Gd(DTPA)^{2-}$, $Gd(BOPTA)^{2-}$ and Gd(DTPA-BMA) at pH= 6.5, are $1.8x10^{-7}$ s^{-1}, $1.4x10^{-7}$ $s^{-1}$and $4.0x10^{-6}$ s^{-1}, respectively.[67,68,76] However, the k_p values obtained for the ligand exchange reactions for the $Gd(DTPA)^{2-}$, $Gd(BOPTA)^{2-}$ and Gd(DTPA-BMA) at pH= 6.5 and $[TTHA]_t$= $1x10^{-2}$ M, are $7.6x10^{-6}$ s^{-1}, $5.1x10^{-6}$ s^{-1} and $1.3x10^{-4}$ s^{-1}, respectively. The comparison of these rate data shows that the proton assisted dissociation of complexes is relatively slow even at the highest H^+ concentration (the contribution of these pathways is 2.4 %, 2.8 % and 3.1 %, respectively), so it has practically no role in the ligand exchange reactions at pH > 6.5 and in the presence of TTHA excess.

The k_L ($M^{-1}s^{-1}$) values, calculated for the GdL complexes (Equation (IV.1. 4) and Figure IV.1.1.), which characterize the efficiency of the attack

of the $H_iTTHA^{(6-i)-}$ species on the $Gd(DTPA)^{2-}$, $Gd(BOPTA)^{2-}$ and Gd(DTPA-BMA) at pH= 7.4, were found to be $(7.4\pm0.9)x10^{-4}$ $M^{-1}s^{-1}$, $(3.1\pm0.2)x10^{-4}$ $M^{-1}s^{-1}$ and $(2.3\pm0.03)x10^{-2}$ $M^{-1}s^{-1}$, respectively. These rate data, similarly to the k_p values, reveal that the behavior of $Gd(DTPA)^{2-}$ and $Gd(BOPTA)^{2-}$ in the ligand exchange reactions differs considerably from that of Gd(DTPA-BMA). The k_L values, thus the rates of reactions of Gd(DTPA-BMA) are more than two orders of magnitude higher than those of the $Gd(DTPA)^{2-}$ and $Gd(BOPTA)^{2-}$.

The pH-dependence of the rates of the ligand exchange reactions also differs considerably for the negatively charged $Gd(DTPA)^{2-}$ and $Gd(BOPTA)^{2-}$ and for the neutral Gd(DTPA-BMA). Figures IV.1.2. and 3. show the pseudo-first-order rate constants as a function of pH. The k_p values obtained for the reactions of $Gd(DTPA)^{2-}$ and $Gd(BOPTA)^{2-}$ vary according to minimum curves, with minima at pH about 8.5. The trend of the k_p values determined for the reactions of Gd(DTPA-BMA) is different. The k_p values slightly increase in the pH range 6.5-7.5, then at pH> 7.5 the rate constants increase abruptly. At pH> 9 the reactions are too fast to be followed by measuring the proton relaxation rates. A comparison of the rate data presented in Figure IV.1.2. and 3. also shows that the rates of the exchange reactions of Gd(DTPA-BMA) are about two to three orders of magnitude higher than those of the $Gd(DTPA)^{2-}$ and $Gd(BOPTA)^{2-}$.

To understand the mechanisms of the ligand exchange reactions and to interpret the difference in the behavior of the negatively charged and neutral complexes, we have to take into account the structure of the complexes and the flexibility of the coordinated ligands. The structure of the GdL complexes in solution is similar as it was found by ^{1}H- and ^{13}C-NMR studies.[77-79] The ligands are coordinated in octadentate fashion and the ninth coordination site of Gd^{3+} is occupied by a water molecule. This water

exchanges fast with the bulk water, which is of primary importance for the relaxation effect of the Gd^{3+} complexes. This coordination site is presumably very important in the ligand exchange, because as a first step of the reaction a carboxylate group of the attacking $H_iTTHA^{(6-i)-}$ can be coordinated to this site, when a ternary intermediate is formed. The stability of this intermediate is very low and the dissociation of TTHA from the latter is very probable. However, in a favourable case, due to the intramolecular rearrangement of the donor atoms in the complex, a second and then further donor atoms of TTHA can be coordinated to the Gd^{3+}, and slowly, step by step, the whole coordinated L ligand is displaced by the TTHA, which leads to the formation of the Gd(TTHA) complex.

There are probably several reasons why the ligand exchange reactions of Gd(DTPA-BMA) are considerably faster than the similar reactions of $Gd(DTPA)^{2-}$ and $Gd(BOPTA)^{2-}$. One of the possible reasons is the stronger electrostatic interaction between the uncharged Gd(DTPA-BMA) and $H_iTTHA^{(6-i)-}$ in comparison to the interaction between the $Gd(DTPA)^{2-}$ or $Gd(BOPTA)^{2-}$ and $H_iTTHA^{(6-i)-}$ (The Gd(DTPA-BMA) has a partial positive charge because of the coordination of the two uncharged amide oxygen atoms[80]).

The other reason leading to the faster ligand exchange reaction of Gd(DTPA-BMA) is probably the higher rate of the intramolecular rearrangements of its donor atoms.[79] The rearrangements may result in the transitional presence of free coordination site(s) on the complexed Gd^{3+}, when the attack of the $H_iTTHA^{(6-i)-}$ species on the complex can be more efficient.

The rates of the intramolecular rearrangements have been studied for several $Ln(DTPA)^{2-}$ and Ln(DTPA-BPA) complexes by ^{1}H- and ^{13}C-NMR spectroscopy in a broad temperature range (0-100 ^{o}C) (DTPA-BPA= DTPA-

bis(propylamide)).[79,81] Both in the $Ln(DTPA)^{2-}$ and Ln(DTPA-BPA) complexes the inversion of the three nitrogen atoms of the diethylenetriamine backbone is precluded. In the $Ln(DTPA)^{2-}$ complexes the middle nitrogen, while in the Ln(DTPA-BPA) complexes all three of the nitrogen atoms are chiral. Consequently, the $Ln(DTPA)^{2-}$ complexes have two isomers, which were detected by ^{1}H-NMR spectroscopy for the paramagnetic complexes at low temperatures.[78,79] For the DTPA-bis(amide) derivative complexes the formation of eight isomers is expected and in the ^{13}C-NMR spectrum of Nd(DTPA-BPA) the signals of the eight isomers could be observed.[81] At lower temperatures slow exchange was observed between the different isomers. The rates of isomerisation increased with the increase of temperature and both the ^{1}H and ^{13}C signals broadened and coalesced at higher temperatures. The NMR studies have shown that two exchange processes occur in the complexes: (i) the relatively rapid racemization of the middle nitrogen atom, associated with the interconversions of the two gauche conformations of the ethylenediamine groups; (ii) the slow racemization at the terminal nitrogens, which can take place with the decoordination of a nitrogen and its neighbouring acetate and amide oxygens. The latter process is very slow for the $Ln(DTPA)^{2-}$ complexes, because the iminodiacetate (IMDA) groups are strongly bound to the Gd^{3+}, so this process can not be observed in the temperature range studied. For the Ln(DTPA-BPA) complexes the inversion of both the middle and the terminal nitrogens was observed by ^{13}C-NMR spectroscopy, because the amide oxygen- Ln^{3+} bond is weaker.[81]

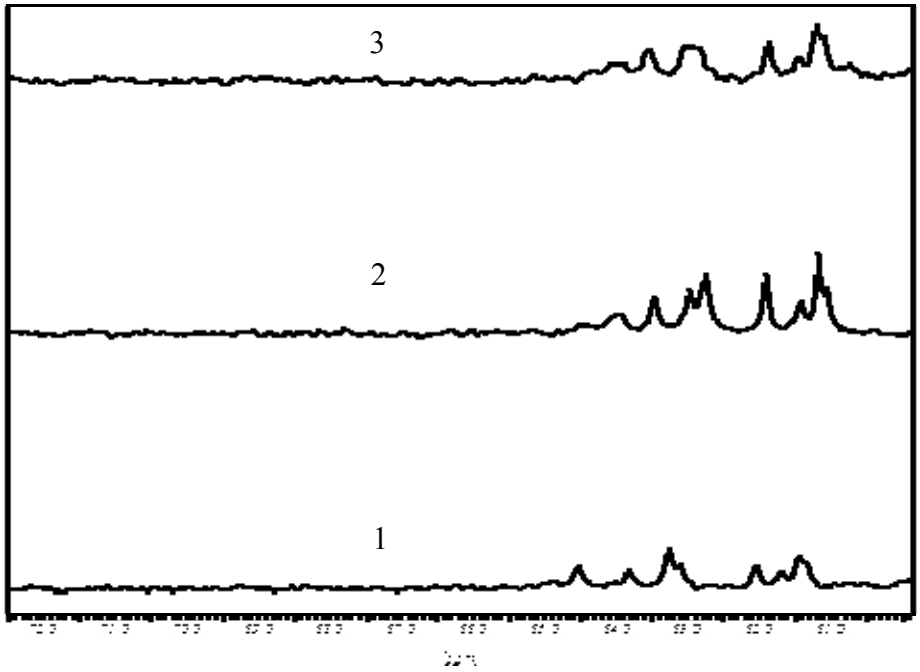

Figure IV.1.7. A part of the ^{13}C-NMR spectra of 0.1 M La(DTPA-BMA) at 35 ^{o}C (1) and 50 ^{o}C (2) and that in the presence of 0.4 M DTPA-BMA excess at 35 ^{o}C (3) (pH= 6.8, ethanol was used as internal standard).

In the ^{13}C-NMR spectra of La(DTPA-BMA) (Figure IV.1.7.) the broadening of the signals can also be observed with the increase of temperature. Similar broadening effect can be observed in the presence of DTPA-BMA ligand excess, when the exchange between the coordinated and free ligands is slow (the signals are separated). In this study we used DTPA-BMA excess instead of TTHA, because in the La(DTPA-BMA) – DTPA-BMA system, where the exchange takes place between the coordinated and free DTPA-BMA ligands, the investigation by NMR spectroscopy is simpler. It can be assumed that the mechanisms of the slow ligand exchange reaction between La(DTPA-BMA) and DTPA-BMA are similar to those occurring between the La(DTPA-BMA) and TTHA, so in the presence of DTPA-BMA

excess a second DTPA-BMA can be coordinated to the La^{3+} and in the intermediate formed, the second ligand can slowly displace the other ligand. In the presence of DTPA-BMA excess the signals of the La(DTPA-BMA) broaden, which indicates the increase in the rate of the mobility of the donor atoms. In Figure IV.1.7. the signals at about 64 ppm belong to the acetate methylene carbons, so the broadening indicates the increase of the rate of the racemization of the terminal nitrogens.[81] The increase in the rate of decoordination of the terminal iminodiacetate methylamide groups may result in the increase of the ligand exchange processes both in the La(DTPA-BMA)-DTPA-BMA and Gd(DTPA-BMA)-TTHA systems.

The increase in the rates of the intramolecular rearrangements has been detected for the $Eu(DTPA)^{2-}$ in the presence of DTPA excess by ^{1}H NMR spectroscopy. At low temperatures (0-5 ^{o}C) the proton spectra of $Eu(DTPA)^{2-}$ consist of 18 signals which average to 9 signals at high temperatures (70-100 ^{o}C).[79,80] In this temperature range the increase of temperature results in the narrowing of the signals, which indicates the increase in the rates of the intramolecular rearrangements. In the spectrum of a 0.1 M $Eu(DTPA)^{2-}$, recorded at 85 ^{o}C the half-widths of the signals observed at -9.13, -1.35 and 7.13 ppm are 135, 65 and 138 Hz, respectively (The signals at -9.13 and -1.35 ppm belong to the terminal acetate methylene, while that at 7.13 ppm, to the ethylene protons).[80] At 90 ^{o}C the signals are narrower, their half-widths are 95, 51 and 114 Hz, respectively. In the presence of 0.4 M DTPA excess, the signals of $Eu(DTPA)^{2-}$ at 85 ^{o}C are narrower than in the absence of DTPA; the widths are 118, 51 and 135 Hz, respectively. These data also indicate that in the presence of free DTPA, because of the encounter of the complexes and the free ligands, the rates of the intramolecular rearrangements in $Eu(DTPA)^{2-}$ are higher and it can be assumed that the presence of TTHA in the solution results in a similar effect.

The rates of the ligand exchange reactions of $Gd(DTPA)^{2-}$ and $Gd(BOPTA)^{2-}$ vary according to minimum curves as a function of pH (Figure 2.) To understand the pH dependence of the k_p values, we have to know the concentration of the attacking $H_iTTHA^{(6-i)-}$ species at different pH values. To calculate the species distribution, the protonation constants of the TTHA have been determined in 0.15 M NaCl, because at such ionic strength there were no data in the literature. The protonation constants determined are as follows: $logK_1^H$= 9.99 (0.003); $logK_2^H$= 9.11 (0.003); $logK_3^H$= 6.00 (0.005); $logK_4^H$= 4.02 (0.006); $logK_5^H$= 2.76 (0.007); $logK_6^H$= 2.15 (0.01). The protonation constants obtained are lower than those determined in 0.1 M KCl, because the stability constants of the Na^+-TTHA complexes are expectedly higher than those of the K^+-TTHA species. The species distribution calculations show that in the pH range 6.5-11 the species H_3X^{3-}, H_2X^{4-}, HX^{5-} and X^{6-} are present, but the concentration of the H_3X^{3-} species is low and negligible at pH> 7.5

The attack of the $H_iTTHA^{(6-i)-}$ species on the Gd^{3+} complexes is expected to be more efficient, if one of its IMDA groups is deprotonated. The infrared and ^{1}H-NMR spectroscopic studies on the protonation scheme of TTHA indicate that the first three protons protonate three nitrogen atoms of the amine backbone. Deprotonated IMDA group is present in the species X^{6-}, HX^{5-} and H_2X^{4-}, but the ratio of the H_3X^{3-} species, bearing a deprotonated IMDA group, is low.[81]

The inspection of the rate data presented in Figure IV.1.2. show that the k_p values do not vary considerably between pH 6.5 and 11. This finding suggests that the reactivity of the predominating TTHA species (H_2X^{4-}, HX^{5-} and X^{6-}) do not differ considerably. The increase of the k_p values from pH 8.5 to 11 can be interpreted with the increase of the concentration of the TTHA species containing less proton (HX^{5-} and X^{6-}), which can more efficiently

attack the Gd^{3+} complexes. By considering this statement, it is difficult to explain the decrease in the k_p values from pH 6.5 to 8.5. For interpreting these data we have to assume that in the ternary intermediates formed by the encounter of the Gd^{3+} complexes and TTHA, the protons from the protonated H_3X^{3-} and H_2X^{4-} species can be transferred to the coordinated DTPA and BOPTA, which accelerates the displacement of these ligands by the TTHA. The realization of these reaction pathways means the validity of the general acid catalysis in these reactions, which was observed earlier in the dissociation reactions of the amine and aminopolycarboxylate complexes.[82,83]

In the ligand exchange reactions of Gd(DTPA-BMA) the k_p values increase with the increase of pH (Figure 1. 3.). The stronger interaction between the Gd(DTPA-BMA) and the $H_iTTHA^{(6-i)-}$ species and the higher rate of the intramolecular rearrangements in the complex make the ligand exchange reactions relatively rapid, so the validity of the general acid catalysis can not be observed.

On the basis of these considerations the rates of the ligand exchange reactions can be expressed as follows:

$$-\frac{d[GdL]}{dt} = \left(k_{H_3X}[H_3X] + k_{H_2X}[H_2X] + k_{HX}[HX] + k_X[X]\right)[GdL] \quad \text{(IV.1. 5)}$$

where k_{H3X}, k_{H2X}, k_{HX} and k_X are the rate constants characterizing the rates of the ligand exchange reactions taking place with the attack of the TTHA species H_3X^{3-}, H_2X^{4-}, HX^{5-} and X^{6-}, respectively. By comparing the Equations (IV.1.3) and (IV.1.5), the pseudo-first-order rate constants can be given by Equation (IV.1. 6):

$$k_p = k_{H_3X}[H_3X] + k_{H_2X}[H_2X] + k_{HX}[HX] + k_X[X] \quad \text{(IV.1.6)}$$

By fitting the k_p values (Figures IV.1.2. and IV.1.3.) to Equation (IV.1.6) the k_{HiX} rate constants have been calculated and presented in Table IV.1.1.

Table IV.1.1. Rate constants characterizing the ligand exchange reactions between the $Gd(DTPA)^{2-}$, $Gd(BOPTA)^{2-}$ and Gd(DTPA-BMA) complexes and TTHA (25 ^oC, 0.15 M NaCl).

	$GD(DTPA)^{2-}$	$GD(BOPTA)^{2-}$	GD(DTPA-BMA)
k_X $(M^{-1}s^{-1})$	$(1.16\pm0.05)\times10^{-3}$	$(7.9\pm0.4)\times10^{-4}$	-
k_{HX} $(M^{-1}s^{-1})$	$(5.9\pm0.4)\times10^{-4}$	$(3.5\pm0.3)\times10^{-4}$	0.58±0.04
k_{H2X} $(M^{-1}s^{-1})$	$(5.6\pm0.2)\times10^{-4}$	$(3.1\pm0.1)\times10^{-4}$	$(1.1\pm0.1)\times10^{-2}$
k_{H3X} $(M^{-1}s^{-1})$	$(2.2\pm0.2)\times10^{-3}$	$(1.8\pm0.2)\times10^{-3}$	-

By the calculation of the rate constants, k_{HiX}, the concentration of the protonated H_iX species was figured out with the use of the protonation constants of TTHA. By calculating the k_{HiX} rate constants, characterizing the reaction of the Gd(DTPA-BMA), the lowest errors were obtained, when in the Equation (IV.1.6) the second and third terms were considered only (In the pH range 6.5-9 the concentration of the species H_3X^{3-} and X^{6-} is low and so the reactions with the H_2X^{4-} and HX^{5-} species are more efficient).

The rate constants k_X, k_{HX}, k_{H2X} and k_{H3X}, obtained for the ligand exchange reactions of $Gd(DTPA)^{2-}$ and $Gd(BOPTA)^{2-}$ do not differ considerably, probably because in each of the X^{6-} , HX^{5-} and H_2X^{4-} species a free IMDA group is available[81], however, the proton transfer from the H_3X^{3-} and H_2X^{4-} species to the GdL complex can take place efficiently. The k_{H2X} and k_{HX} rate constants determined for the reaction of Gd(DTPA-BMA) are

considerably higher than those obtained for the $Gd(DTPA)^{2-}$ and $Gd(BOPTA)^{2-}$, which also indicates that the ligand exchange reactions of Gd(DTPA-BMA) occur significantly faster.

The pseudo-first-order rate constants, k_p, increase with the increase in the concentration of the endogenous citrate, phosphate and carbonate ligands, as it is seen in Figures IV.1.4-6. The increase in the reaction rates may be the result of the formation of low stability ternary complexes between the endogenous ligands and the GdL species (first of all with CO_3^{2-} ions), which accelerate the intramolecular rearrangements and so the dissociation of the complexes[84] The other possibility is the proton transfer from the HPO_4^{2-}, $H_2PO_4^-$ or HCO_3^- ions to the coordinated L ligand, which also increases the dissociation rate of the Gd^{3+} complexes also, that is the general acid catalysis is valid.[64,83] The increase in the reaction rates is significant for the citrate (and probably for the other oxycarboxylic and dicarboxylic acids, present in the blood plasma) (Figure IV.1.4.), in the presence of phosphate the increase in the rates of the exchange reactions of $Gd(DTPA)^{2-}$ and $Gd(BOPTA)^{2-}$ is very low, while in the case of Gd(DTPA-BMA) the effect is larger (Figure IV.1. 5.). Carbonate ions increase the reaction rates only slightly, but since the concentration of the carbonate in the blood plasma is larger (25 mM), so its effect is observable under biological conditions. The k_p values determined for the $Gd(DTPA)^{2-}$, $Gd(BOPTA)^{2-}$ and Gd(DTPA-BMA) in the presence of 25 mM carbonate at pH= 7.4 are larger by 37 %, 20 % and 63 %, respectively. The kinetics of the ligand exchange reactions in the presence of endogenous ligands was not studied in detail. The data obtained indicate that the rates of dissociation of the Gd^{3+} complexes used as MRI contrast agents, are practically not affected by the presence of citrate and phosphate in the plasma, because of their low concentrations, but carbonate ions may slightly increase the rate of dissociation. However, phosphate ions can increase the

rates of the dissociation of Gd^{3+} complexes in those experiments, where phosphate buffers of large concentration are used to study the rates of the reactions. In such experiments the presence of phosphate can result in an apparent increase in the reaction rates, in particular, for the reaction of the Gd(DTPA-BMA) complex.[85]

IV. 2. Physico-chemical characterization of lanthanide(III) complexes formed with a macrocyclic ligand based on 1,7-diaza-12-crown-4

Recently, a series of acyclic chelators bearing picolinate arms and carboxylate or phosphonate groups have been reported for the design of Gd^{3+} complexation in aqueous solution (Scheme IV.2.1).[86,87] These ligands form thermodynamically stable lanthanide complexes.[88] Interestingly, the water exchange rate on the phosphonate derivative Gd^{3+} complex of L^2 (Scheme IV. 2. 1.)has been found to be extremely high, comparable to that on the aqua ion itself.[86] This fast water exchange has been related to the flexible nature of the chelate, and indeed, the rigidification of the ligand backbone by introducing a cyclohexyl ring (L^3) resulted in a decrease of the water exchange rate.[86] We studied the complexation properties of a novel picolinate-derivative molecule based on the 1,7-diaza-12-crown-4 platform ($bp12c4^{2-}$, Scheme IV.2.1).[89] This macrocyclic chelator is expected to form kinetically more inert complexes with respect to the previous acyclic picolinate analogues, which will be an advantage to prevent toxicity. On the other hand, the optimal water exchange characteristics reported for complexes with picolinate arms could be preserved.

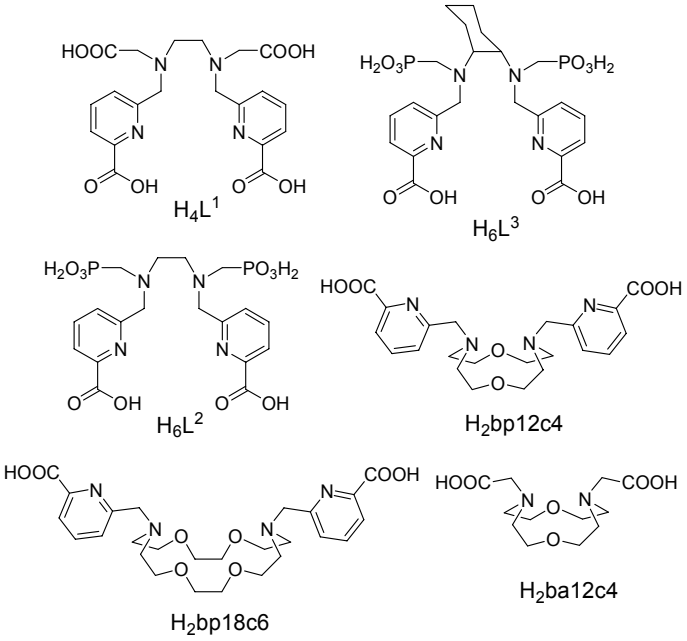

Scheme IV.2.1. Formulas of the ligands

Ligand protonation constants and stability constants of the complexes

The protonation constants of $bp12c4^{2-}$, as well as the stability constants of its metal complexes formed with Ln^{3+} and biologically relevant divalent ions were determined by pH-potentiometric titrations; the constants and standard deviations are given in Table IV.2.1, which also lists the protonation constants of $bp18c6^{2-}$ and the stability constants of its Ln^{3+} complexes.[90] The titration curves of the lanthanide complexes all show a deprotonation step at high pH (> 8) indicating the formation of a monohydroxo complex (Figure IV.2.1). The formation of these monohydroxo complexes has been characterized by the protonation constant K_{MLOH}, as defined in Eq. (IV.2.1)

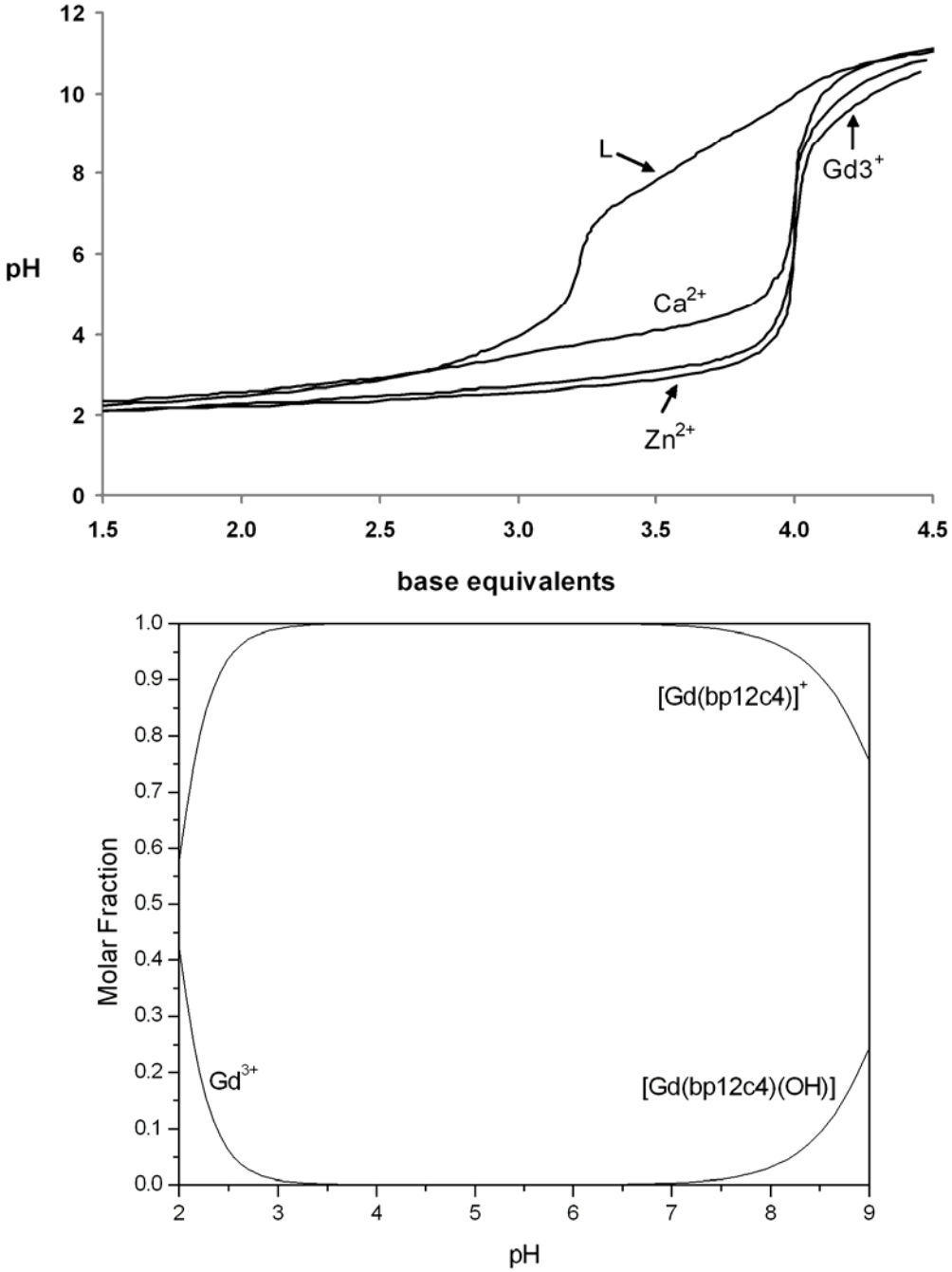

Figure IV.2.1. Top: Potentiometric pH titration curves for the ligand $bp12c4^{2-}$ in the absence and in the presence of some of the metal ions studied

at 1:1 metal to ligand ratio. Bottom: Species distribution of the $[Gd(bp12c4)]^+$ system at 1: 1 Gd:bp12c4 ratio, $[Gd^{3+}]$ = 1 mM [I = 0.1 M KCl, 25 ºC].

$$K_{MLOH} = \frac{[ML]}{[ML(OH)][H^+]} \qquad \text{(IV.2. 1)}$$

Four protonation constants could be determined for the $bp12c4^{2-}$ ligand. The first two $\log K_i$ values correspond to the protonation of the macrocyclic nitrogens. $\log K_1$ is somewhat lower for $bp12c4^{2-}$ than for the bisacetate derivative of the same macrocycle (ba12c4, Scheme IV.2.1.). It is in accordance with previous observations where a diminution of the amine basicity, though more important than here, has been observed on replacement of the acetate arm by 6-methyl-2-pyridinecarboxylate groups.[91] The third and fourth protonation steps of $bp12c4^{2-}$ are likely associated to the carboxylic acid groups.[92]

Table IV.2.1. Protonation constants of $bp12c4^{2-}$ and related ligands and stability constants of their Ln^{3+} and M^{2+} complexes (25 ºC; I=0.1 M (KCl)).

	bp12c4	**bp18c6**[90]	**ba12c4**[90]	**EDTA**[75]	**DTPA**[75]
$\log K_1$	9.16 (0.03)	7.41	9.53	10.17	10.34
$\log K_2$	7.54 (0.04)	6.85	7.46	6.11	8.59
$\log K_3$	3.76 (0.05)	3.32	2.11	2.68	4.25
$\log K_4$	2.79 (0.04)	2.36			2.71
$\log K_5$		1.69			2.18
$\log K_{LaL}$	16.81 (0.06)	14.99		15.46	18.23
$\log K_{LaHL}$		2.28			
$\log K_{LaLOH}$	10.87 (0.08)				
$\log K_{CeL}$	16.94 (0.09)	15.11		15.94	19.09
$\log K_{CeHL}$		2.07			
$\log K_{CeLOH}$	9.78 (0.07)				
$\log K_{EuL}$	18.62 (0.08)	13.01		17.32	20.87
$\log K_{EuHL}$		1.97			
$\log K_{EuLOH}$	9.96 (0.07)				
$\log K_{GdL}$	18.82 (0.01)	13.02		17.35	20.73
$\log K_{GdHL}$		2.48			
$\log K_{GdLOH}$	9.49 (0.03)				
$\log K_{DyL}$	18.11 (0.08)	11.72		18.28	21.11
$\log K_{DyHL}$		2.42			
$\log K_{DyLOH}$	10.0(0.1)				

$\log K_{YbL}$	18.08 (0.05)	8.89		19.48	22.59
$\log K_{YbLOH}$	10.15 (0.08)				
$\log K_{CaL}$	12.09 (0.06)		8.50	10.8	10.7
$\log K_{CaLOH}$	10.01 (0.09)				
$\log K_{ZnL}$	18.12 (0.03)		12.28	16.5	18.29
$\log K_{CuL}$	19.56 (0.04)		15.95	18.8	21.5
$\log K_{CuHL}$	6.52 (0.09)				4.8

The stability constants of the lanthanide complexes of $bp12c4^{2-}$ could be obtained from direct potentiometric titrations, as the complex formation was fast. The complex stability increases from the early lanthanides to the middle of the series, then remains relatively constant or slightly declines for the heavier lanthanides. In this respect, this chelator is similar to DTPA, in contrast to most of the poly(amino carboxylate) ligands, such as EDTA, which form complexes of increasing stability all across the lanthanide series due to the increase of charge density on the metal ions. Given its much medium size, this twelve-membered macrocycle provides an optimal fit for smaller lanthanides. For the first half of the lanthanide series (Ln = La-Gd), the stability constants determined for $Lnbp12c4^{+}$ complexes fall in between those reported for EDTA and DTPA complexes. For the heaviest lanthanides, the stability constants are somewhat lower for $bp12c4^{2-}$ complexes than for EDTA ones, as a consequence of the different trend of the stability constants of $bp12c4^{2-}$ and EDTA complexes along the lanthanide series.

At high pH, all lanthanide complexes undergo deprotonation, likely occurring on the coordinated water molecule, to form monohydroxo complexes.[93] The K_{MLOH} constants characterizing this deprotonation step

decrease from the beginning to the middle of the series to reach the lowest value for [Gd(bp12c4)(OH)], then again slightly increase for the heavier lanthanides. The trend observed in the first part of the series can be easily rationalized by the increasing charge density of the metal ions. The increase observed towards the end of the series could be related to a diminution in the hydration from two to one for the small lanthanides. The species distribution diagram obtained for the representative Gd^{3+} complex is depicted in Figure IV.2.1. The diagram shows that at a 10^{-3} M concentration the dissociation of the complex starts at pH ~ 3.5, while the formation of the monohydroxo complex is observed at pH > 7.

In order to better compare the stability of $Gd(bp12c4)^{+}$ to other Gd^{3+} complexes, we have calculated its the p*Gd* value at pH 7.4, $c_L = 1\times10^{-5}$ M and $c_{Gd} = 1\times10^{-6}$ M (p*Gd* = -log$[Gd^{3+}]_{free}$). p*Gd* values reflect the influence of the ligand basicity and the protonation of the complex on the stability; the higher the p*Gd*, the more stable is the complex under the given conditions. For the Gd^{3+} complex of $bp12c4^{2-}$ we obtain p*Gd* = 17.6, a slightly lower value than that calculated for $Gd(DTPA)^{2-}$ (p*Gd* = 19.1), which clearly shows the good complexing ability of our ligand towards lanthanides.

Kinetic studies on $[Ln(bp12c4)(H_2O)_q]^{+}$ complexes

The kinetic inertness of the complexes plays a critical role in determining the Gd^{3+} release *in vivo*. The kinetic stability can be characterized by rate constants of exchange reactions that might take place in the plasma. Among those, the most important is probably the displacement of Gd^{3+} from a given complex by the endogenously abundant Cu^{2+} and Zn^{2+} ions in a metal exchange reaction. Since the dissociation of the complexes and the metal exchange reactions are relatively slow processes around

physiological pH, the dissociation of many complexes has been studied in acidic solutions.[94] More recently, detailed kinetic studies have been conducted at higher pHs (3.5-6) to investigate the role of transmetallation with Zn^{2+} and Cu^{2+}.[68] In general terms, linear DTPA-type Gd^{3+} chelates are kinetically much less inert than the macrocyclic, DOTA-type complexes. At physiological pH, the dissociation of linear chelates proceeds mainly *via* transmetallation, which largely takes over the acid-assisted pathway. Indeed, the reaction rates of the metal exchange between $Gd(DTPA)^{2-}$ and Cu^{2+} or Zn^{2+} are independent of pH above pH 4.5, indicating that the exchange predominantly occurs *via* direct attack of these metals on the Gd^{3+} complex.[68] In contrast, the dissociation of macrocyclic chelates is much slower and independent of the exchanging metal ion concentration, showing that it occurs mainly through proton-assisted pathways.[95,96,97]

We have assessed the kinetic inertness of the $Ln(bp12c4)^{+}$ complexes by following the acid-assisted dissociation in strongly acidic solutions for the Ce^{3+} complex, and the transmetallation with Zn^{2+} and Cu^{2+} at pH 4.5-5.5 for the Gd^{3+} analogue. In the presence of a large excess of acid (0.001 – 0.3 M HCl), the complex is thermodynamically unstable. The reaction was followed for the Ce^{3+} complex by monitoring the decrease of the absorbance of the complex at 280 nm. The observed first order dissociation rate constants follow a quadratic dependence on the proton concentration, as given in Eq. IV.2.2, showing the role of proton-catalyzed pathways in the dissociation (Figure IV.2. 2).

$$k_{obs} = k_0 + k' \times [H^+] + k'' \times [H^+]^2 \qquad \text{(IV.2.2)}$$

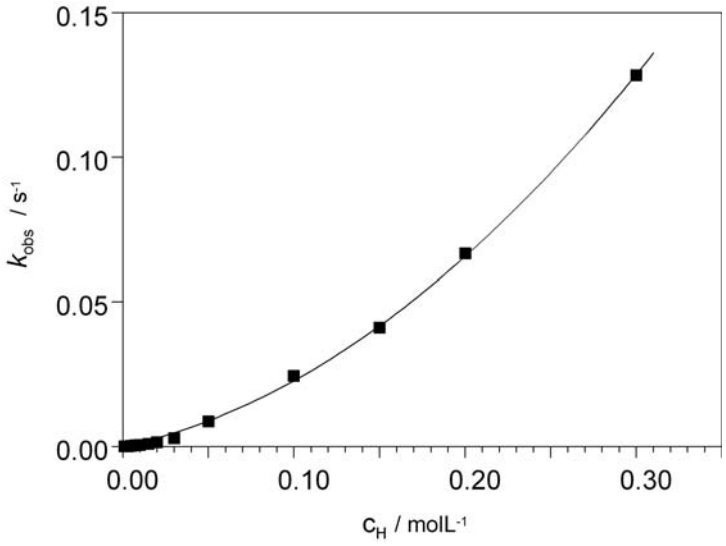

Figure IV.2. 2. Pseudo-first-order rate constants, k_{obs}, as a function of the proton concentration in the dissociation of $Ce(bp12c4)^{+}$ (0.0001 M; I = 0.1 M KCl).

Similar behavior was reported for the dissociation of various acyclic Ln^{3+} complexes, including DTPA and pyridine-aminocarboxylate ligands.[98] This equation indicates that the dissociation might take place by proton-independent (characterized by k_0) and proton-assisted pathways, presumably with the formation and dissociation of mono- and diprotonated complexes (characterized by k' and k'', respectively). The constants fitted are k' = 0.143±0.009 M^{-1} s^{-1} and k''= 0.96±0.03 M^{-2} s^{-1}, while k_0 had to be fixed to 0. When fitting k_0, we obtained a small negative value with a large error. This is not surprising since in such strongly acidic solutions the dissociation pathways involving protonated complexes are much more important than the spontaneous dissociation.

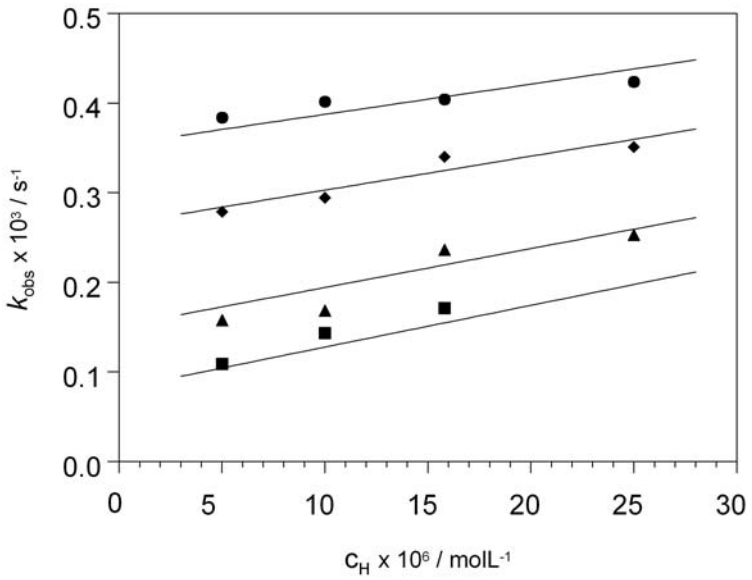

Figure IV.2.3. Plots of k_{obs} versus hydrogen ion concentration for the reaction between $Gd(bp12c4)^+$ (0,2 mM) and Zn^{2+}. c_{Zn} = 5 mM (■), 10 mM (▲), 20 mM (◆) and 30 mM (●).

In the exchange reaction between $Gd(bp12c4)^+$ and Zn^{2+}, the observed pseudo-first order rate constants depend both on the proton and the Zn^{2+} concentration in the pH range investigated (pH 4.6-5.3; Fig. IV.2.3). They increase by increasing proton and increasing metal ion concentration, indicating that both proton- and metal-assisted pathways play a role in the dissociation process. In this respect, this system is intermediate between DTPA-type and macrocyclic chelates, for which the dissociation is predominated by metal- or proton-assisted pathways, respectively. Taking into account previous studies on the metal-assisted dissociation of Ln^{3+} poly(aminocarboxylates)[95], the following possible reaction pathways are assumed to describe the experimental rate data in the exchange of $Gd(bp12c4)^+$ with Zn^{2+} (Scheme IV.2.2.):

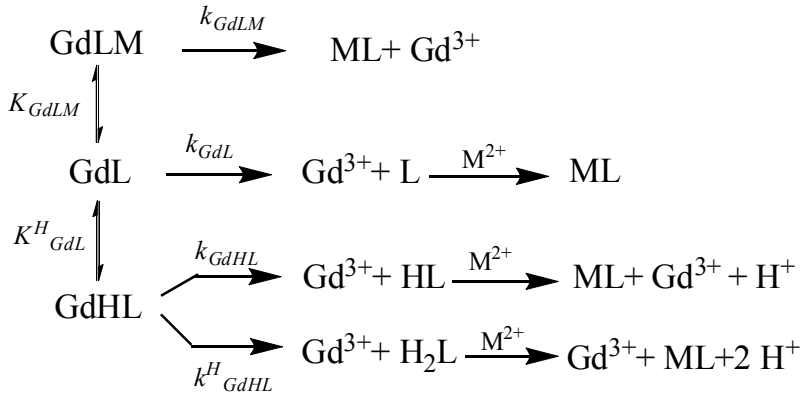

Scheme IV.2.2. Possible reaction pathways for the dissociation of a Gd^{3+} complex in the presence of a divalent metal ion M^{2+}.

According to this reaction scheme, the rate of the exchange reaction can be given as in Eq. (IV.2. 3):

$$-\frac{d[GdL]_t}{dt}=k_{GdL}[GdL]+k_{GdHL}[GdHL]+k^{H}_{GdHL}[GdHL][H^+]+k_{GdLM}[GdLM] \qquad \text{(IV.2.3)}$$

By taking into account the total concentration of the complex, the following expression can be derived for the pseudo-first-order rate constant of the dissociation process:

$$k_{obs}=\frac{k_0+k_1[H^+]+k_2[H^+]^2+k_3[M]}{1+K_{HGdL}[H^+]+K_{GdLM}[M]} \qquad \text{(IV.2.4)}$$

with $k_0 = k_{GdL}$, $k_1 = k_{GdHL} \times K^H_{GdL}$, $k_2 = k^H_{GdHL} \times K^H_{GdL}$ and $k_3 = k_{GdLM} \times K_{GdLM}$. In the potentiometric study, we could not identify any protonated complex at pH > 1.8, which means that if there is any, its protonation constant $\log K_{HGdL}$ has to be very low. The pseudo-first-order rate constants shown in Fig. IV.2.3. were fitted to Eq. (IV.2.4). During the fitting procedure k_0 was fixed zero, otherwise small negative values with a large error being obtained. The fitting of k_2 also turned to be impossible, showing that in the pH region of the experiment the dissociation pathway *via* diprotonated complexes is negligible. Therefore, the rate constants k_1 and k_3, as well as the protonation constant K_{HGdL} and the stability constant of the dinuclear complex, K_{GdLZn}, were calculated. All constants obtained are listed and compared to those for $Gd(DTPA)^{2-}$ in Table IV.2.2.

Table IV.2.2. Rate constants obtained for the exchange reaction of $[Gd(bp12c4)]^+$ with Zn^{2+} and Cu^{2+} at 25 ºC.

	$Gd(bp12c4)^+$		**$Gd(DTPA)^{2-}$**	
	Zn^{2+}	**Cu^{2+}**	**Zn^{2+}**	**Cu^{2+}**
k_1 / $M^{-1}s^{-1}$	5.0±1.0	*b*	0.58[c]	
k_2 / M^{-2} s^{-1}	*b*	*b*	9.7×10^4 [c]	
k_3^M / $M^{-1}s^{-1}$	0.018±0.006	0.047±0.010	0.056	0.93
K_{GdLM} / M^{-1}	16±10	10±7	7	13
$\log K^H_{GdL}$	1.6±0.6	1.6 [d]	2.0	
k_4^{OH} / $M^{-2}s^{-1}$	-	$(2\pm0.9)\times10^8$	-	-

c Ref. [68]

The observed rate constants for the metal-exchange reaction between $[Gd(bp12c4)]^+$ and Cu^{2+} also depend on both the proton and the Cu^{2+}

concentration; however, their proton dependency shows an unexpected trend (Figure IV.2.4). In contrast to previously reported complexes and to the exchange between $[Gd(bp12c4)]^{+}$ and Zn^{2+}, here the rate constants decrease with increasing proton concentration indicating an unusual reaction pathway. The pH dependency is more important when the Cu^{2+} is in high concentration, while at lower copper concentration the k_{obs} values remain almost constant with the pH, as it has been observed for the metal exchange of various DTPA-type Ln^{3+} complexes. This phenomenon could be explained by the formation of a protonated $H[Gd(bp12c4)]^{2+}$ complex that dissociates slower than the dinuclear $Cu\text{-}[Gd(bp12c4)]^{3+}$ complex transitionally formed by the direct attack of the exchanging metal ion. However, protonated complex could not be identified in the potentiometric titration, which can be rationalized by the positive charge of $Gd(bp12c4)^{+}$ which is unfavorable for protonation. An attempt to fit the k_{obs} data to Eq. (IV.2.4) resulted in the following values: k_1 = 10 $M^{-1}s^{-1}$, k_2 = 0, k_3 = 1.2 $M^{-1}s^{-1}$, K_{GdLCu} = 11 and $\log K^{H}_{GdL}$ = 5.6. While all the other parameters have reasonable values, the value of $\log K^{H}_{GdL}$ = 5.6 is unconceivable, since such high protonation constant should be well detectable on the pH-potentiometric titration curve, and therefore this model cannot account for the unprecedented pH-dependency of the rate constants observed for the Cu^{2+} transmetallation. In another hypothesis that we could think of, the transitionally formed dinuclear $Cu\text{-}[Gd(bp12c4)]^{3+}$ species would dissociate *via* a hydroxide-assisted pathway which is faster than the proton-assisted dissociation of the $Gd(bp12c4)^{+}$ complex itself. This hypothesis is based on the three positive charges of the dinuclear species which makes it more prone to an eventual hydroxide-catalyzed dissociation. The lanthanide complexes of $bp12c4^{2-}$ all have shown a tendency to form monohydroxo complexes in the potentiometric study. On the other hand, Cu^{2+} is known to form hydroxo-

complexes at lower pH than Zn^{2+}, which could explain the different behavior of the two metals.[99] In order to take into account such a pathway in the dissociation, we can include a term $k_4^{OH}\times[Cu^{2+}]\times[OH^-]$ in the numerator of the expression of k_{obs} to give Eq. (IV.2. 5):

$$k_{obs}=\frac{k_0+k_1[H^+]+k_2[H^+]^2+k_3[M]+k_4^{OH}[M][OH^-]}{1+K_{HGdL}[H^+]+K_{GdLM}[M]}$$

(IV.2.5)

The fit of the experimental data to this equation is shown in Figure 4 and the fitted parameters are reported in Table IV.2.2. It must be pointed out that we do not have proofs that a hydroxide-assisted dissociation is responsible for the unprecedented pH dependence of the Cu^{2+}-exchange kinetics observed for $Gd(bp12c4)^+$. Thus, the data reported in Table IV.2.2. for the Cu^{2+} exchange should be understood as the result of a tentative explanation of the experimental evidence.

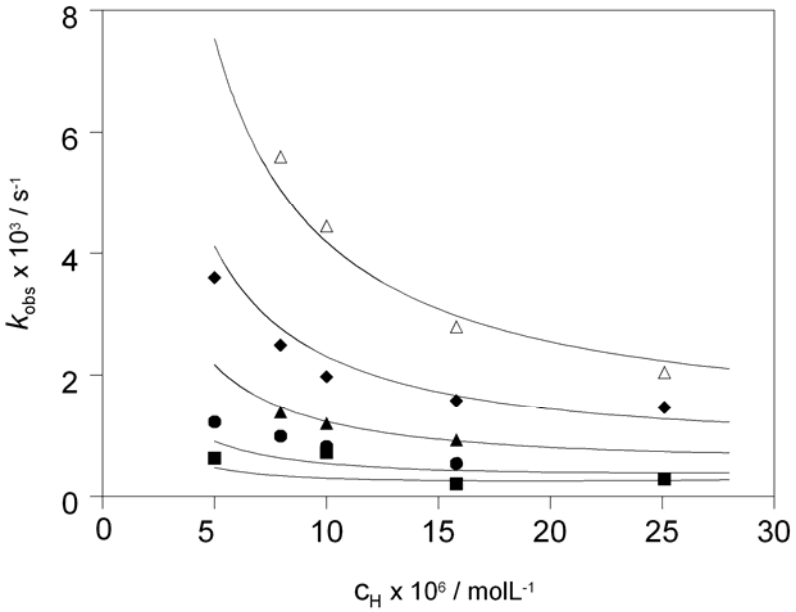

Figure IV.2.4. Plots of k_{obs} versus hydrogen ion concentration for the reaction between $Gd(bp12c4)^+$ (0,1 mM) and Cu^{2+}. C_{Cu} = 1 mM (■), 2 mM (●), 5 mM (▲), 10 mM (◆) and 20 mM (Δ).

In comparison to $Gd(DTPA)^{2-}$, the proton-assisted dissociation is more rapid, while the zinc- or copper-assisted transmetallation is less efficient for $Gd(bp12c4)^+$. If we consider that at physiological pH the acid-catalyzed pathway becomes negligible, the $Gd(bp12c4)^+$ complex is more resistant to dissociation than its DTPA analogue. In overall, however, the kinetic inertness of $[Gd(bp12c4)]^+$ is not considerably higher than that of $GdDTPA^{2-}$.

^{17}O NMR measurements and water exchange on $Gd(bp12c4)(H_2O)_q^+$

In order to assess parameters characterizing the water exchange and rotational dynamics on $Gd(bp12c4)(H_2O)_q^+$, we have measured variable temperature transverse and longitudinal ^{17}O NMR relaxation rates and

chemical shifts at 11.7 T. Previous luminescence and high resolution UV-Vis absorbance data obtained on the corresponding Eu^{3+} analogue proved the existence of a hydration equilibrium, with an average hydration number of q_{av} = 1.4 at 298 K.[89] The temperature dependence of the hydration equilibrium has been also described by the UV-Vis absorbance study which yielded the reaction enthalpy (ΔH^{o} = 9.5 kJ mol^{-1}) and the reaction entropy (ΔS^{o} = 33 J mol^{-1} K^{-1}). Based on the similar size of the neighbouring Eu^{3+} and Gd^{3+} ions, we assume that the same hydration equilibrium, characterized by these thermodynamic parameters, exists for $Gd(bp12c4)(H_2O)_q^{+}$ as well. The reduced ^{17}O relaxation rates and chemical shifts have been therefore obtained from the experimental relaxation rates and chemical shifts by taking into account the temperature dependency of the hydration equilibrium, which allows calculating the average q value at each temperature. The data are presented in Figure IV.2.5.

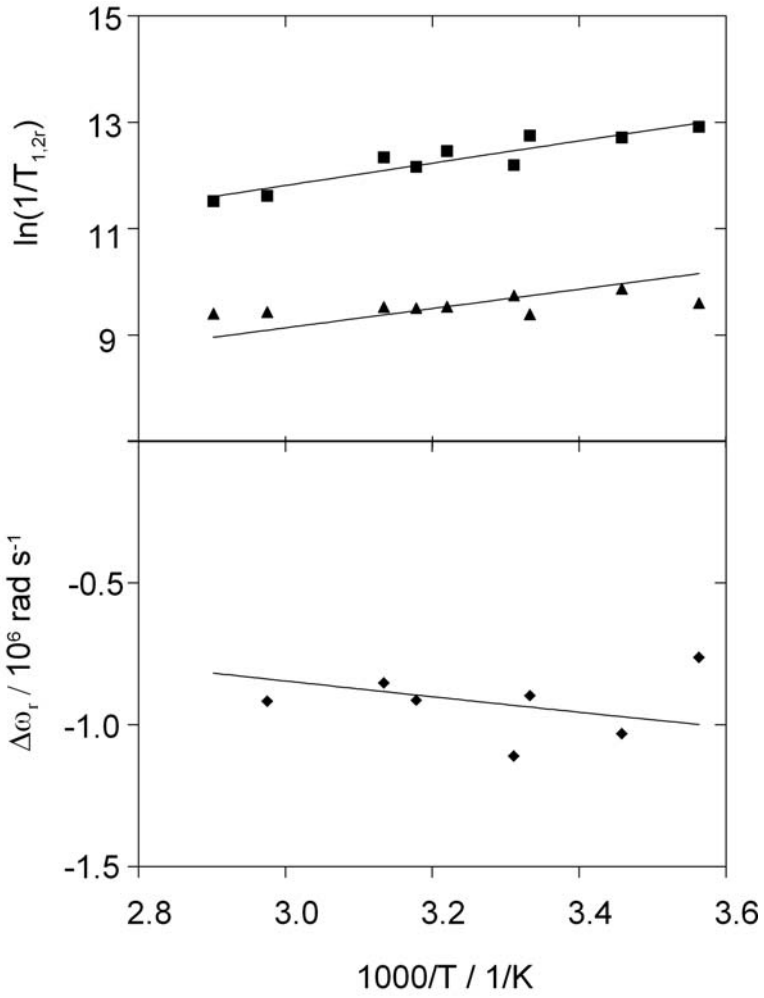

Figure IV.2.5. Reduced longitudinal (▲) and transverse (■) ^{17}O NMR relaxation rates and ^{17}O NMR chemical shifts (◆) of a $[Gd(bp12c4)(H_2O)_q]^+$ solution at 11.75 T and pH = 6. The lines represent the best fit of the data as explained in the text.

The ^{17}O reduced transverse relaxation rates ($1/T_{2r}$) decrease with increasing temperature in the whole temperature range investigated, indicating that they are in the fast exchange region. In the fast exchange regime, the reduced transverse relaxation rate is defined by the transverse

relaxation rate of the bound water oxygen, $1/T_{2m}$, which is in turn influenced by the water exchange rate, k_{ex}, the longitudinal electronic relaxation rate, $1/T_{1e}$, and the scalar coupling constant, $A/\hbar$. The reduced ^{17}O chemical shifts are determined by $A/\hbar$. Transverse ^{17}O relaxation is governed by the scalar relaxation mechanism, thus contains no information on the rotational motion of the system. In contrast to $1/T_{2r}$, the longitudinal ^{17}O relaxation rates, $1/T_{1r,}$ are determined by dipole-dipole and quadrupolar relaxation mechanisms, both related to rotation. The dipolar term depends on the Gd^{3+}-water oxygen distance, r_{GdO}, while the quadrupolar term is influenced by the quadrupolar coupling constant, $\chi(1+\eta^2/3)^{1/2}$. The experimental data have been fitted simultaneously to the common Solomon-Bloembergen-Morgan theory of paramagnetic relaxation using the equations presented in Section III. 4. In the fitting procedure, r_{GdO} has been fixed to 2.50 Å, based on available crystal structures[100,101] and recent ESEEM results[102]. The quadrupolar coupling constant, $\chi(1+\eta^2/3)^{1/2}$, has been set to the value for pure water, 7.58 MHz. We should note that a r_{GdO} value of 2.585 Å was obtained for $[Gd(bp12c4)(H_2O)]^+$ from DFT calculations performed in vacuo.[89] However, a shorter distance is expected in aqueous solution, where a stronger water ion-Gd^{3+} interaction arises from solvent polarization effects that increase the dipole moment of the free water molecules.[103] The empirical constant describing the outer sphere contribution to the ^{17}O chemical shift, C_{os}, was also fixed to 0. The following parameters have been adjusted: the water exchange rate, k_{ex}^{298}, the activation entropy, $\Delta S^{\ddagger}$, the activation enthalpy for water exchange, $\Delta H^{\ddagger}$, the scalar coupling constant, $A/\hbar$, the rotational correlation time (τ_R^{298}) and its activation energy, E_R, and the parameters characterizing the electron spin relaxation, such as the correlation time for the modulation of the zero-field-splitting, τ_v^{298}, and its activation energy, E_v, and the mean-square zero-field-splitting energy, Δ^2. The values obtained for these

parameters are presented in Table IV.2.3. For the parameters characterizing electron spin relaxation, we calculated τ_v^{298} = 27±9 ps, Δ^2 = 1.1×10^{19} s^{-2}, while E_v was fixed to 1 kJ/mol, otherwise small negative values being obtained.

Table IV.2.3. Parameters obtained from the fitting of the ^{17}O NMR relaxation rates and chemical shifts at 11.7 T.

	Gd(bp12c4)$(H_2O)_q^+$	Gd(DTPA)$(H_2O)^{2-}$	$[Gd(H_2O)_8]^{3+}$
$k_{ex}^{298}/10^6$ s^{-1}	220±15	3.3	800
$\Delta H^{\ddagger}$/kJ mol^{-1}	14.8±3.0	51.6	15.3
$\Delta S^{\ddagger}$ /J mol^{-1} K^{-1}	-35±8	+56	-23
$A/\hbar$ /10^6 rad s^{-1}	-3.4±0.3	-3.8	-5.3
τ_R^{298} /ps	105±16	103	41
E_R /kJ mol^{-1}	15.0±4.2	17.3	15

The water exchange rate is very high on $[Gd(bp12c4)(H_2O)_q]^+$, being within the same order of magnitude as for the $Gd(H_2O)_8^{3+}$ aqua ion or for the previously studied $Gd(L^2)^{3-}$ complex (Scheme IV.2.1). To the best of our knowledge, this is the fastest water exchange on a macrocyclic Gd^{3+} complex ever reported. In the fast exchange regime, the ^{17}O transverse relaxation rates are influenced by both the water exchange and the electron spin relaxation. We should note that in our case, the electron spin relaxation, $1/T_{1e}$, has a very limited contribution, representing maximum 10 % in the correlation time τ_c governing the relaxation rate of the bound water oxygen, $1/T_{2m}$ ($1/\tau_c = k_{ex} + 1/T_{1e}$). Therefore, the water exchange rate can be obtained with a very good certitude. Indeed, by varying the values of either τ_V^{298} or Δ^2 by a factor of 5

as compared to those obtained in the fit, the value of k_{ex}^{298} calculated in this way changed maximum by 5 %.

The activation entropy that we obtained has a strongly negative value, indicating that the water exchange process has an associative character. In associatively activated water exchange processes, the incoming water enters the inner coordination sphere of the complex before the departure of the leaving water molecule. So far, very few Gd^{3+} complexes have been reported to have associative water exchange.[104,105,106,107] All of them, including the aqua ion, are octa-coordinate complexes. Most of the Gd^{3+} complexes studied so far with respect to their water exchange, poly(aminocarboxylates) in majority, were nine-coordinate and presented dissociatively activated water exchange. This could be related to the nature of Gd^{3+} that prefers the typical coordination numbers 8 or 9 in solution. Consequently, the water exchange of octa-coordinate complexes will proceed *via* an associatively activated mechanism, involving a nine-coordinate transition state, while that of the nine-coordinate complexes will go through an eight-coordinate transition state in a dissociatively activated process. As a general rule, the water exchange rate is higher for associatively activated processes. In our case, the hydration equilibrium is between a nine-coordinate, monohydrated, and a ten-coordinate, bishydrated species, which are present in comparable quantities. Given the large negative value obtained for the activation entropy pointing to an associatively activated water exchange, one could speculate that the water exchange on the nine-coordinate species, which can be expected to proceed *via* an associative pathway, is mainly responsible for the observed T_2 effect in the ^{17}O NMR, while the contribution of the ten-coordinate, bishydrated species, which should proceed *via* a dissociative mechanism, would be negligible. We should also note that the positive charge of the complex could be another factor that contributes to the fast

water exchange in an associatively activated process. The approaching of the second water molecule with its oxygen bearing a partial negative charge should be indeed favored by a positive charge on the complex. Consequently, the water exchange on the bishydrated complex should be considerably slower than that on the monohydrated one. This would be in accordance with the general observation that associative exchanges are faster than dissociative ones. Based on this reasoning, we tried to fit the $1/T_{2r}$ values by assuming that the only species that contributes to the water exchange is the monohydrated complex. By taking into account the temperature-dependent variation of its ratio (based on the UV-Vis study on the Eu^{3+} analogue, see above), we obtained $k_{ex}^{298} = (8.0\pm1.0)\times10^8$ s^{-1} for $Gd(bp12c4)(H_2O)^+$ ($\Delta H^{\ddagger}$ = 18.7 kJ/mol). We also tried to fit the $1/T_{2r}$ values by assuming two species (q=1 and q=2) that undergo water exchange independently. The resulting values were $k_{ex}^{298} = (3.9\pm1.2)\times10^8$ s^{-1} and $(1.7\pm1.3)\times10^8$ s^{-1} for $Gd(bp12c4)(H_2O)^+$ and $Gd(bp12c4)(H_2O)_2^+$, respectively. Although this latter fit resulted in a smaller k_{ex}^{298} for the bishydrated complex, it still shows a very fast exchange. In overall, we do not possess any tool to decide whether the nine-coordinate species with an associatively activated exchange is the only contributor to the reduced ^{17}O transverse relaxation rates or there is also a contribution from the exchange of the ten-coordinate species. Therefore, we prefer to report the effective k_{ex} value as shown in Table IV.2.3. In any case, if we consider practical applications of this complex as an MRI contrast agent, it is the effective k_{ex} value that will determine the efficiency of the chelate in enhancing water proton relaxation.

The very fast exchange observed for $Gd(bp12c4)(H_2O)_q^+$ is likely related to the hydration equilibrium of the complex, and more importantly, to the very flexible inner coordination sphere around the metal ion. Other Gd^{3+} complexes which also present hydration equilibrium do not necessarily have

such extreme water exchange rates. For instance, $Gd(DO3A)(H_2O)_q$ and $Gd(DO2A)(H_2O)_q^+$ both have differently hydrated species in aqueous solution (q_{ave} = 1.8 and 2.8, respectively), but they show only a limited increase of the water exchange rate as compared to the monohydrated $Gd(DOTA)(H_2O)^-$.[108] For these macrocyclic complexes, the most important factor that limits water exchange is probably the rigidity of the inner sphere.

Concerning the other parameters calculated in the fit, the rotational correlation time has a reasonable value for a small molecular weight complex. For the scalar coupling constant, $A/\hbar$, we obtained $-(3.4\pm0.3)\times10^6$ rad s^{-1}, which is in good accordance with values reported for Gd^{3+} complexes.[105] This also confirms that the hydration number used in the calculations is correct. We should also note that the slope of the curve of the reduced chemical shifts versus inverse temperature is nicely reproduced by the fit, which supports that the parameters characterizing the temperature dependency of the hydration equilibrium are correct (Figure IV.2. 5).

Anion binding studies

Coordinatively unsaturated lanthanide complexes containing two inner-sphere water molecules, such as Ln^{3+} DO3A-like complexes, are known to bind biologically relevant anions such as hydrogencarbonate, phosphate or citrate.[109] The ability of these lanthanide complexes to form ternary complexes with anions is likely related to the presence of the two inner-sphere water molecules coordinated to the Ln^{3+} ion in adjacent positions. Indeed, several coordinatively unsaturated q = 2 lanthanide complexes either do not bind anions or the observed binding is very weak[110] Most likely this is due to an unfavourable, non adjacent location of the inner-sphere water molecules around the metal ion. In a previous study on the

solution structure of Ln(bp12c4)$(H_2O)_q^+$ complexes, we have shown that in q = 2 complexes the two inner-sphere water molecules occupy adjacent positions in the metal ion coordination sphere.[89] Thus, these Ln^{3+} complexes of $bp12c4^{2-}$ are expected to bind anions in aqueous solution. The formation of ternary complexes between Gd(bp12c4)$(H_2O)_q^+$ and hydrogencarbonate, phosphate and citrate ions has been studied by measuring the longitudinal relaxation rates ($1/T_1$) of water protons at 500 MHz and 25 ^oC (pH = 7.4, 0.01 M HEPES, I = 0.15 M NaCl). The concentration of the Gd^{3+}-complex was ~1 mM while the concentration of each anion varied between 0-36 mM. Anion addition caused a decrease in relaxivity, in agreement with the replacement of inner-sphere water molecules by the anion, for citrate see Figure IV.2.6. Plots of the relaxivity versus the [anion]/[complex] ratio show saturation profiles for all investigated anions. The least-squares fitting of the titration profiles allowed us to determine the binding constants listed in Table IV.2.4. The fitting of the experimental data also provides the relaxivity of the ternary complexes ($r_{1,t}$, Table IV.2.4). The Gd(bp12c4)$(H_2O)_q^+$ complex binds the three investigated anions rather strongly, as expected for a positively-charged complex, with binding constants ranging between ca. 250 and 630 M^{-1}, in the following binding trend: hydrogencarbonate > phosphate ≈ citrate. The relaxivities calculated for the three ternary complexes are very similar, being consistent with that expected for a q = 0 complex.

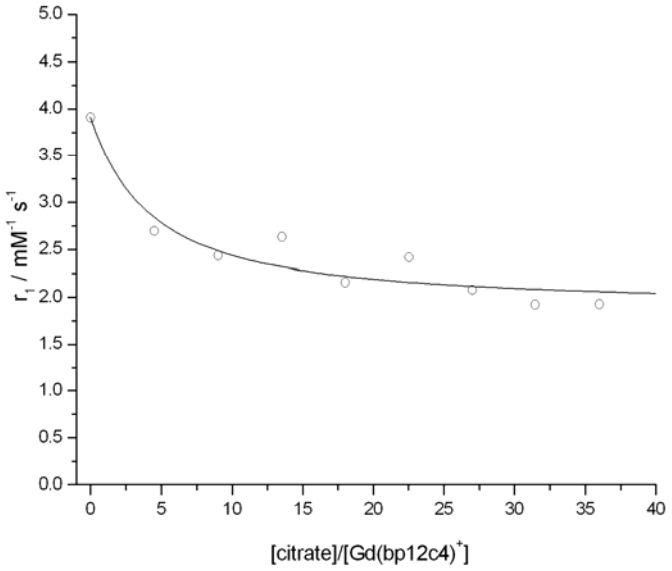

Figure IV.2.6. Relaxivity of Gd(bp12c4)$(H_2O)_q^+$ (~1 mM) in the presence of increasing citrate concentration.

Table IV.2.4. Binding constants (K_{aff}, M^{-1}) for the interaction of Gd(bp12c4)$(H_2O)_q^+$ with different anions and relaxivity ($r_{1,t}$, $mM^{-1}s^{-1}$) of the ternary complex obtained from the fit of the relaxivity measurements at 25 ºC (pH = 7.4, 0.01 M HEPES, I = 0.15 M NaCl).

	CITRATE	**HCO_3^-**	**PHOSPHATE**
K_{aff}	280±20	630±50	250±20
$r_{1,t}$	1.90±0.02	2.15±0.02	1.90±0.03

IV. 3. Physico-chemical characterisation of lanthanide complexes formed with a novel oxa-aza macrocyclic ligand, L^1

A novel macrocyclic ligand (Scheme IV.3.1.) - based on an oxa-triaza ring - was synthesized as a potential chelating agent of lanthanide complexes for MRI applications. The ligand L^1 was prepared by dr. Gyula Tircsó. It was known from preliminary luminescence lifetime measurements that the lanthanide complexes formed with this new ligand contain two inner sphere water molecules. This finding indicates that the efficiency (relaxivity) of the GdL^1 complex might be higher than that for currently used MRI contrast agents containing one water molecule, provided that water exchange is sufficiently fast. On the other hand, the presence of the three amine protons might give PARACEST activity to the YbL^1 or EuL^1 complexes. These two favorable features suggested that we can design a PARACEST and a classical T_1 MRI contrast agent with the same ligand.

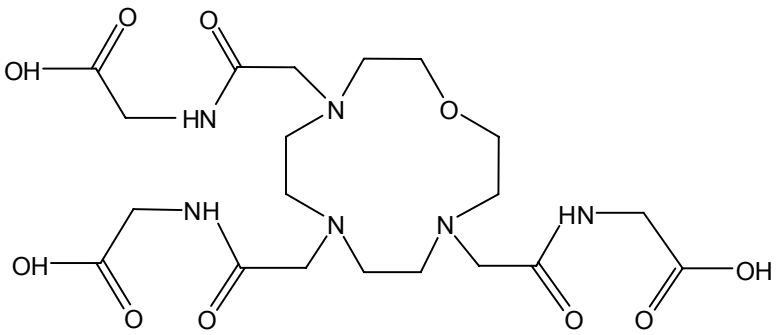

Scheme IV.3. 1. Structure of ligand L^1

The objective of this study was to determine the thermodynamic stability constants for the series of LnL^1 complexes and compare them to

those of complexes formed with structurally similar macrocyclic ligands, especially DOTA, DO3A (1,4,7,10-tetraazacyclododecane-1,4,7,-triacetic acid) and their derivatives. The kinetics of LnL^1 complex formation, the acid catalyzed dissociation of LnL^1 complexes, and the transmetallation reactions with biologically relevant metal ions were also investigated and compared to other systems described previously. Based on the structural features of L^1, additional physico-chemical measurements were performed on the lanthanide(III)-complexes involving ^{17}O-NMR, PARACEST and anion binding studies.

Ligand protonation constants and stability constants of the complexes

The ligand L^1 has seven protonation sites, and five protonation steps of these were detected in the pH range 1.9–11.5, when the ligand was titrated with a strong base (NaOH). The protonation constants obtained by pH-potentiometric measurements are presented in Table IV.3.1.

Table IV.3.1. Calculated protonation constants of L^1.

	L^1
$\log K_1$	8,38(0,07)
$\log K_2$	5,33(0,09)
$\log K_3$	3,92(0,08)
$\log K_4$	3,44(0,08)
$\log K_5$	2,77(0,05)

The first two protonation constants can be assigned to two nitrogen atoms of the macrocyclic ring, while the next three protonation steps occur

most likely on the acetate groups of the glycinate arms. It is in accordance with previous observations reported for tetraaza macrocyclic polyamino-polycarboxylate ligands.[12] The overall basicity ($\Sigma\log K_i^H$) of L^1 is 23.9. Although this value seems to be high enough for stable complexation of Ln(III) ions, it is about 4-5 orders of magnitude lower than those of DO3A and DOTA. Therefore, the thermodynamic stability constants for the complexes of L^1 are expected to be significantly lower than that of the corresponding DOTA-, or DO3A analogues.

It was confirmed by preliminary spectrophotometric measurements that the formation of the CeL^1 complex is immediate under the given conditions (pH=4.5, metal-ligand ratio 1:1). Based on this finding, and on the highly similar coordination behaviour of all Ln(III) ions, the formation of all LnL^1 complexes was considered to be fast, too, and thus the stability constants of these complexes have been determined by direct pH-potentiometric titrations.

The stability constants of L^1 complexes with trivalent lanthanide(III) ions are listed in Table IV.3.2. along with the stabilities of endogenous bivalent ML^1 complexes.

Table IV.3.2. Stability constants of the complexes formed with L^1

	ML	**MHL**	**MH_2L**	**$MH_{-1}L$**	**MOHL**
Ca(II)	7,97(0,02)	4,51(0,03)	-	-	-
Mg(II)	3,04(0,04)	-	-	-	-
Zn(II)	11,57(0,03)	4,13(0,02)	-	-	9,39(0,02)
Cu(II)	13,42(0,03)	3,66(0,02)	3,43(0,03)	6,42(0,09)	10,79(0,04)
La(III)	9,23(0,10)	3,99(0,09)	3,36(0,06)	-	-
Ce(III)	11,31(0,05)	3,66(0,07)	3,29(0,07)	-	-
Nd(III)	11,98(0,05)	3,55(0,07)	3,06(0,07)	-	-
Eu(III)	12,85(0,05)	3,53(0,06)	2,83(0,07)	-	-
Gd(III)	12,47(0,09)	3,97(0,08)	2,81(0,11)	-	-
Dy(III)	12,94(0,04)	3,6(0,03)	2,56(0,10)	-	-
Yb(III)	12,45(0,05)	3,62(0,05)	2,78(0,08)	-	-
Lu(III)	11,28(0,04)	3,56(0,05)	-	-	-

As it was expected by taking into account the total basicity of L^1, the stability constants obtained from pH-potentiometric titrations of the LnL^1 complexes are relatively low in comparison to the complexes formed with other macrocylic ligands; several orders of magnitude lower than for instance those of the corresponding M(DOTA) chelates.[111] The stability constants of LnL^1 complexes increase from Ce(III) to Eu(III), then remain relatively constant. (Figure IV.3. 1.)

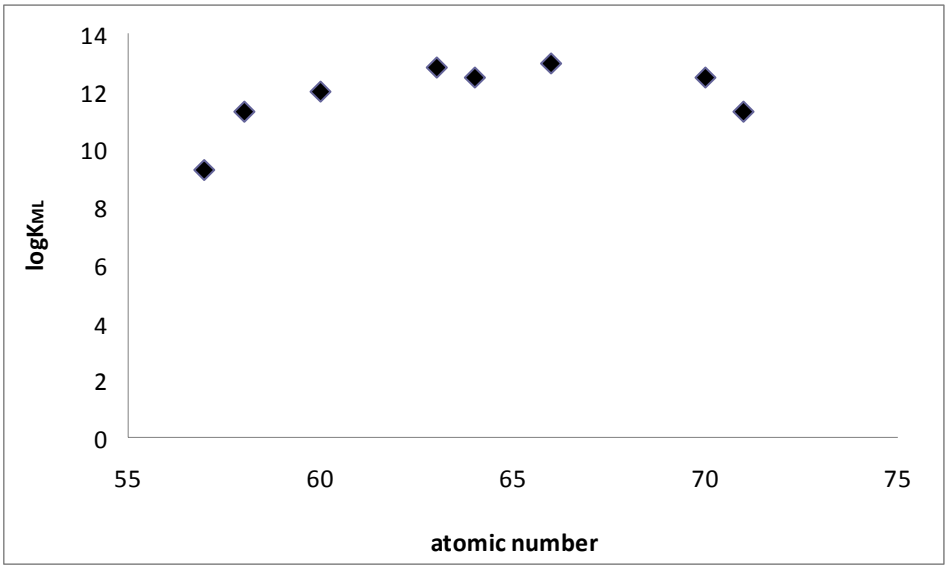

Figure IV.3.1. Stability constants of LnL^1 complexes as a function of atomic number

Regarding this trend, this ligand is more similar to the linear DTPA and its derivatives than to macrocyclic polyamino-polycarboxylate chelators. As it was mentioned in the Bibliographic review section, the stabilities of macrocyclic lanthanide(III) complexes depend on many parameters, and among these, in general, the size of the macrocyclic ring has a primordial role. In this case, the substitution of one of the ring N-atoms with an ether oxygen probably makes the macrocyclic ring smaller and more rigid, which leads to the diminution of the stability constants.

All LnL^1 complexes exist in mono- and diprotonated (except LuL^1) forms under acidic conditions (pH< 4.0). The presence of differently protonated species were detected in the case of Ca(II), Cu(II) and Zn(II) complexes, too. CuL^1 and ZnL^1 complexes loose one equimolar proton above pH > 9.0 as a consequence of the deprotonation of one of the coordinated

water molecule in the complexes. Similar monohydroxo species have been reported for a number of Cu(II)- and Zn(II)-polyamino-polycarboxylate chelates.[112] Interestingly, a second deprotonated complex was detected preceeding the formation of $Cu(OH)L^1$ at pH= 6.4 which is probably the result of the deprotonation of one amide-NH group. It should be noted, however, that additional UV-Vis measurements would be required for assessing the deprotonation sequence of CuL^1.

Kinetic studies on LnL^1 complexes

Although the thermodynamic stability of LnL^1 complexes is relatively low, a high kinetic inertness of the complexes might compensate for that and result in a safe *in vivo* use. Therefore, a detailed kinetic study – including proton assisted dissociation and metal exchange reactions with Cu(II), Zn(II) and Eu(III) - was performed in order to assess the possible dissociation pathways of LnL^1 complexes.

The proton assisted dissociation of CeL^1 has been studied in excess of HCl by UV-Vis spectrophotometry. The reactions were followed at 270 nm, where the absorbance changes are significantly high. The rate of dissociation is directly proportional to the concentration of the complex:

$$-d[CeL^1]_t/dt= k_d[CeL^1]_t \qquad \text{(IV.3. 1)}$$

where k_d is a pseudo-first-order rate constant.

The pseudo-first-order rate constants vs. HCl concentration curve shows saturation kinetics (Figure IV.3.3). This can be interpreted by accumulation of a diprotonated intermediate complex with increasing H^+-

concentration. Taking into account all possible dissociation pathways the pseudo-first-order rate constant can be expressed with Eq. (IV.3.2):

$$k_{obs} = \frac{k_0 + k_1 K_1 [H^+] + k_2 K_1 k_2 [H^+]^2}{1 + K_1 [H^+] + K_1 K_2 [H^+]^2} \qquad \text{(IV.3.2)}$$

where k_0 is a constant that describes dissociation independent of the acid concentration, k_1 and k_2 are rate constants describing acid-catalyzed dissociation, and K_1 and K_2 are the protonation constants of the mono- and diprotonated CeL^1 complexes. The calculated k_d values were fitted to Eq. (IV.3. 2) with the program SCIENTIST, k_0 was fixed to zero, K_1 and K_2 were known from pH potentiometric studies. The fitting of the k_d data gave k_1= 0.0186 ± 0,002 $M^{-1}s^{-1}$ and k_2= 0.0157 ± 0.002 $M^{-2}s^{-1}$. The experimental data and the fitted curve are shown in Figure IV.3.3.

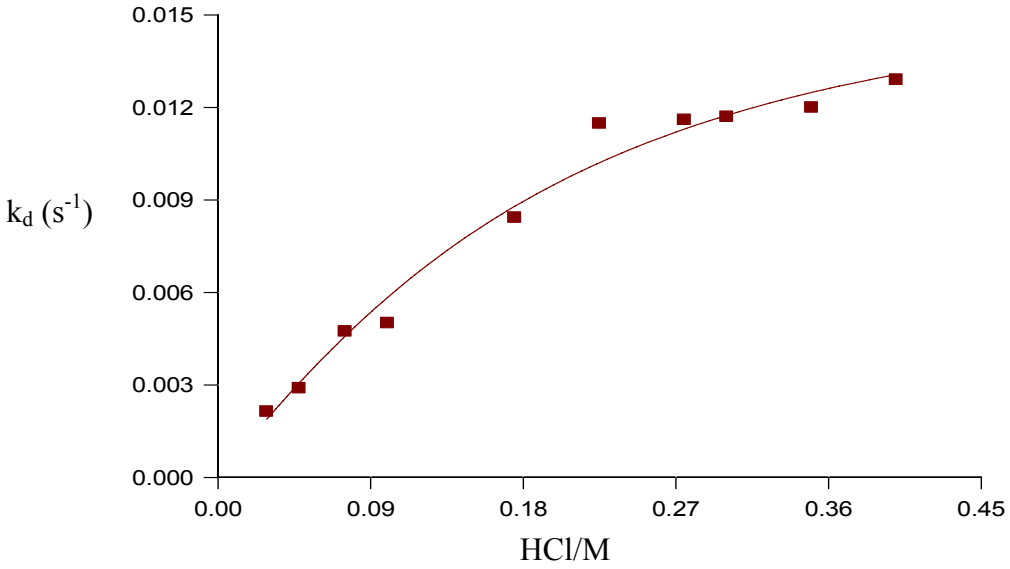

Figure IV.3.3. Dissociation rate constants for CeL^1 (0,1 mM) as a function of the H^+ concentration, t= 25 °C, I=0,15 M NaCl

Considering that the concentration of H^+-ions is negligible at physiological pH, the biologically more relevant transmetallation reactions were also studied between GdL^1 and Cu(II), Zn(II) and Eu(III) under pseudo-first-order conditions. Since the stability constants of CuL^1, ZnL^1 and EuL^1 are comparable with that of GdL^1, these metal exchange reactions take place completely if metal ion excess is used. Surprisingly, no quantitative data could be obtained in the case of Cu(II)-exchange, because the calculated pseudo first order rate constants are independent both on the H^+-ion and the Cu(II)-concentration. The only explanation for this unusual mechanism might be the formation of a relatively stable GdL^1Cu mixed complex that is formed immediately after mixing GdL^1 and Cu(II) and dissociates slowly to free Gd(III) and CuL^1. Thus, instead of Cu(II), Eu(III) was used in order to get more quantitative information about the possible transmetallation reactions of GdL^1.

The transmetallation pathways of GdL^1 with Zn(II) and Eu(III) differ essentially (Figure IV.3. 4-5.).

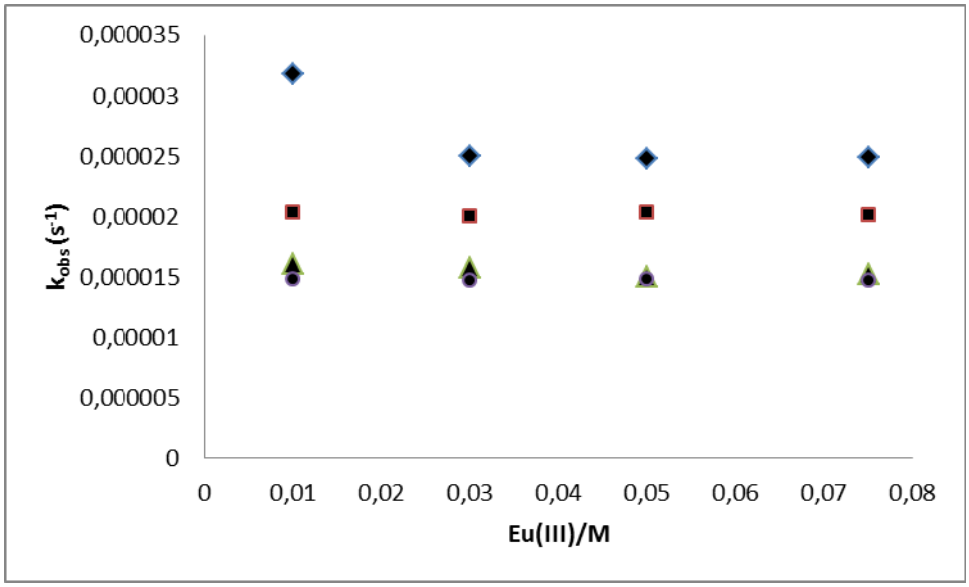

Figure IV.3. 4 . Dependence of k_{obs} on the Eu(III)-concentration at pH= 3,5 (♦), 3,75 (■), 4,3 (▲) and 4,75 (●), [GdL^1]= 1 mM, I=0,15 M NaCl

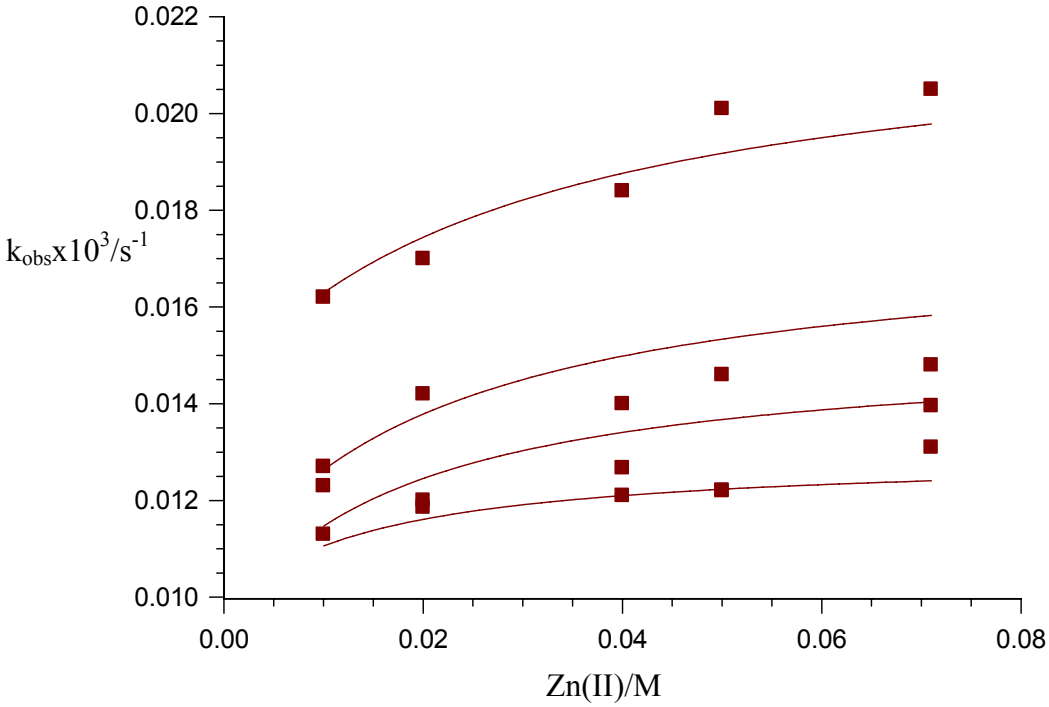

Figure IV.3. 5. Dependence of k_{obs} on the Zn(II)-concentration, [GdL^1]= 1 mM, I=0,15 M NaCl

Practically, the pseudo first order rate constants obtained for the Eu(III)-exchange depend only on the H^+ -ion concentration, which indicates that the exchange reaction takes place mainly by proton-assisted pathway. From this dependency, two constants could be calculated: k_0 = 1x10^{-5} s^{-1} (spontaneous dissociation) and k_1 = 0.038 $M^{-1}s^{-1}$ (proton-assisted dissociation). It is worth mentioning that the spontaneous dissociation pathway is quite unusual among the lanthanide(III)-polyamino-polycarboxylate complexes. This finding suggests that the GdL^1 complex itself is not stable enough neither thermodynamically, nor kinetically.

The rate constants calculated for the Zn(II)-exchange depend both on the H^+-ion and Zn(II)-concentration showing that L^1 complexes behave similarly to DTPA analogues. Taking into account all possible dissociation pathways, the pseudo first order rate constants were fitted to Equation (IV.3. 3):

$$k_{obs} = \frac{k_0 + k_1[H^+] + k_2[H^+]^2 + k_3[M]}{1 + K_{HGdL}[H^+] + K_{GdLM}[M]} \qquad \text{(IV.3.3)}$$

The calculated rate constants are summarized in Table IV.3.3.

Table IV.3.3. Rate constants obtained for the exchange reaction of GdL^1 with Zn^{2+} and Cu^{2+} at 25 ºC.

	GdL^1		**$Gd(DTPA)^{2-}$, [68]**	
	Zn^{2+}	**Eu^{3+}**	**Zn^{2+}**	**Cu^{2+}**
k_1 / $M^{-1}s^{-1}$	(1.36±0.02)x10^{-5}	(1.36±0.02)x10^{-5}	0.58	-
k_2 / M^{-2} s^{-1}	0.0364±0.001	0.0364±0.001	9.7×10^4	-
k_3^M / $M^{-1}s^{-1}$	1116±155	-	0.056	0.93
K_{GdLM} / M^{-1}	(9.3±3.5)x10^{-4}	-	7	13
logK^H_{GdL}	74±31	-	2.0	-

The most important difference between the behaviour of GdL^1 and $Gd(DTPA)^{2-}$ is that the direct attack of the exchanging metal ions and the proton assisted dissociation pathway are more efficient in the case of $Gd(DTPA)^{2-}$, while the spontaneous dissociation plays a crucial role in the decomplexation of GdL^1. Based on these facts, the formation of relatively stable Gd(L)M intermediates and their unexpectedly high kinetic activities can be the explanation for the low kinetic inertness of GdL^1.

Aninon-binding studies

The formation of ternary complexes between GdL^1 and carbonate, phosphate, lactate and citrate ions has been studied by measuring the longitudinal relaxation rates ($1/T_1$) of water protons on a Stelar relaxometer at 7.2 MHz at 25 ^oC. The concentration of the Gd(III) complex was 1 mM while the concentration of each anion varied between 0-300 mM. 0.01 M HEPES was used as buffer to maintain a constant pH (pH= 7.4) and the ionic strength was maintained by 0.15 M NaCl.

No interaction could be detected with phosphate and citrate. In the case of carbonate and lactate, strong ternary complex formation was observed in agreement with the replacement of one inner sphere water molecule (Figures IV.3. 6. and 7.). The calculated binding constants for carbonate and lactate are 62 (15), and 52 (3) M^{-1}, respectively.

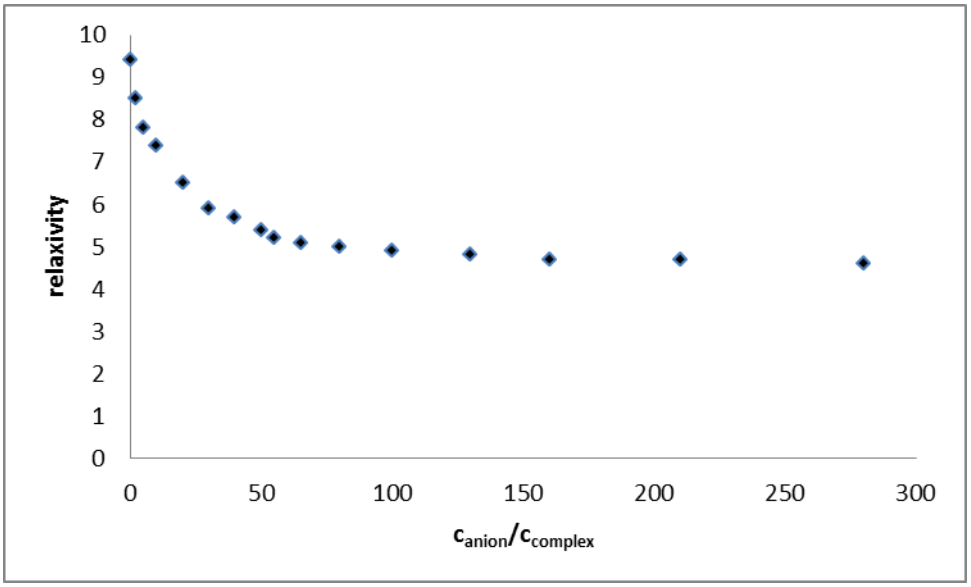

Figure IV.3.6. Relaxivity of GdL^1 (1 mM) in the presence of increasing carbonate concentration, 25 ^oC

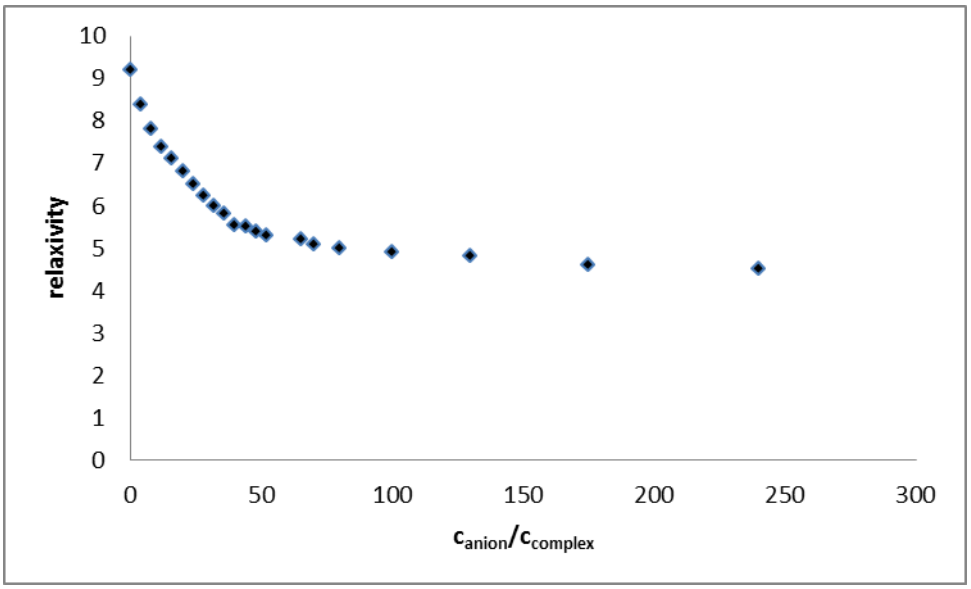

Figure IV.3.7. Relaxivity of GdL^1 (1 mM) in the presence of increasing lactate concentration, 25 ^oC

Thus, unfortunately, GdL^1 has no specificity towards the corresponding anions, but might have a significantly decreased relaxivity in the presence of low molecular weight metabolites, which leads to less efficiency.

^{17}O NMR studies, determination of the water exchange rate

It has become clear from the results presented so far that the ligand L^1 has probably no potential for the complexation of gadolinium(III) for MRI applications. Nevertheless, we have performed variable-temperature ^{17}O-NMR measurments on the GdL^1 complex to assess parameters describing water exchange and rotational dynamics.

The variable temperature ^{17}O NMR data, including reduced transverse and longitudinal relaxation rates and chemical shifts have been evaluated

according to the Solomon-Bloembergen-Morgan theory of paramagnetic relaxation. The reduced transverse relaxation rates and chemical shifts (Figure IV.3. 8) clearly show that the system is in the slow exchange limit up to ~320 K (the maximum on the $\ln(1/T_{2r})$ curve). Therefore, in the fit the scalar coupling constant has to be fixed to -3.6 MHz, a typical value for Gd^{3+} complexes. Also, given the limited number of points outside the slow exchange regime, the parameters describing electron spin relaxation can only be obtained with a relatively high error, therefore not reported in Table IV.3.4. We should note, however, that the rate and the enthalpy of water exchange as well as the rotational correlation times and its activation energy are determined with a good certitude.

As it is seen in Table IV.3. 4., the water exchange rate determined is indeed relatively low, one order of magnitude lower than that on $Gd(DOTA)^-$. Such slow water exchange might offer the possibility for YbL^1 to act as a PARACEST agent. As for the rotational correlation time, it is remarkably higher than the τ_R^{298} value for $Gd(DOTA)^-$. This difference can be likely related to the larger size of the ligand, and to the non-coordinating, deprotonated carboxylate functions that keep a second sphere hydration shell around the complex which therefore tumbles more slowly than $Gd(DOTA)^-$.

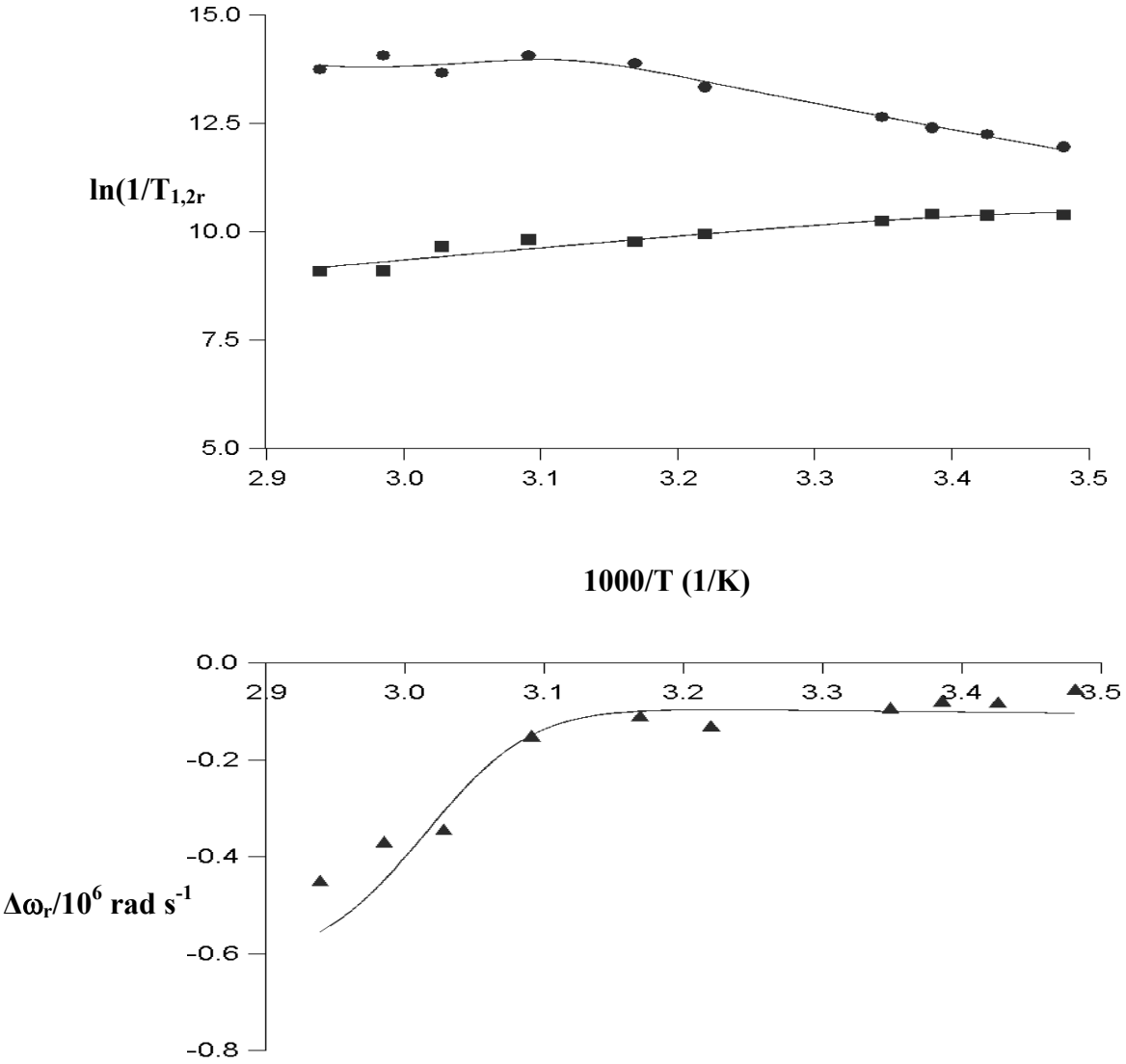

Figure IV.3. 8. Reduced tranverse (circles) and longitudinal (squares) ^{17}O relaxation rates (top) and chemical shifts (bottom) for GdL[1]. The lines represent the least-square fit according to the Solomon-Bloembergen-Morgan theory

Table IV.3. 4. Water exchange rate and rotational parameters obtained from ^{17}O NMR data for GdL^1 and GdDOTA

	GdL^1	**$Gd(DOTA)^{-a}$**
k_{ex}^{298}/s^{-1}	**$(3.1 \pm 0.3)x10^5$**	**$48x10^5$**
$\Delta H^{\ddagger}$ / kJ mol^{-1}	46.4 ± 0.6	48.8
τ_{rO}^{298} / ps	186 ± 12	90
E_R / kJ mol^{-1}	23.7 ± 2.2	17

a. from D. H Powell, O. M. Ni Dhubhghaill, D. Pubanz, L. Helm,Y. S. Lebedev, W. Schlaepfer, A. E. Merbach, *J. Am. Chem. Soc.* **1996,** *118,* 9333-9346

PARACEST measurements

PARACEST spectra of YbL^1 were recorded in the absence and presence of lactate and carbonate ions at 37 ^oC. The concentration of YbL^1 was 20 mM, the concentration of carbonate was varied between 0-1.0 M, while concentration of the lactate was 1.5 M. 0.01 M HEPES was used as buffer to maintain a constant pH=7.4. As shown above, ternary complex formation has been proved between the GdL^1 complex and carbonate and lactate ions and therefore we were interested to see if this has an effect on the PARACEST spectrum.

As it was expected, given the exchangable amide protons on the ligand, a PARACEST effect could be detected for YbL^1 at approximately +28 ppm (Fig. 3. 9.).

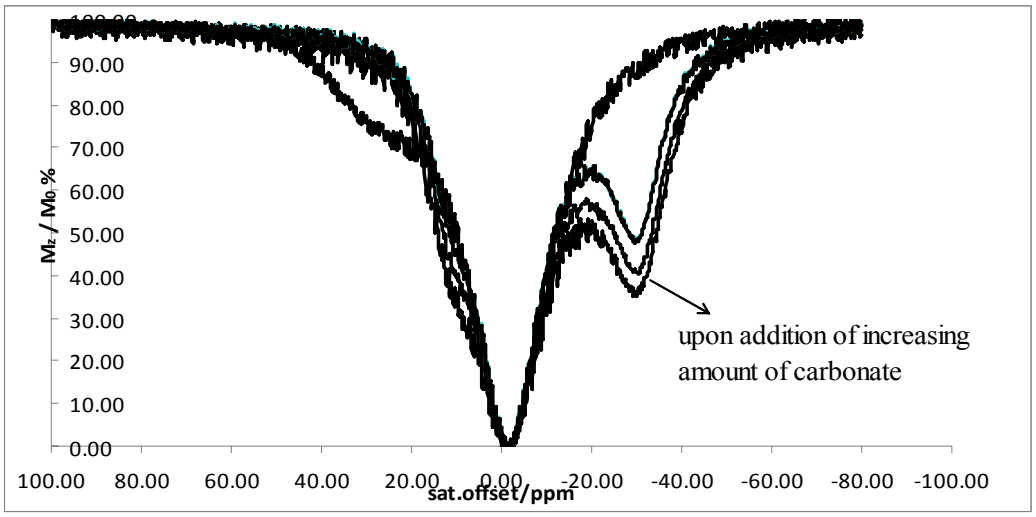

Figure IV.3.9. PARACEST spectra of YbL^1 in the absence and presence of carbonate ion.

Surprisingly, upon addition of carbonate, a new PARACEST peak appears at -30 ppm which is inreasing with increasing carbonate ion concentration, while the original peak at +28 ppm disappears. Lactate addition has no effect on the PARACEST spectrum of the complex. So far we do not have a clear explanation of the different behaviour of lactate and carbonate with respect the PARACEST effect, given the fact that very similar binding constants were calculated from the relaxometric titrations for both anions. Since the PARACEST effect is linked to the exchange of the amide protons, this difference indicates that the binding of carbonate or lactate ions does not have the same influence on the amide protons, even if the coordinated water molecule is expelled in both cases.

V. Experimental section

V. 1. Materials

The $LnCl_3$ stock solutions were prepared by dissolving the corresponding Ln_2O_3 (99.9%, Fluka) in 6 M HCl and the excess of acid was evaporated off. The concentration of the lanthanide(III) (Ln(III)) stock solutions was determined by complexometric titration using standardized Na_2H_2EDTA solution in the presence of xylenolorange as an indicator. The stock solutions of the DTPA (Fluka), BOPTA (Bracco Imaging S.p.A.), DTPA-BMA (Bracco Imaging S.p.A.) and TTHA (Fluka) were prepared by dissolving the solid ligands in double distilled water. The ligand concentrations were determined by pH-potentiometry on the basis of the titration curves obtained in the absence and presence of a 50 fold excess of Ca^{2+}. Phosphate, citrate, hydrogen-carbonate, NaCl, and the other metal chloride stock solutions were prepared from analytical grade salts in double distilled water.

V. 2. pH-potentiometry

In the case of DTPA, BOPTA, DTPA-BMA and TTHA, the pH-potentiometric titrations were made with standardized NaOH solution at 25 ^{o}C at a constant ionic strength, (0.15 M NaCl). The samples (10 ml) were stirred with a magnetic stirrer, while a constant N_2 flow was bubbled through the solutions. A Metrohm 6.0233.100 combined electrode was used to measure the pH. The pH-meter was calibrated using standard KH-phtalate (pH= 4.004) and borax (pH= 9.177) buffers. The potentiometric measurements were carried out with the use of a computer-controlled

Methrom 702 SM Titrino automatic burette. The H^+ ion concentrations have been calculated from the measured pH values by the method, suggested by Irving et al.

The protonation constants of $bp12c4^{2-}$ and stability constants of its metal complexes (Ln : La, Ce, Eu, Gd, Dy and Yb) were determined by pH-potentiometric titration at 25ºC in 0.1 M KCl. The samples (3 ml) were stirred while a constant N_2 flow was bubbled through the solutions. The titrations were carried out adding standardized KOH solution with a Methrom 702 SM Titrino automatic burette. A Metrohm 692 pH/ion-meter was used to measure pH.

The protonation constants of L^1 and stability constants of its metal complexes (Ln: La, Ce, Nd, Eu, Gd, Dy, Yb, Lu and M: Mg, Ca, Zn, Cu) have been determined in 0.15 M NaCl at 25 ^oC. The protonation constants of the ligand were calculated from the potentiometric data obtained by titrating 2 mM samples with a standardized NaOH solution in the absence of Ca^{2+} in the pH range 1.8-11.5.

The stability constants of ML^1 metal complexes were calculated by titrating samples containing equimolar amounts of ligand and metal ion (2 mM) in the pH range 1.8-5.5. The samples (3 ml) were stirred while a constant N_2 flow was bubbled through the solutions. A Metrohm 692 pH/ion-meter was used to measure pH. The pH/ion-meter was calibrated using standrad pH=4.00 and pH=7.00 buffers. The potentiometric measurments were carried out by use of a computer-controlled Methrom 702 SM Titrino automatic burette.

The protonation and stability constants were calculated from parallel titrations with the program PSEQUAD. The errors given correspond to one standard deviation.

V. 3. Kinetic studies

The progress of the ligand exchange reactions between the Gd^{3+} complexes formed with the DTPA derivatives (GdL) and H_iTTHA (H_iX) in the absence and presence of the endogenous anions was followed by measuring the water proton relaxation rates ($1/T_1$) of the samples with an MS-4 NMR spectrometer (Institute Jozef Stefan, Ljubljana) at 9 MHz or a Bruker minispec mq20 NMR analyzer at 20 MHz. The longitudinal relaxation times were measured by the inversion recovery method (180^o - τ - 90^o) by using 8-10 different τ values. The concentration of the GdL complexes in the samples was generally 1.0 mM.

For studying the effect of TTHA on the reaction rates, the concentration of TTHA was varied between 5-40 mM, while the pH of the samples was maintained constant (pH= 7.4) by a non-coordinating buffer, HEPES. In the pH-dependent measurements the pH of the samples was varied in a broad pH range (6.5-11.0), when the concentration of TTHA was 10 mM.

In the samples containing the different endogenous anions, the concentration of TTHA was 2.0 mM, the pH was adjusted to 7.4, the citrate-, phosphate- and hydrogen-carbonate concentrations were varied between 0-20 mM and 0-40 mM, respectively.

The kinetic measurements were started (t= 0 s) by mixing the calculated volume of the GdL complex with a solution containing the ligand TTHA, or the ligand TTHA and the Na-salt of the corresponding endogenous anion. The GdL complex and the TTHA solutions were pre-thermostated at 25 ^oC. All kinetic measurements were carried out at 25 ^oC in 0.15 M NaCl solution to maintain a constant ionic strength. The first-order rate constants (k_{obs}) have been calculated with the use of Equation (V. 1):

$$r_{1t} = (r_{10} - r_{1e})\exp(-k_{obs}t) + r_{1e} \qquad \text{(V. 1)}$$

where r_{10}, r_{1t}, and r_{1e} are the measured relaxivity values at the start, at time t, and at equilibrium of the reaction.

The proton assisted dissociation of the Ce^{3+} complex of $bp12c4^{2-}$ has been studied in the presense of a large excess of HCl, where the complex is unstable. The reaction was followed at 25 °C by monitoring the decrease of the absorbance of the complex at 280 nm in the range of proton concentrations 0.001-0.04 M. The concentration of the complex was 0.0001 M.

The exchange reactions between $Gd(bp12c4)(H_2O)_q^+$ and Zn^{2+} have been studied by measuring the longitudinal relaxation rates ($1/T_1$) of water protons on a Bruker Avance 500 (11.75 T) NMR spectrometer in the pH range 4.6-5.3. The Zn^{2+} concentration varied between 0.005 M and 0.03 M, while the concentration of the Gd^{3+} complex was 0.0002 M. 0.02 M N-methyl-piperazine was used as buffer and the ionic strength was 0.1 M KCl. The relaxivities, r_1, were calculated from the measured $1/T_{1obs}$ water proton relaxation rates according to Eq. (1), where $1/T_{1w}$ is the relaxation rate of water at the given temperature, and [Gd] is the Gd^{3+} concentration in mM.

$$\frac{1}{T_{1obs}} = \frac{(1}{T_{1w}} + \frac{1}{T_{1p}} = \frac{1}{T_{1w}} + r_1 \times [Gd] \qquad \text{(V. 2)}$$

The pseudo-first-order rate constants (k_{obs}) were calculated by fitting the relaxation rate data to Eq. (V. 2) (see above).

The dissociation rate constants of the metal exchange reaction with Cu^{2+} were determined by UV-vis measurements following the increase of the

absorbance at 300 nm. The concentration of the gadolinium(III)-complex was 0.0001 M, the Cu^{2+} concentration varied between 0.001 M and 0.02 M and MES was used as buffer. The rate of the exchange reaction was studied at different pHs (4.6-5.3).

The proton assisted dissociation of CeL^1 has been studied in the presence of a large excess of HCl, where the complex is unstable. The reaction was followed by monitoring the decrease of the absorbance of the complex at 270 nm in the range of proton concentrations 0.03-0.4 M. The concentration of the CeL^1 was 0.1 mM.

The exchange reactions between GdL^1 and Zn^{2+} and Eu^{3+} have been studied by measuring the longitudinal relaxation rates ($1/T_1$) of water protons on a Stelar relaxometer (7.2 MHz) in the pH range 3.5-5.3, at 25 ^oC. The temperature in the sample holder was maintained with an air stream. The Zn^{2+} concentration varied between 0.01 M and 0.071 M, the Eu^{3+} concentration varied between 0.01 M – 0.075 M, while the concentration of the Gd^{3+} complex was 0.001 M. 0.02 M N-methyl-piperazine was used as buffer and the ionic strength was 0.15 M NaCl.

The dissociation rate constants of the metal exchange reaction with Cu^{2+} were determined by UV-vis measurements following the increase of the absorbance at 272 nm. The concentration of the gadolinium(III)-complex was 0.0001 M, the Cu^{2+} concentration varied between 0.0004 M and 0.02 M and N-methyl piperazine was used as buffer. The rate of the exchange reaction was studied at different pHs (4.3-5.25).

V. 4. NMR measurements

^1H- and ^{13}C-NMR spectra of La(DTPA-BMA) and $Eu(DTPA)^{2-}$ were recorded on a Bruker Avance 500 MHz spectrometer in the temperature

range 274-298 K in the absence and presence of ligand excess. The pH of the samples was adjusted to 7.4. The concentration of La(DTPA-BMA) and $Eu(DTPA)^{2-}$ were 0.1 M, while the concentration of DTPA-BMA and DTPA excess were varied between 0.25 and 0.5 M.

PARACEST spectra of YbL^1 were measured on a Brucker Avance 500 (11.75 T) NMR spectrometer in the absence and presence of lactate and carbonate ions at 37 ^oC. The concentration of YbL^1 was 20 mM, the concentration of carbonate was varied between 0-1.0 M, while concentration of the lactate was 1.5 M. 0.01 M HEPES was used as buffer to maintain a constant pH=7.4, in case of lactate binding measurements the pH was varied between 6.5-8.0. 10 % D_2O was added to the samples.

V. 5. ^{17}O NMR measurements

The transverse and longitudinal ^{17}O relaxation rates ($1/T_{1,2}$) and the chemical shifts were measured in a $Gd(bp12c4)(H_2O)_q^+$ aqueous solution in the temperature range 280–345 K, on a Bruker Avance 500 (11.75 T, 67.8 MHz) spectrometer.

Variable-temperature ^{17}O-NMR measurments on the GdL^1 complex were performed on Bruker Avance 500 (11.75 T, 67.8 MHz) spectrometer. Transverse and longitudinal ^{17}O relaxation times and chemical shifts were measured between 287,2 K and 343,3 K. GdL^1 was prepared by mixing ligand stock solution with a $GdCl_3$ solution. A slight excess of ligand (3 %) was used to ensure complete coordination of Gd(III), and the pH was adjusted to 5,55 with addition of NaOH. The absense of free Gd(III) was controlled with the xylenolorange test.

The temperature was calculated according to previous calibration with ethylene glycol and methanol. An acidified water solution was used as reference ($HClO_4$, pH 3.3). Longitudinal ^{17}O relaxation times (T_1) were measured by the inversion-recovery pulse sequence, and the transverse relaxation times (T_2) were obtained by the Carr-Purcell-Meiboom-Gill spin-echo technique. The samples were sealed in glass spheres fitted into 10 mm NMR tubes, to eliminate susceptibility corrections to the chemical shifts. To improve sensitivity in ^{17}O NMR, ^{17}O-enriched water (10 % $H_2{}^{17}O$, CortecNet) was added to the solutions to yield around 1 % ^{17}O enrichment. The ^{17}O NMR data have been evaluated according to the Solomon-Bloembergen-Morgan theory of paramagnetic relaxation.

V. 6. Ternary complex formation

The formation of ternary complexes between $Gd(bp12c4)(H_2O)_q^{+}$ and carbonate, phosphate and citrate ions has been studied by measuring the longitudinal relaxation rates ($1/T_1$) of water protons on a Bruker NMR spectrometer at 500 MHz and 25 ^{o}C. The concentration of the Gd^{3+} complex was 1 mM while the concentration of each anion varied between 0-36 mM by adding 15 μl portions of the anion stock solution to 0.5 ml complex solution in the NMR tube. The exact concentration of the complex and the anions were calculated in each point; 0.01 M HEPES was used as buffer to maintain a constant pH (pH= 7.4), while the ionic strength was 0.15 M NaCl.

The formation of ternary complexes between GdL^1 and carbonate, phosphate, lactate and citrate ions as well as some endogenous metal ions (Cu, Zn, Ca) has been studied by measuring the longitudinal relaxation rates ($1/T_1$) of water protons on a Stelar relaxometer at 7.2 MHz at 25 ^{o}C. The concentration of the Gd(III)-complex was 1 mM while the concentration of

each anion varied between 0-300 mM depending on the relaxivity changes by adding small portions of known concentration of cation/anion stock solution to 1.0 ml complex solution in a 10 mm NMR tube. The exact concentration of the complex and the added ions were corrected at each point. 0.01 M HEPES buffer was used, and the samples were contained 0,15 M NaCl.

VI. Summary

The $Gd(DTPA)^{2-}$, $Gd(BOPTA)^{2-}$ and Gd(DTPA-BMA) complexes, used as contrast agents in MRI, undergo exchange reactions with multidentate ligands, like TTHA. The dissociation of Gd^{3+} complexes through the ligand exchange reactions occurs significantly faster at pH=7.4 than the dissociation via the proton assisted pathway. The ligand exchange reactions take place with the direct attack of the $H_iTTHA^{(6-i)-}$ species on the Gd^{3+} complexes, through the formation of ternary intermediates. The formation of ternary intermediates is related to the intramolecular rearrangements, occurring in the Gd^{3+} complexes. The rate of the rearrangements is higher in the Gd(DTPA-BMA) (it is indicated by NMR studies) and so the rates of the ligand exchange reactions of this complex are about two to three orders of magnitude higher than those of the $Gd(DTPA)^{2-}$ and $Gd(BOPTA)^{2-}$. The lower kinetic inertness of Gd(DTPA-BMA) is consistent with the experiences, showing that it dissociates faster than $Gd(DTPA)^{2-}$ or $Gd(BOPTA)^{2-}$, so the amount of retained Gd^{3+} in the living systems can be higher when Gd(DTPA-BMA) (Omniscan) is used as MRI contrast agent.

The rates of the ligand exchange reactions of Gd(DTPA-BMA) increase with the increase of pH from 6.5 to 9, because the attack of the less protonated $H_iTTHA^{(6-i)-}$ species via the formation of the ternary intermediates is more efficient. The increase of the rates of the exchange reactions of $Gd(DTPA)^{2-}$ and $Gd(BOPTA)^{2-}$ from pH 8.5 to 11 can be interpreted similarly, but on the contrary, the increase of pH from 6.5 to 8.5 results in a decrease in the rates of the reactions. This unexpected trend has been interpreted by assuming the validity of the general acid catalysis, which has a lower effect at higher pH. The proton(s) from the $H_iTTHA^{(6-i)-}$ species, can be

transferred to the coordinated DTPA or BOPTA, when the dissociation of these ligands from the Gd^{3+} complex is more probable.

The ligand exchange reactions take place faster in the presence of the endogenous citrate, phosphate and carbonate ions at pH= 7.4. The rates of the exchange reactions increase with the increase in the concentration of these ions, but the effect of the citrate and phosphate is very low at their physiological concentrations. Phosphate ions may have significant effect on the reaction rates, particularly on that of the Gd(DTPA-BMA), when the kinetic studies are carried out in phosphate buffer. The effect of the carbonate ions on the reaction rates is well measurable, because of its higher physiological concentration, when the increase in the rates of the exchange reactions is the largest for the Gd(DTPA-BMA).

The stability constants of the $Ln(bp12c4)^{+}$ complexes have been obtained from direct potentiometric titrations, as the complex formation is fast. The stability increases from the early lanthanides to the middle of the series, then remains relatively constant or slightly declines for the heavier lanthanides, similarly to $Ln(DTPA)^{2-}$ chelates. In the presence of Zn^{2+}, the dissociation of $Gd(bp12c4)^{+}$ proceeds both *via* proton- and metal-assisted pathways, and in this respect, this system is intermediate between DTPA-type and macrocyclic chelates, for which the dissociation is predominated by metal- or proton-assisted pathways, respectively. The Cu^{2+} exchange shows an unexpected pH-dependency, with the observed rate constants decreasing with increasing proton concentration.

The $Gd(bp12c4)(H_2O)_q^{+}$ complex is present in hydration equilibrium between nine-coordinate, monohydrated and ten-coordinate, bishydrated species. The rate of water exchange as assessed by ^{17}O NMR is extremely high, close to that of the Gd^{3+} aqua ion itself. This fast exchange can be accounted for by the flexible nature of the inner coordination sphere. The

activation entropy suggests a strong associative character for the water exchange which presumably involves only the nine-coordinate, monohydrated species. Relaxometric and luminescence measurements, together with DFT calculations, indicate strong anion binding to $Ln(bp12c4)(H_2O)_q^+$ complexes, consistent with the complete replacement of the inner sphere water molecules.

For the novel ligand L^1, based on an oxa-aza macrocyclic ring, a comprehensive study was performed, including thermodynamic, kinetic, relaxometric, ^{17}O-NMR and PARACEST measurements of its lanthanide(III)- complexes. Lanthanide ions form stable complexes with L^1. Strong ternary complex formation was observed between GdL^1 and lactate and carbonate ions.

In the presence of carbonate ions, a strong PARACEST effect was detected which increases with increasing carbonate concentration. It is necessary to make a complex ^{1}H-NMR study in order to understand the origin of this effect.

The constants characterizing the metal-exchange reactions between GdL^1 and Eu(III)and Zn(II) ions, as well as the water exchange rate were determined at 25 ^{o}C. Surprisingly, the most important pathway in the transmetallation reactions is the spontaneous dissociation, which makes the GdL^1 complex kinetically much less inert (half time of dissociation is approximately 14 h) than Gd(III) complexes formed with other macrocyclic ligands.

VI. Összefoglalás

Vizsgáltuk a $[Gd(DTPA)]^{2-}$, $[Gd(BOPTA)]^{2-}$ és [Gd(DTPA-BMA)] komplexek és a TTHA kicserélő ligandum között lejátszódó ligandumcsere reakciók sebességét. Megállapítottuk, hogy a reakció a TTHA közvetlen támadásával játszódik le, és sokkal gyorsabb a biszamid-származék komplex esetében, mint a másik két ligandumnál. A különböző pH értékeknél kapott eredmények alapján elmondható, hogy a $[Gd(DTPA)]^{2-}$ és $[Gd(BOPTA)]^{2-}$ reakciójának sebessége minimum görbe szerint változik a pH-val, míg a [Gd(DTPA-BMA)] esetén a reakciósebesség közel exponenciálisan nő a pH növelésével. A semleges [Gd(DTPA-BMA)] komplex és a kicserélő TTHA ligandum között nem lép fel taszítás, így nagy a cserereakció sebessége. A $Gd(DTPA)]^{2-}$ és $[Gd(BOPTA)]^{2-}$ két negatív töltésű: pH> 8.5 esetén a reakciósebesség növekedés a TTHA kevésbé protonált formáinak közvetlen támadásával magyarázható, míg a pH csökkenésével tapasztalt sebességcsökkenés a protonált H_3TTHA és H_2TTHA ligandumról a Gd-komplexre történő protontranszfer lehetőségével értelmezhető.

Vizsgáltuk a plazmában lévő ligandumok hatását a $[Gd(DTPA)]^{2-}$ és $[Gd(BOPTA)]^{2-}$ és Gd(DTPA-BMA) ligandumcsere reakcióra. Mindhárom ligandum növelte a Gd(III)-komplexek ligandumcsere reakcióinak sebességét: a karbonát-ionnak van a legjelentősebb hatása: a $[Gd(DTPA)]^{2-}$ és $[Gd(BOPTA)]^{2-}$ ligandumcsere sebessége közelítőleg 50%-kal, míg a [Gd(DTPA-BMA)]-é 100%-kal nő meg a karbonát-iont nem tartalmazó mintákéhoz képest. A citrát-ionnak csak a [Gd(DTPA-BMA)]-komplex ligandumcsere reakciójára van észlelhető hatása, míg a foszfátionok sebességnövelő hatása gyakorlatilag elhanyagolható mindhárom komplex esetében. Az általunk tanulmányozott ligandumcsere reakciók tapasztalatai

alapján a komplexek kinetikai inertsége a $[Gd(BOPTA)]^{2-}$>$[Gd(DTPA)]^{2-}$ >[Gd(DTPA-BMA)] irányban csökken.

Megállapítottuk, hogy az bp12c4 ligandum és a lantanida(III)ionok között pillanatszerűen gyors a komplexképződés. Megállapítottuk a direkt pH-potenciometriás mérések alapján, hogy a ligandum stabil komplexeket képez a lantanida(III)ionokkal, a [Zn(bp12c4)]- és [Cu(bp12c4)]-komplex stabilitása pedig közel azonos a $[Gd(bp12c4)]^{+}$ stabilitásával.

Vizsgáltuk a Gd(bp12c4) és a Zn(II), valamint Cu(II)-ionok között lejátszódó fémcsere reakciók lefolyását. Megállapítottuk, hogy a Zn(II) jelenlétében lezajló fémcsere reakció lejátszódhat a Zn(II)-ionok közvetlen támadásával, illetve protonkatalizált úton is. A Cu(II)-csere esetében nem várt pH-függést tapasztaltunk: a sebességi állandók értékei a pH növelésével nőttek. Magyarázatul a Cu(II)-ionok hidroxokomplex képződési hajlama szolgálhat, ami alacsonyabb pH-n bekövetkezhet, mint Zn(II)-ionok esetében. A fémcsere reakciók során kapott sebességi állandók összevetéséből az látszik, hogy a $[Gd(bp12c4)]^{+}$ kinetikai inertsége nem nagyobb, mint a $[Gd(DTPA)]^{2-}$-komplexé.

A Gd(III)-komplexek relaxációs hatását befolyásolhatja a belső szférában kötött vízmolekula cseresebessége, ezért ^{17}O-NMR vizsgálatok segítségével meghatároztuk a $[Gd(bp12c4)]^{+}$-komplexben kötött vízmolekula/vízmolekulák cseresebességét az oldószer vízmolekulákkal. Vizsgálatainkból kiderült, hogy a mért vízcsere sebesség értéke közelítőleg azonos a Gd^{3+}(aqua)-ion vízcseresebességével, és a második legnagyobb érték az irodalomban mindezidáig fellelhető értékek között.

Megvizsgáltuk egy új, általunk előállított makrociklusos ligandum (L^1) komplexképződési sajátságait lantanida(III)-, és biológiai szempontból jelentős fémionokkal. A kapott eredmények alapján elmondható, hogy az L^1 ligandum viszonylag stabilis komplexet képez a lantanida(III)ionokkal,

azonban a fémioncsere reakciók vizsgálata alapján a GdL^1 komplex kinetikai inertsége messze elmarad a várttól. Ennek oka feltehetőleg a spontán disszociáció nagymértékű hozzájárulása a különböző fémionokkal lejátszódó reakcióutakhoz.

Minthogy a GdL^1 komplex két vízmolekulát tartalmaz a belső koordinációs szférában, erős vegyeskomplex képződést figyeltünk meg laktát- és hidrogénkarbonát ionokkal, mely a GdL^1 *in vivo* relaxivitásának csökkenéséhez vezethet. Meghatároztuk a GdL^1 vízcseresebességét, és vizsgáltuk az Yb-komplex PARACEST tulajdonságait laktát- és hidrogénkarbonát ionok jelenlétében.

VII. References

1. É. Tóth and A. E. Merbach Eds. *The Chemistry of Contrast Agents in Medical Magnetic Resonance Imaging,* John Wiley & Sons, New-York: **2001**.
2. É. Tóth; L. Helm; A. E. Merbach, *MRI Contrast Enhancement Agents*. in Comprehensive Coordination Chemistry II., Elsevier: **2003**; Vol. 9.
3. M. F. Tweedle, Relaxation Agents in NMR Imaging. J.-C. G. Bünzli, G. R. Choppin, Eds. *Lanthanide Probes in Life, Chemical and Earth Sciences: Theory and Practice*, Elsevier-Amsterdam **1989** 127.
4. R. J. Weinmann; M. Laniado; W. Muetzel, *Physiol. Chem. Phys. & Med. NMR*, **1984**, 16, 167.
5. Simon Cotton, *Lanthanides and actinides*, Macmillan Physical Science Series, **1991**
6. Cotton, F. A.; Wilkinson, G. *Advanced Inorganic Chemistry*, John Wiley & Sons, Inc, **1988**.
7. Carnall, W. T.; Fields, P. R.; Ralnak, K. *J. Chem. Phys.* **1968**, *49*,
8. H. D.Carr; J. Brown; G. M. Bydder; R. E. Steiner; H.J. Wienmann; U. Speck; A. S. Hall; I. R. Young; *Am. J. Roentgenol* **1984**, 143.
9. H. Gries; H. Miklautz; *Physiol. Chem. Phys. Med. NMR* **1984,** 16, 105.
10. Bünzli, J. C. G.; Choppin, G. R.; eds., *Lanthanide Probes in Life, Chemical and Earth Sciences: Theory and Practice.* Elsevier, Amsterdam, **1989**
11. Uggeri, F.; Aime, S.; Anelli, P. L.; Botta, M.; Brochetta, M.; de Haen, C.; Ermondi, G.; Grandi, M.; Paoli, P.; *Inorg. Chem.*, **1995**, 34
12. J. F. Desreux, E. Merciny, M. F. Loncin, *Inorg. Chem.* **1979,** 20, 987.
13. É. Tóth; E. Brücher, *Inorg. Chim. Acta* **1994,** 221, 165.
14. L. Burai; I. Fabian; R. Kiraly; E. Szilagyi; E. Brücher, *J. Chem. Soc. Dalton Trans.* **1998**, 243.
15. E. T. Clarke; A. E. Martell, *Inorg. Chim. Acta* **1991,** 190, 37.
16. A. Ringbom Ed. *Complexation in Analytical Chemistry*., New York: Interscience Publishers: **1963**.
17. P. M. May; P. W. Linder; D. R. Williams, *J. Chem. Soc. Dalton Trans.* **1977**, 588.
18. G.E. Jackson; S. Wynchank; S. Woudenberg, *Magn. Reson. Med.* **1990,** 16, 57.
19. W. P. Cacheris; S. C. Quay; S. M. Rocklage, *Magn. Reson. Imaging* **1990,** 8, 467.
20. L. Sarka; L. Burai; Brücher, E., *Chem. Eur. J.* **2000,** 6, 719.

21. E. Brücher, Kinetic Stabilities of Gadolinium(III) Chelates Used as MRI Contrast Agents, in *Contrast Agents I. Magnetic Resonance Imaging* Krause, W. Ed. Topics in Current Chemistry, Springer Verlag-Berlin: Berlin, **2002**; Vol. 221, 104.
22. E. Toth; E. Brucher; I. Lazar; I. Toth, *Inorg. Chem.* **1994,** 33, 4070
23. C. A. Chang; Y.-L. Liu; C.-Y. Chen; Chou, X.-M., *Inorg. Chem.* **2001,** 40, 3448.
24. S. P. Kasprzyk; R.G. Wilkins, *Inorg. Chem.* **1982,** 21, 3349.
25. E. Brücher; G. Laurenczy; Z.S. Makra, *Inorg. Chim. Acta,* **1987,** 139, 141.
26. X. Wang; T. Jin; V. Comblin; Lopez-Mut; E. Merciny; J. F. Desreux, *Inorg. Chem.* **1992,** 31, 1095.
27. K. Kumar; M. F. Tweedle, *Inorg. Chem.* **1993,** 32, 4193.
28. L. Wu; W.D. Horrocks, *Inorg. Chem.* **1995,** 34, 3724.
29. L. Burai; I. Fabian; R. Kiraly; E. Szilagyi; E. Brücher, *J. Chem. Soc. Dalton Trans.* **1998**, 243.
30. Bloembergen, N.; Purcell, E. M.; Pound, R. V. *Phys. Rev.* **1948**, *73*, 679.
31. Solomon, I. *Phys. Rev.* **1955**, *99*, 559.
32. Bloembergen, N.; Morgan, L. O. *J. Chem. Phys.* **1961**, *34. 3.*, 842.
33. Caravan, P; Ellison, J. J.; McMurry, T. J.; Lauffer, R. B. *Chem. Rev.* **1999**, 99, 2293.
34. Aime, S.; Botta, M.; Fasano, M.; Terreno, E. in *The Chemistry of Contrast Agents in Medical Resonance Imaging,* A.E.Merbach, É. Tóth (eds), John Wiley & Sons, Chichester, **2001**, p. 193.
35. S. Torres, S.; André, J. P.; Martins, J. A.; Geraldes, C. F. G. C.; Merbach, A. E.; Tóth, E. *Chem. Eur. J.* **2006,** 12, 940.
36. Tóth, E. ; Pubanz, D.; Vauthey, S.; Helm, L.; Merbach, A. E. *Chem. Eur. J.* **1996**, 2, 1607.
37. Zhang, S. ; Wu, K. ; Sherry, A. D. *Angew. Chem. Int. Ed. Engl.* **1999**, *38*, 3192.
38. Hovland, R.; Gløgård, C.; Aasen, A. J.; Klaveness, J. *J. Chem. Soc., Perkin Trans. 2* **2001**, 6, 929.
39. Tóth, E.; Bolskar, R. D.; Borel, A.; Gonzalez, G.; Helm, L.; Merbach, A. E. *J. Am. Chem. Soc.* **2005**, 127, 799.
40. Esqueda, A. C.; Lopez, J. A.; Andreu-de-Riquer, G.; Alvarado-Monzon, J. C.; Ratnakar, J.; Lubag, A. J. M.; Sherry, A. D.; De Leon-Rodriguez, L. M. *J. Am. Chem. Soc.* **2009**, 131, 11387.
41. Li W-H, Fraser SE, Meade TJ. *J. Am. Chem. Soc.* **1999**; 121: 1413-1414.
42. Dhingra K, Fousková P, Angelovski G et al. *J. Biol. Inorg. Chem.* **2008**, 13, 35.

43. Mishra A, Fousková P, Angelovski G et al. *Inorg. Chem.* **2008**, 47, 1370.
44. Angelovski, G.; Fousková, P.; Mamedov, I.; et al. *Chem. Bio. Chem.* **2008**, 9, 1729.
45. Ward, K. M.; Balaban, R. S. *J. Magn. Reson.* **2000**, 143, 79.
46. Ward, K. M.; Balaban, R. S. *Magn. Reson. Med.* **2000**, 44, 799.
47. Zhang, S. R.; Winter, P.; Wu, K. C.; Biewer, M. C.; Sherry, A. D. *J. Am. Chem. Soc.* **2001**, 123, 1517.
48. Aime, S.; Barge, A.; Castelli, D. D.; Fedeli, F.; Mortillaro, A.; Nielen, F. U.; Terreno, E. *Magn. Reson. Med.* **2002**, 47, 639.
49. Urbanczyk-Pearson, L. M.; Femia, F. J.; Smith, J.; Parigi, G.; Duimstra, J. A.;
50. Eckermann, A. L.; Luchinat, C.; Meade, T. J. *Inorg. Chem.* **2008**, 47, 56.
51. Trokowski, R.; Ren, J.; Kalman, F. K.; Sherry, A. D. *Angew. Chem. Int. Ed.* **2005**, 44, 6920.
52. Aime, S.; Delli Castelli, D.; Terreno, E. *Angew. Chem. Int. Ed. Engl.* **2002**, 41, 4334.
53. Parker, D. L.; Smith, V.; Sheldon, P.; Crooks, L. E.; Fussell, L. *Med. Phys.* **1983**, 10, 321.
54. Weinmann H. J., Laniado M., Muetzel W., *Physiol. Chem. Phys. Med. NMR.* **1984**, *16,* 167.
55. Van Vagoner M., Worah D., *Invest. Radiol.* **1993**, 28 (Suppl. 1), 544.
56. Port M., Idee J.-M., Medina C., Robic C., Sabaton M., Carot C., *Biometals* **2008**, 21, 469.
57. Caravan P., Ellison J. J., McMurry T. J., Lauffer R. B., *Chem. Rev.* **1999**, 99, 2293.
58. Mann J. S., J. *Comput. Assist. Tomography,* **1993**, 17 (Suppl. 1), 519.
59. Wedeking P., Kumar K., Tweedle M. F., *Magn. Res. Imag.* **1992**, 10, 641.
60. Kasokat T., Urich K., Arzneim.-Forch., *Drug Res.* **1992**, 42(I), 869.
61. Puttagunta N. R., Wendel A., Gibby W. A., Smith G. T., *Invest. Radiol.* **1996**, 31, 739.
62. White G. W., Gibby W. A., Tweedle M. F., *Invest. Radiol.* **2006**, 41, 272.
63. Morcos S. K., Br. *J. Radiol.* **2007**, 80, 73.
64. Perazella M. A., *Clin. J. Am. Soc. Nephrol.* **2007**, 2, 200.
65. Choi K. Y., Kim K. S., Kim J. C., *Polyhedron,* **1994**, 13, 567.
66. Rothermel G. J., Rizkalla E. N., Choppin G. R*., Inorg. Chim. Acta,* **1997**, 262, 133.
67. Sarka L., Burai L., Király R., Zékány L., Brücher E., *J. Inorg. Biochem.* **2002**, 91, 320.

68. Sarka L., Burai L., Brücher E., *Chem. Eur. J.* **2000**, 6, 719.
69. Brücher E., *Top. Curr. Chem.* **2002**, 221, 203.
70. Jackson G. E., Wynchank S., Woudenberg M., *Magn. Reson. Med.* **1990**, 16, 57.
71. Normann P. T., Froysaand A., Svaland M., *Scand. J. Clin. Lab. Invest.* **1995**, 55, 421.
72. Lin J., Idee J.-M., Port M., Diai A., Berthomier C., Robert M., Raynal I., Devoldere I., Carot C., *J. Pharmaceut. Biomed. Anal.* **1999**, 21, 931.
73. Puttagunta N. R., Gibby W. A., Puttagunta V. L., *Invest. Radiol.* **1996**, 31, 619.
74. Yantassee W., Fryxell G. E., Porter G. A., Pattamakomsan K., Sukwarotwat V., Chouyyok W., Koorsiripaiboon V., Xu J., Raymond K. N., *Nanomedicine: Nanotechnology, Biology and Medicine*, **2010**, 6, 1.
75. Stability Constants Database, Academic Software, Royal Society of Chemistry, **2001**, (version 5.7)
76. Baranyai Zs., Pálinkás Z., Uggeri F., Brücher E., *Eur. J. Inorg. Chem.* **2010**, 13, 1948.
77. Jenkins B. G., Lauffer R. B., *Inorg. Chem.* **1988**, 27, 4730.
78. Aime S., Botta M., *Inorg. Chim. Acta,* **1990**, 177, 101.
79. Geraldes C. F. G. C., Urbano A. M., Hoefnagel M. A., Peters J. A., *Inorg. Chem.* **1993**, 32, 2426.
80. Powell H. D., NiDhubhghaill O. M., Pubanz D., Helm L., Lebedev Y., Schlaepfer W., Merbach A. E., *J. Am. Chem. Soc.* **1996**, 118, 9333.
81. Fried A. R., Martell A. E., *J. Coord. Chem.* **1971**, 1, 47.
82. Bannister CE., Margerum D. W., *Inorg. Chem*. **1981**, 20, 3149.
83. Hauröder M., Schütz M., Wannowins K. J., Elias H., *Inorg. Chem.* **1989**, 28, 736.
84. Burai L., Hietapelto V., Király R., Tóth É., Brücher E., *Magn. Reson. Med.* **1997**, 38, 146.
85. Laurent S., Vander Elst L., Capoix MA., Muller R. N., *Invest. Radiol.* **2001**, 36, 115.
86. Mato-Iglesias, M.; Platas-Iglesias, C.; Djanashvili, K.; Peters, J. A.; Toth, E.; Balogh, E.; Muller, R. N.; Vander Elst, L.; de Blas, A.; Rodríguez-Blas, T. *Chem. Commun.* **2005**, 4729-4731
87. Platas-Iglesias, C.; Mato-Iglesias, M.; Djanashvili, K.; Muller, R. N.; Vander Elst, L.; Peters, J. A.; de Blas, A.; Rodríguez-Blas, T. *Chem Eur. J.* **2004**, 10, 3579-3590.
88. Mato-Iglesias, M.; Balogh, E.; Platas-Iglesias, C.; Toth, E.; de Blas, A.; Rodríguez-Blas, T. *Dalton Trans.* **2006**, 5404-5415.
89. Mato-Iglesias, M.; Roca-Sabio, A.; Palinkas, Z.; Esteban-Gomez, D.; Platas-Iglesias, C.; Toth, E.; de Blas, A.; Rodriguez-Blas, T. *Inorg. Chem.* **2008**, 47, 7840-7851.

90. Amorim, M. T. S. ; Delgado R. ; Frausto da Silva, J. J. R. *Polyhedron* **1992**, 11, 1891-1899.
91. Chatterton, N.; Gateau, C.; Mazzanti, M.; Pecaut, J.; Borel, A.; Helm, L.; Merbach, A. *Dalton Trans.* **2005**, 1129-1135.
92. Ferreiros-Martinez, R.; Esteban-Gomez, D.; Platas-Iglesias, C.; de Blas, A.; Rodriguez-Blas, T. *Dalton Trans.* **2008**, 5754-5765
93. Nonat, A.; Fries, P. H.; Pecaut, J.; Mazzanti, M. *Chem. Eur. J.* **2007**, 13, 8489-8506.
94. Tóth, E.; Brücher, E.; Lazar, I.; Toth, I. *Inorg. Chem.* **1994**, 33, 4070-4076.
95. Balogh, E.; Tripier, R.; Ruloff, R.; Toth, E. *Dalton Trans.* **2005**, 1058-1065.
96. Brucher, E.; Sherry, A. D. *Inorg. Chem.* **1990**, 29, 1555-1559.
97. Pellegatti, L.; Zhang, J.; Drahos, B.; Villette, S.; Suzenet, F.; Guillaumet, G.; Petoud, S.; Toth, E. *Chem. Commun.* **2008**, 6591-6593.
98. Jakab, S., Kovacs, Z., Burai, L., Brücher, E. *Magy. Kém. Foly.* **1993**, 99, 391-396.
99. Dale W. Margerum, B. A. Zabin, D. L. Janes, *Inorg. Chem.,* **1966**, 5, 250
100. Spirlet, M.-R.; Rebizant, J.; Desreux, J. F.; Loncin, M.-F. *Inorg. Chem.* **1984**, 23, 359-363.
101. Stezowski, J. J.; Hoard, J. L. *Isr. J. Chem.* **1984**, 24, 323-334.
102. Raitsimring, A. M.; Astashkin, A. V.; Baute, D.; Goldfarb, D.; Caravan, P. *J. Phys. Chem. A*. **2004**, 108, 7318-7323.
103. Djanashvili, K.; Platas-Iglesias, C.; Peters, J. A. *Dalton Trans.* **2008**, 602-607.
104. Powell, H. D.; Ni Dhubhghaill, O, M.; Pubanz, D.; Helm, L.; Lebedev, Y.; Schlaepfer, W.; Merbach, A. E. *J. Am. Chem. Soc.* **1996**, 118, 9333-9346.
105. Toth, E.; Helm, L.;, Merbach, A. E.; Hedinger, R.; Hegetschweiler, K.; Jánossy, A. *Inorg. Chem.* **1998**, 37, 4104-4113.
106. Thompson, M. K., Botta, M., Nicolle, G. M., Helm, L., Aime, S., Merbach, A. E., Raymond, K. N *J. Am. Chem. Soc*. **2003**, 125, 14274-14275.
107. Burai, L.; Toth, E.; Bazin, H.; Benmelouka, M.; Jaszberenyi, Z.; Helm, L.; Merbach, A. E. *Dalton Trans.* **2006**, 629-634.
108. Toth, E.; Ni Dhubhghaill, O. M.; Besson, G.; Helm, L.; Merbach, A. E. *Magn. Reson. Chem.* **1999**, 37, 701-708.
109. Aime, S.; Botta, M.; Bruce, J. I.; Mainero, V.; Parker, D.; Terreno, E. *Chem. Commun.* **2001**, 115-116.
110. Loureiro de Sousa, P.; Livramento, J. B.; Helm, L.; Merbach, A. E.; Meme, W.; Doan, B.-T.; Beloeil, J.-C.; Prata, M. I. M.; Santos, A. C.; Geraldes, C. F. G. C.; Toth, E. *Contrast Media Mol. Imaging* **2008**, 3, 78-85.

111. Clarke E.T., Martell A.E., *Inorg Chim Acta*. **1991**, 190:37–46.
112. H. Sigel, R. B. Martin, *Chem. Rew.* **1982,** 82, 385

Acknowledgements

First of all, special thanks to my supervisiors, prof. Éva Jakab Tóth, prof. Ernő Brücher and prof. Imre Tóth, for their continuous support during the last few years. To Imre, who invited me to the "Rare-earth" research group in the University of Debrecen seven years ago. To prof. Brücher, who introduced me to the chemistry of MRI contrast agents and gave me useful advices every day to solve the problems. Thank to Éva, for offering me the opportunity to spend an unforgettable time in Orléans; she helped me not only in the laboratory, but in the adaptation in the new country. Here, I would like to thank the financial support for the Ministére de l'Education Nationale, France (Programme RFR).

During these years, I have learned a number of new experimental methods and techniques, and their difficulties and problems, as well. Of course, I would not have been able to solve these problems alone. Thus, I need to say thanks to dr. Róbert Király for his very useful help in equilibrium measurements, to dr. Krisztián Ferenc Kálmán for his help in relaxometric experiments and in the evaluation of the data, to dr. Zsolt Baranyai for teaching me how to perform NMR measurements. I also very grateful to Béla Rózsa for his technical help. Thanks to László Zékány for the useful computational support.

Special thanks to dr. Gyula Tircsó, dr. Marta-Mato Iglesias and dr. Carlos-Platas Iglesias for the synthesis of the ligands.

Thanks to all the recent and ancient members of the Jakab Tóth and Brücher group for the nice atmosphere in the laboratory: Célia Bonnet, Thomas Chauvin, Petra Fouskova, André Martins, Bohuslav Drahos; Tamara Kócs, Judit Bodnár, Erika Ruscsák, Zoltán Garda.

Last but not least, I want to say thanks to my family for their faithful support. Anya, Apa, Emi, köszönöm!

Zoltan Palinkas

Etudes thermodynamiques, cinétiques et de relaxation de complexes de lanthanides avec des ligands linéaires et macrocycliques

Résumé:
La thèse se porte sur l'étude des réactions d'échange de ligands sur les agents de contraste IRM cliniques (GdDTPA, GdBOPTA, Gd(DTPA-BMA)) avec le TTHA, ainsi que sur la caractérisation physico-chimique de complexes de gadolinium(III) avec de nouveaux ligands macrocycliques (bp12c4^{2-} et L^1= oxa-triaza tris(glycinate)). Les réactions d'échange de ligands impliquent la formation d'intermédiaires ternaires. Les vitesses d'échange sont 2-3 ordres de grandeurs plus élevées pour Gd(DTPA-BMA) que pour Gd(DTPA) ou Gd(BOPTA). Les réactions sont accélérées par des anions endogènes (carbonate, citrate, phosphate), bien que l'effet des deux derniers soit limité dans les conditions physiologiques. Le ligand 1,7-diaza-12-crown-4 avec des bras picolinates (bp12c4^{2-}) forme des complexes de Ln^{3+} stables. En présence du Zn^{2+}, la dissociation de [Gd(bp12c4)]$^+$ est catalysée par les protons et par le métal, donc ce système est intermédiaire entre des chélates macrocycliques de type DOTA et des complexes de type DTPA. L'échange d'eau est extrêmement rapide sur le [Gd(bp12c4)(H_2O)q]$^+$, similaire à celui de l'aqua ion Gd^{3+}. Sur les complexes de lanthanides du ligand L^1, nous avons mené des études thermodynamique, cinétique, relaxometrique, de RMN de l'^{17}O NMR et PARACEST très approfondies. Les ions Ln^{3+} forment des complexes stables avec L1. Nous avons constaté la formation de complexes ternaires entre GdL^1 et des ions lactate ou carbonate. Etonnamment, la dissociation spontanée est la voie la plus importante pour la dissociation, ce qui réduit sensiblement l'inertie cinétique du complexe GdL^1.
Mots clés: complexes de gadolinium(III), IRM, constante de stabilité, inertie cinétique, dissociation, relaxometrie, RMN de l'^{17}O, complexe ternaire, échange de métal, échange de ligand, échange d'eau

Thermodynamic, kinetic and relaxation studies on lanthanide complexes of open-chain and macrocyclic ligands

Summary:
The thesis is focused on the investigation of ligand exchange reactions of currently used MRI contrast agents (GdDTPA, GdBOPTA and Gd(DTPA-BMA)) with TTHA, and on the physico-chemical characterization of gadolinium(III) complexes formed with novel macrocyclic polyamino polycarboxylate ligands (bp12c4^{2-} and L^1= oxa-triaza tris(glycinate)). The ligand exchange reactions take place through the formation of ternary intermediates. The rates of the ligand exchange reactions of Gd(DTPA-BMA) are 2-3 orders of magnitude higher than those of Gd(DTPA) and Gd(BOPTA). They are faster in the presence of the endogenous citrate, phosphate and carbonate ions, though the effect of citrate and phosphate is limited at physiological concentrations. The picolinate-derivative ligand based on 1,7-diaza-12-crown-4 (bp12c4^{2-}) forms stable Ln^{3+} complexes. In the presence of Zn^{2+}, the dissociation of [Gd(bp12c4)]$^+$ proceeds both via proton- and metal-assisted pathways, thus this system is intermediate between DTPA- and DOTA-type chelates. The water exchange is extremely fast on [Gd(bp12c4)(H_2O)q]$^+$, and is similar to that on the Gd^{3+} aqua ion. For LnL^1 complexes, a comprehensive study

included thermodynamic, kinetic, relaxometric, ^{17}O NMR and PARACEST measurements. Ln^{3+} ions form stable complexes with L^1. Strong ternary complex formation occurs between GdL^1 and lactate or carbonate ions. Surprisingly, spontaneous dissociation is the most important pathway of dissociation, which remarkably reduces the inertness of GdL^1.
Keywords: Gadolinium(III) complexes, MRI, stability constant, kinetic inertness, dissociation, relaxometry, ^{17}O NMR, ternary complex, metal exchange, ligand exchange, water exchange

Centre de biophysique moléculaire, CNRS,
Rue Charles Sadron, 45071 Cedex 2 Orléans,
France

Department of Inorganic and Analytical Chemistry, DE
H-4010 Debrecen, Egyetem tér 1., Hungary

DE TTK